TRANSPORTATION RESEARCH
RECORD

No. 1315

Bridges, Other Structures, and Hydraulics and Hydrology

Culverts and Pipelines: Design, Monitoring, Evaluation, and Repair 1991

A peer-reviewed publication of the Transportation Research Board

TRANSPORTATION RESEARCH BOARD
NATIONAL RESEARCH COUNCIL
WASHINGTON, D.C. 1991

Transportation Research Record 1315
Price: $18.00

Subscriber Category
IIC bridges, other structures, and hydraulics and hydrology

TRB Publications Staff
Director of Publications: Nancy A. Ackerman
Senior Editor: Naomi C. Kassabian
Associate Editor: Alison G. Tobias
Assistant Editors: Luanne Crayton, Norman Solomon
Graphics Coordinator: Diane L. Ross
Production Coordinator: Karen S. Waugh
Office Manager: Phyllis D. Barber
Production Assistant: Betty L. Hawkins

Printed in the United States of America

Library of Congress Cataloging-in-Publication Data
National Research Council. Transportation Research Board.

Culverts and pipelines : design, monitoring, evaluation, and repair, 1991.
p. cm—(Transportation research record, ISSN 0361-1981 ; no. 1315)
ISBN 0-309-05152-5
1. Culverts. 2. Pipelines. I. National Research Council (U.S.). Transportation Research Board. II. Series: Transportation research record ; 1315.
TE7.H5 no. 1315
[TE213]
388 s—dc20
[625.7'342] 91-38546
CIP

Sponsorship of Transportation Research Record 1315

GROUP 2—DESIGN AND CONSTRUCTION OF TRANSPORTATION FACILITIES
Chairman: Raymond A. Forsyth, Sacramento, California

Structures Section
Chairman: Robert C. Cassano, Imbsen & Associates, Inc.

Committee on Culverts and Hydraulic Structures
Chairman: A. P. Moser, Utah State University
Gordon A. Alison, James D. Arnoult, A. E. Bacher, Kenneth J. Boedecker, Jr., Thomas K. Breitfuss, Dennis L. Bunke, Bernard E. Butler, James E. Cowgill, William D. Drake, J. Michael Duncan, James B. Goddard, James J. Hill, Jey K. Jeyapalan, Iraj I. Kaspar, Michael G. Katona, Timothy J. McGrath, John C. Potter, Russell B. Preuit, Jr., Harold R. Sandberg, James C. Schluter, David C. Thomas, Corwin L. Tracy, Robert P. Walker, Jr.

Soil Mechanics Section
Chairman: Michael G. Katona, Air Force Engineering and Services Center, Tyndall AFB

Committee on Subsurface Soil-Structure Interaction
Chairman: J. Michael Duncan, Virginia Polytechnic Institute and University
George Abdel-Sayed, Arnold Aronowitz, Baidar Bakht, Sangchul Bang, Timothy J. Beach, Mike Bealey, Lester H. Gabriel, James B. Goddard, William A. Grottkau, John Owen Hurd, Jey K. Jeyapalan, Michael G. Katona, Kenneth K. Kienow, Richard W. Lautensleger, L. R. Lawrence, Donald Ray McNeal, Samuel C. Musser, Thomas D. O'Rourke, James C. Schluter, Raymond B. Seed, Ernest T. Selig, H. J. Siriwardane, Mehdi S. Zarghamee

Frank R. McCullagh, G. P. Jayaprakash, Transportation Research Board staff

Sponsorship is indicated by a footnote at the end of each paper. The organizational units, officers, and members are as of December 31, 1990.

Transportation Research Record 1315

Contents

Impact Effects on Pipelines Beneath Railroads

HARRY E. STEWART AND MICHAEL T. BEHN

Design methods being developed for uncased crossings of high-pressure gas pipelines use impact factors to account for the increase in live load response due to the effects of vehicle speed, track stiffness, vehicle suspension characteristics, or irregularities in the running surface. Field experiments to measure impact effects were conducted on an instrumented pipeline 36 in. (914 mm) in diameter buried 5.75 ft (1.75 m) below the Facility for Accelerated Service Testing track at the Transportation Test Center in Pueblo, Colorado. Ranges of vehicle speeds and surface geometry conditions were investigated, and impact factors based on measured pipeline strains were determined. The results indicated that train speeds of 5 to 40 mph (8 to 64 km/hr) had a relatively minor influence on impact response, whereas changes in surface geometry resulted in a range of dynamic pipeline strains, with the maximum values nearly 1.6 times larger than previously recorded under baseline operating conditions.

When high-pressure gas pipelines cross beneath railroads, the owner of the railroad generally requires that the carrier pipeline be installed within a metallic casing. The main design criterion for the cased carrier is that the circumferential (hoop) stress due to internal pressurization be less than some percentage of the specified minimum yield strength. The allowable percentage is based on the population density in the vicinity of the pipeline, the type of pipeline welds, and the operating temperature. Because the casing is designed to carry the earth and live loads, the carrier design for cased pipelines is unaffected by additional live load effects due to impacts at the surface.

Research focused on the development of design procedures for uncased gas pipelines is under way. Uncased pipelines must be designed to withstand live load stresses imposed by vehicular traffic as well as stresses due to internal pressure and earth load. Rational methods to account for impact forces are an important part of design procedures.

Two instrumented high-pressure steel pipelines were installed without casings, using auger boring methods, at the Transportation Test Center (TTC) in Pueblo, Colorado. Field experiments were conducted to measure pipeline response to train loading. The effects of vehicle speed, internal pressure, and time since pipeline installation were investigated during a 2-year period. Figure 1 shows profiles of the two pipelines. The pipeline 12 in. (305 mm) in diameter has a wall thickness of 0.25 in. (6.4 mm) and a specified minimum yield strength of 42,000 psi (290 MPa). The pipeline 36 in. (914 mm) in diameter has a wall thickness of 0.61 in. (15.5 mm) and a specified minimum yield strength of 60,000 psi (414 MPa). The depth from the top of the railroad crossties to the crown of both pipes at the track centerline is 5.75 ft (1.75 m).

Both pipelines were instrumented before field installation. Instrumentation consisted of strain gauges, both internal and external, on the pipes, accelerometers, pressure transducers, and temperature sensors. Strain gauges also were mounted on the rails directly above the pipes to measure the applied wheel loads. The strain gauges on the pipes were oriented to measure both circumferential and longitudinal strains at the inside and outside crown, springlines, and invert. The locations of the instrument stations are shown in Figure 1 as solid circles. The gauge locations correspond to locations on the pipelines directly beneath the outside rail, track centerline, inside rail, and other locations along the pipe's long axis sufficient to measure the distribution of strains along the pipeline.

Testing of the pipelines began in July 1988. Measurements were made at 4- to 6-month intervals through the spring of 1990. Although measurements of live load response were recorded for both pipes, special impact testing was conducted only with the 36-in. (914-mm) pipeline. The remaining discussion focuses on the 36-in. (914-mm) pipeline data.

BASELINE TESTING

Field data were measured for a range of train speeds and internal pressures from the summer of 1988 through the spring of 1990. After the installation of the 36-in. (914-mm) pipeline, the annulus left by the 1.5-in. (38-mm) auger overbore remained partially open and did not collapse fully. The resulting pipeline strains were small, because contact between the pipe and the soil was limited. To replicate long-term loading conditions, the remaining annulus around the pipe was injected with a slurry of native sand and water in May 1989. Field data indicated that the annulus had collapsed partially between July 1988 and May 1989, and strains had been increasing. The decision to fill the annulus and increase live load transfer was necessary, because long-term response was desired and the field testing program had a duration of 2 years. There is little doubt that, given several years, the annulus would have collapsed fully because of repeated traffic. Between May and June 1989, the field measurements increased and stabilized at a consistent level. Measurements in July 1989 confirmed that the annulus around the pipeline was in a steady-state condition.

Figure 2 shows the longitudinal pipeline strains at the crown and invert of the 36-in. pipe measured in May 1989 before the annulus was filled, in May 1989 just after the annulus was

School of Civil and Environmental Engineering, Cornell University, Ithaca, N.Y. 14853-3501.

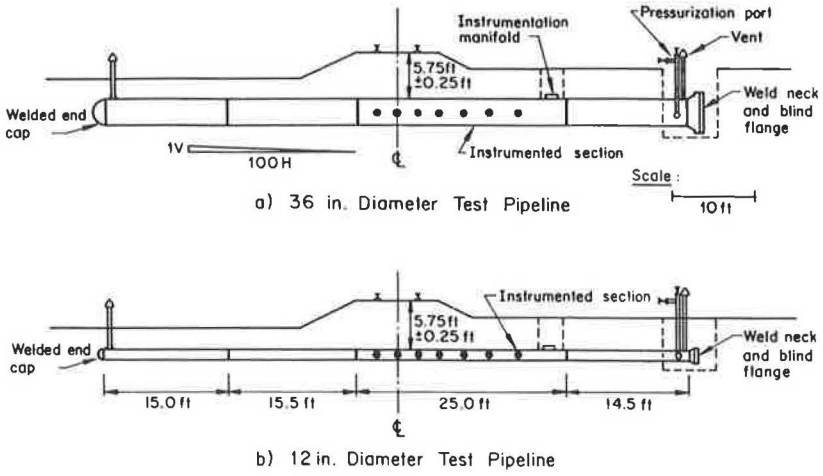

FIGURE 1 Profile views of test pipelines (looking west).

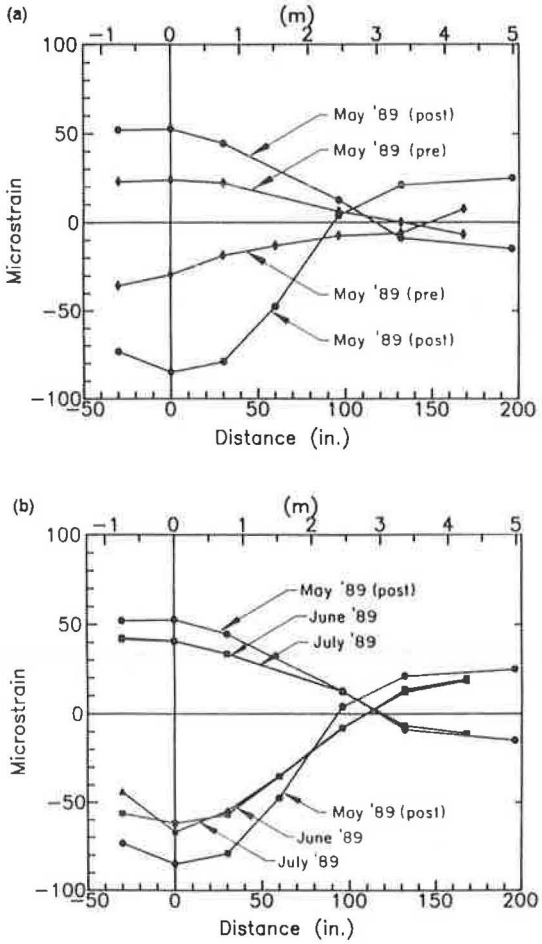

FIGURE 2 Changes in longitudinal strains at crown and invert over time.

injected with the native sand and water slurry, in June 1989, and in July 1989. (Distance 0 corresponds to the track centerline.) The rail surface at this time was level, without irregularities. Train loading was generated by slowly rolling loaded freight cars weighing 315,000 lb (1400 kN), producing 39.4-kip (175-kN) wheel loads. The freight cars are referred to as 125-ton cars and are representative of the heavy loadings anticipated in the near future on U.S. revenue lines. As shown in Figure 2, the strains before the annulus was filled were substantially smaller than those after the annulus was filled in May 1989. Strain decreased from May 1989 to June 1989, as any locked-in injection pressures dissipated. The June 1989 and July 1989 data indicate that the contact conditions between the pipe and soil had stabilized and were taken to represent the long-term condition. The relative changes in pipe strain from May 1989 to July 1989 shown in Figure 2 are representative of the changes of circumferential strain at the pipe crown, invert, and springline over time.

Train speeds above the instrumented pipeline were varied from a slow roll of roughly 5 mph (8 km/hr) to 40 mph (64 km/hr). The upper limit was based on the maximum speed that the train could achieve through the test section. Figure 3 shows dynamic longitudinal strains at the crown and invert of the 36-in. (914-mm) pipe, at the gauge station directly below the centerline of the track. The data indicate that at the pipeline depth of 5.75 ft (1.75 m), there was no measurable effect of train speed for the baseline field condition, without surface irregularities. Thus, for the normal track conditions at the Facility for Accelerated Service Testing (FAST) track at TTC, impacts were not measured.

Figure 4 shows the dynamic wheel loads measured using the strain gauge instrumentation installed on the rails directly

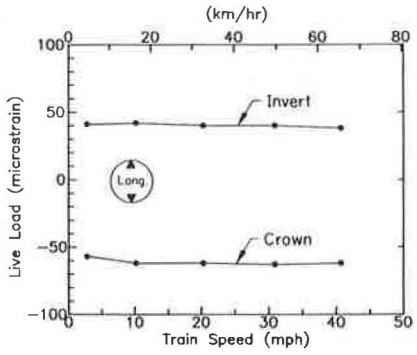

FIGURE 3 Longitudinal strains at crown and invert versus speed, July 1989.

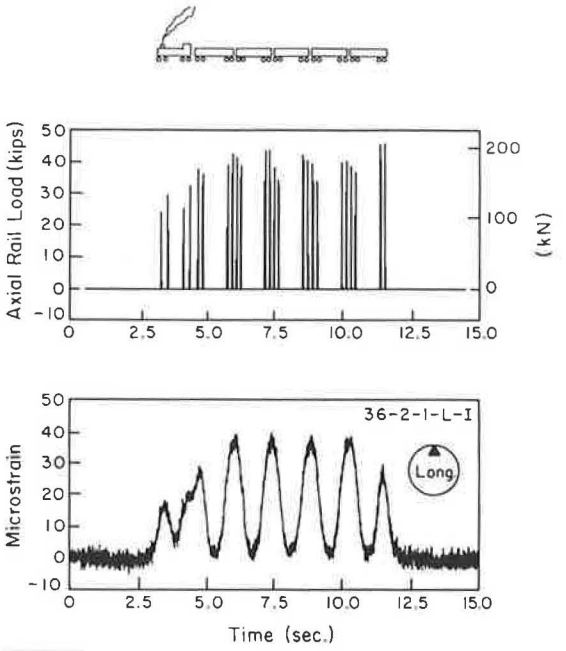

FIGURE 4 Dynamic wheel loads and longitudinal strains at invert for train speed of 30 mph.

above the pipeline for a train speed of 30 mph (48 km/hr) and the corresponding longitudinal strains at the pipe invert beneath the track centerline. The train used for this data run consisted of one locomotive and five freight cars. There is some variation in the dynamic wheel loads from the freight cars. The dynamic loads are approximately 40 ± 4 kips (178 ± 18 kN). The nominal static wheel load for the freight cars was 39.4 kips (175 kN). This indicates that at 30 mph (48 km/hr), the surface impact factor is 1.0 ± 0.1. Figure 4 also shows that four axles result in a single stress pulse at the pipeline depth.

IMPACT FACTORS

Design methods for pipelines subjected to traffic loads generally use some factor to account for the increase in live loading effects due to vehicle dynamics and the quality of the running surface. For railroad loadings on buried pipelines, two approaches are often used. The first is to use an impact factor as a multiplier of the static wheel load and calculate pipe response on the basis of the increased surface loading. This approach is also used for conventional track design, and several methods are available for estimating the surface impact factor. Typical methods are based on a combination of vehicle speed, wheel diameter, track stiffness, track quality, and unsprung mass of the wheel sets (*1–6*). In general, these methods predict surface impact factors on the order of 1.3 to 1.6 for track in good condition at vehicle speeds from 5 to 40 mph (8 to 64 km/hr). Impact factors based on these methods increase to approximately 2.0 to 2.5 at high train speeds for track in poor condition.

The second approach for impact loadings, which is more common for pipeline design, is to predict stresses within the soil mass that are based on a nominal design wheel load and then to increase the predicted stresses by a factor that is greater than unity at the surface and that decreases with depth. This method accounts for the attenuation of dynamic stresses with increasing depth. The two most common formulations for this variable depth impact factor are those recommended by the American Society of Civil Engineers (ASCE) (*7*) and the American Petroleum Institute (API) (*8*). The impact factor recommended in the ASCE method equals 1.5 between 0 and 5 ft (0 and 1.5 m), decreases linearly to 1.0 at a depth of 22 ft (6.7 m), and remains constant below that depth. The API impact factor is 1.75 between 0 and 5 ft (0 and 1.5 m) and decreases linearly by 0.03/ft (0.01/m) between 5 and 30 ft (1.5 and 9.1 m). Below 30 ft (9.1 m), the API method uses an impact factor of 1.0.

IMPACT TESTING

The observation that negligible speed-induced impacts occurred through the test section is consistent with wheel load data reported previously for FAST (*9*), in that only a small percentage of wheel loads at the well-maintained FAST track were significantly larger than the nominal static values.

Because the primary purpose of the field experiments was to provide data to substantiate a pipeline design procedure, it was important to replicate typical field conditions and to generate realistic upper bound loading conditions. Project advisors from the gas and railroad industries, the Association of American Railroads, and the American Railway Engineering Association also were concerned that the loading conditions at FAST might not represent those of revenue lines, because the track maintenance standards are high, and irregular train wheels are removed when they are detected. Thus, a series of impact tests intended to cause increased dynamic loadings representative of lesser-quality track was initiated. In addition, impact loading measurements could be used to substantiate current impact formulations used commonly in pipeline design.

Impact testing consisted of progressively degrading the track quality above the pipeline and operating the train at a range of speeds. The degradation procedure included installing a rail joint directly above the pipeline. The installation of the joint required removal of the wheel load detection circuits. Wood shims were placed between the top of the ties and tie plates at both rails over a distance of roughly 80 ft (24.4 m), so that a uniform rail raise of 3 in. (76 mm) was achieved over the central 30 ft (9.1 m). The wood shims over the central portion of the elevated track were removed in stages beneath the inside rail to produce a dip in one rail and a cross-level variance of up to 3 in. (76.2 mm) between the inside and outside rail. The joint at the rail above the pipeline also could be adjusted to produce either a tight joint or a pulled joint. The gap caused by the pulled joint was approximately 0.8 in. (20.3 mm). In addition, the end of the upstream rail at the joint was progressively ground to simulate a battered joint. The mismatch ranged from 0 to approximately 0.3 in. (7.6 mm) and was increased with increasing cross-level variances. The test conditions were selected to correlate with track class designations specified by the Federal Railroad Administration (FRA) (*10*) so that the track irregularities could be related to revenue track conditions at other sites.

Eight test steps were investigated, for FRA Class 6+ standards down to FRA Class 1 standards. For each test step, train speeds were varied from a slow roll to the maximum permissible or safe train speed, with both a tight and a pulled rail joint. Table 1 summarizes the impact test conditions along with the associated FRA class limits for cross-level and rail mismatch. The maximum joint gaps are also given in Table 1. The joints for the tight joint conditions were made as close as possible, not exceeding 1/16 in. (1.6 mm).

Figure 5 shows the measured cross-level variances between the outside and inside rail variances versus tie number for the test steps given in Table 1. Shims were removed from the inside rail, which caused the dip in the rail profile shown. The test pipeline was located beneath Tie 53, corresponding to the center of the rail dip and maximum cross-level variance.

Test Step 1 represents the nominally smooth track that had been shimmed to provide a uniform 3-in. (76-mm) raise through the test section. A slow roll of the train through the test section indicated that the installation of the shims and rail joint did not cause a change in the strains measured in the 36-in. (914-mm) pipeline from those recorded during the baseline measurements. Thus, the slow roll at Test Step 1 was representative of the baseline test conditions. Impact testing proceeded for each test step by increasing the train speeds from 5 mph (8 km/hr) up to the maximum attainable speeds given in Table 1 with the rail joint tight, and then repeating the speed sequence with a pulled joint. After the completion of a test step, the shims were removed as necessary, and the rail was ground to the rail mismatches given in Table 1.

Figure 6 shows the variation in dynamic strains in the pipe beneath the track from Test Step 5b for several important pipeline locations. Figure 6 indicates that strain increases only slightly as speeds increase from 5 to 40 mph (8 to 64 km/hr). There is a slight subpeak in the dynamic strains near 20 mph (32 km/hr), which corresponds to a resonant effect that frequently has been observed in other testing at TTC using 39-ft (11.8-m) jointed rail sections and trains traveling at 18 mph (29 km/hr). Also, the longitudinal strains are not symmetrical about the unrestrained pipe's neutral axis. This trend is also shown in Figure 2. The circumferential strains at the springline have a greater absolute magnitude than at invert. This trend was observed consistently in all of the experimental data.

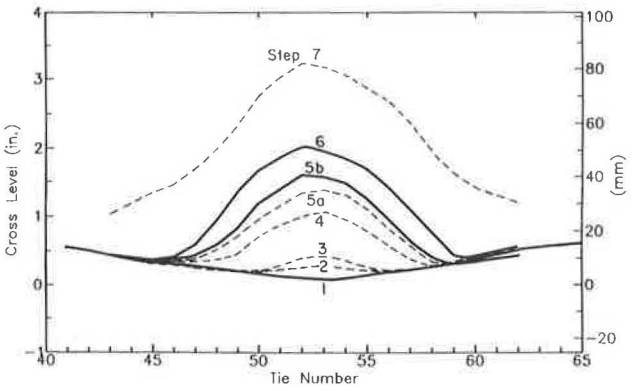

FIGURE 5 Cross-level variances for impact tests.

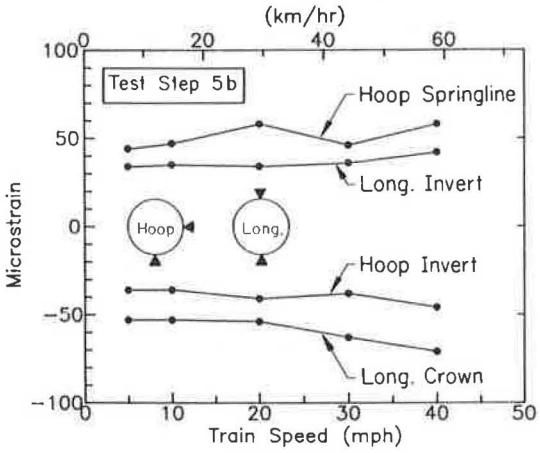

FIGURE 6 Variation of live load strain with train speed, Impact Test Step 5b.

Impact factors for the field tests were defined as the ratio of pipeline strain under impact conditions to the strain measured at the same gauge location from the baseline tests. Table 2 gives the measured impact factors at three critical pipeline locations, determined for the worst surface geometry case and maximum attainable train speed. The impact factors

TABLE 1 SUMMARY OF IMPACT TEST CONDITIONS

Test Step	FRA Class	Speeds (mph)	Cross Level (in.) Test	Cross Level (in.) FRA Max.	Rail Mismatch (in.) Test	Rail Mismatch (in.) FRA Max.	Maximum Joint Gap (in.)
1	6+	0 - 40[a]	0.07	0.00	0.00	0.00	0.88
2	6	0 - 40[a]	0.29	0.50	0.12	0.12	0.81
3	6	0 - 40[a]	0.42	0.50	0.12	0.12	0.94
4	5	0 - 40[a]	1.00	1.00	0.12	0.12	0.75
5a	4	0 - 40[a]	1.38	1.25	0.12	0.12	0.81
5b	3	0 - 40[a]	1.58	1.75	0.19	0.19	0.75
6	2	0 - 25[b]	1.96	2.00	0.25	0.25	0.80
7	1	0 - 10[b]	3.18	3.00	0.28	0.25	0.75

a - Maximum attainable at test section
b - Maximum allowable for FRA Class

TABLE 2 IMPACT FACTORS FOR PULLED JOINT TEST CONDITIONS

Test Step	Train Speed (mph)	Cross Level (in.)	Rail Mismatch (in.)	Joint Gap (in.)	Impact Factor at Station[a] Hoop, Invert	Hoop, Springline	Longitudinal, Invert
1	40	0.07	0.00	0.88	1.30 (2)	1.13 (3)	1.12 (2)
2	40	0.29	0.12	0.81	1.32 (1)	1.19 (3)	1.10 (1)
3	40	0.42	0.12	0.94	1.22 (2)	1.10 (3)	1.12 (1)
4	40	1.00	0.12	0.75	1.15 (2)	1.19 (3)	1.05 (2)
5a	40	1.38	0.12	0.81	1.41 (2)	1.17 (3)	1.12 (1)
5b	40	1.58	0.19	0.75	1.52 (2)	1.25 (3)	1.38 (1)
6	25	1.96	0.25	0.80	1.48 (3)	1.48 (3)	1.17 (1)
7	10	3.18	0.28	0.75	1.36 (1)	1.21 (3)	1.07 (1)

a - Numbers in parentheses refer to pipeline station: 1 = outside rail; 2 = centerline; 3 = inside rail

from Test Steps 1 through 5a did not show a clear trend of increasing with worsened track condition. Test Steps 5b through 7 had increased cross-level variance and rail mismatch, but the maximum allowable test train speeds decreased from 40 mph (64 km/hr) to 10 mph (16 km/hr). The data given in Table 2 suggest that larger impact factors would have been achieved for Test Steps 6 and 7 if the train speeds had been higher.

In general, Test Steps 5b and 6 resulted in the highest measured impact factors. Figure 7 shows comparisons of the pipeline strain from the impact tests with the strain from the initial condition or baseline cases at the same gauge location. Figure 7a shows data from Test Step 5b, and Figure 7b shows data from Test Step 6. The strains at the inside invert, outside crown, and outside springline are shown, using data taken from all instrumented sections along the pipe, as shown in Figure 1. As indicated in Figures 7a and 7b, impact factors can be determined by the ratios of the impact strains to the initial condition strains. There is a distribution of impact factors from roughly 0.8 to 1.6 for both test steps. Impact factors of less than unity are possible due to wheel bounce, load transfer between inside and outside rails, and dynamic interaction effects of the trains passing through the irregular track section.

As described previously, both ASCE and API recommend design impact factors dependent on depth below the track. Figure 8 shows the design impact curves for ASCE and API, along with the maximum impact factor determined from the field testing. Although only one experimental pipeline depth was investigated, the datum shown in Figure 8 suggests that the ASCE recommendation may be unconservative. The field testing had limitations on the maximum train speeds, particularly for the most severe geometric irregularities. Thus, it is likely that greater impacts are possible with revenue train speeds of up to 80 mph (129 km/hr). The API design curve has an impact of 1.75 for the upper 5 ft (1.5 m), which is larger than the maximum field test value of 1.6. Given that higher impacts than measured during the field tests may be possible, the API curve would be preferred for uncased pipeline design.

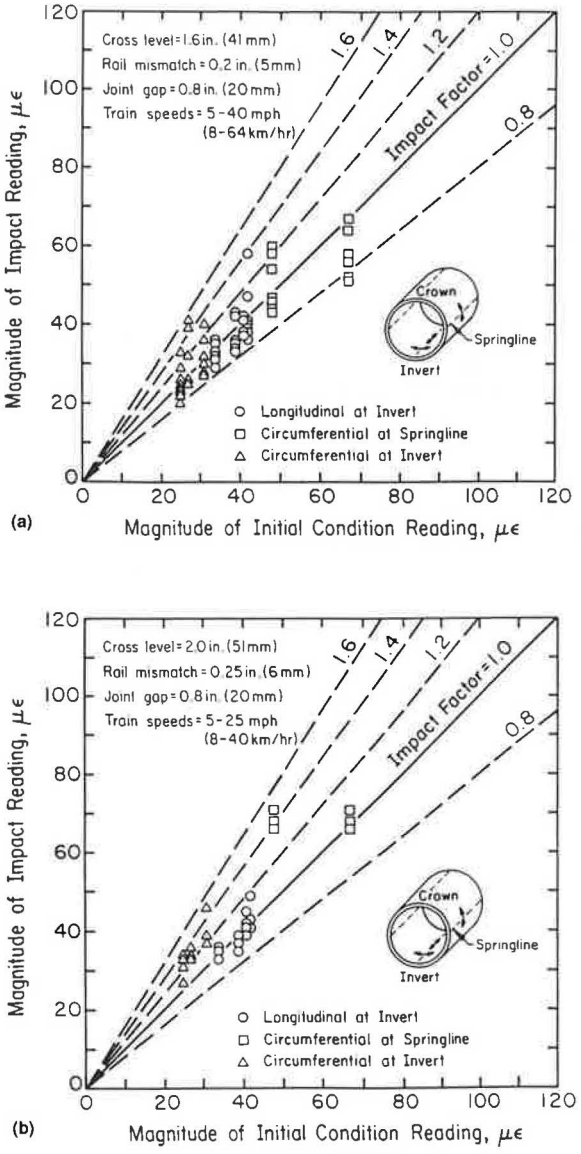

FIGURE 7 Measured impact factors from field tests.

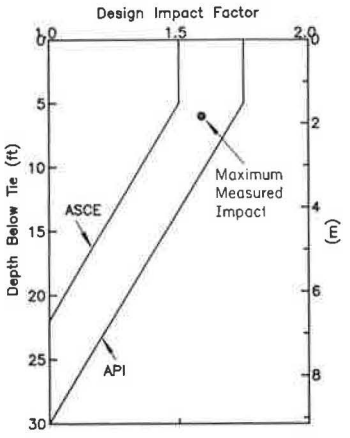

FIGURE 8 ASCE and API design impact factors and maximum measured impact factor from field tests.

SUMMARY

Field testing of live load response on well-maintained track at TTC indicated that negligible dynamic impact effects occurred during baseline field testing. In response to concerns from the gas and railroad industries, and to replicate upper bound conditions to the extent practically possible, a series of special impact tests was conducted to investigate live load response for changes in track quality consistent with FRA class standards. Track quality was degraded progressively by increasing the cross-level variance between the inside and outside rails, producing a condition representative of a dipped joint. Rail mismatch on the order of 0.25 in. (6.4 mm) was included, along with a pulled joint producing a gap of approximately 0.8 in. (20.3 mm). Heavy-axle freight cars were operated over an instrumented steel pipeline 36 in. (914 mm) in diameter buried 5.75 ft (1.75 m) below the top of the tie. Impact factors increased slightly with speed for each of the test configurations. Impact factors based on pipeline strain were measured and ranged from 0.8 to 1.6. On the basis of the maximum measured impact factor of 1.6, and the consideration that higher impacts might have been developed had higher test speeds been possible, the impact formulation given by API is recommended for the design of uncased gas pipelines crossing beneath railroads.

ACKNOWLEDGMENTS

This research was supported by the Gas Research Institute (GRI). Kenneth B. Burnham is the GRI project manager. The participation of gas and railroad industry advisors and TTC personnel is appreciated.

REFERENCES

1. *Manual for Railway Engineering*. American Railway Engineering Association, Washington, D.C., 1989.
2. A. N. Talbot. Stresses in Railroad Track, Report of the Special Committee on Stresses in Railroad Track. *Proceedings*, American Railway Engineering Association. First Progress Report, Vol. 19, 1918, pp. 873–1062. Second Progress Report, Vol. 21, 1920, pp. 645–814.
3. C. W. Clark. Track Loading Fundamentals—Parts 1–7. *Railway Gazette*, 106, London, 1957.
4. M. Srinivasan. *Modern Permanent Way*. Somaiga Publications, Bombay, India, 1969.
5. J. Eisenmann. Germany Gains a Better Understanding of Track Structure. *Railway Gazette International*, Aug. 1972, pp. 305–308.
6. C. O. Frederick and D. J. Round. Vertical Track Loading. *Proceedings, Track Technology for the Next Decade*. Thomas Telford Ltd., London, July 1984, pp. 135–149; discussion pp. 151–169.
7. Committee on Pipeline Crossings for Railroads and Highways. *Interim Specifications for the Design of Pipeline Crossings of Railroads and Highways*. ASCE, New York, Jan. 1964.
8. Recommended Practice for Liquid Petroleum Pipelines Crossing Railroads and Highways. *API Recommended Practice 1102*, 5th ed. American Petroleum Institute, Washington, D.C., Nov. 1981.
9. H. E. Stewart and T. D. O'Rourke. Load Factor Method for Dynamic Track Loading. *Journal of Transportation Engineering*. ASCE, Vol. 114, No. 1, Jan. 1988, pp. 21–39.
10. *Track Safety Standards*. Office of Safety, Federal Railroad Administration, U. S. Department of Transportation, 1982.

Publication of this paper sponsored by Committee on Culverts and Hydraulic Structures.

Evaluation of Flexible Culvert Behavior

DAVID C. COWHERD AND VLAD G. PERLEA

A method of evaluating flexible buried structures that have experienced some degree of flattening and of estimating the potential flattening of flexible structures is presented. The integrity of flexible structures depends on maintaining their shape without becoming too flat. If a flexible buried structure becomes too flat on the top or sides, it experiences distress and might ultimately collapse. A computer program, MULTSPAN, for evaluating the degree of flatness on the basis of measurements of chords and midordinates and for recommending remedial action for deflected structures is described. The recommendations include no action, lowering the load rating of the roadway, and closing the roadway (or airfield, etc.) until further action is taken. A second program, SOILEVAL, which predicts movement of a flexible buried structure, is presented. The program uses soil type to make projections of movement. The average characteristics of seven soil types are built into the program. It is possible to access the program using standard penetration data or other information concerning the degree of compaction. It is also possible to evaluate a flexible structure that is deflected and to predict additional deflection. Whether the ultimate deflection is likely to create collapse can be determined from the evaluation. The program was calibrated with actual data obtained from several deflected or collapsed structures.

All flexible buried underground structures depend on the backfill for varying degrees of their support. It is, therefore, important that in the design and evaluation of such structures the backfill be taken into account. In many applications these structures are not periodically evaluated. Long-span structures under highways have been classified by AASHTO and most states as bridge-type structures and are required to undergo an annual inspection under a bridge inspection program. In many cases these structures were inspected in much the same way as a reinforced concrete or structural steel bridge, that is, by evaluating the structural aspects alone. Specifically, the pipes were analyzed for degree of rusting, missing bolts, torn or damaged plates, and visual structural defects. Little attention was given to deflection of the structure. These types of structures seldom fail because of structure inadequacy, but rather because of excessive deflection resulting from consolidation of backfill or soil outside the backfill envelope. As the structure applies stress to the soil, the soil consolidates by an amount dependent on compaction and allows the sides of the structure to move outward. As the sides move outward, the top moves down. As the top approaches flatness, it no longer maintains its arch structure and is no longer capable of supporting the load above it. At some point, if reverse curvature occurs, the structure collapses.

In most cases, even in evaluations that took shape into account, there were no criteria to determine when the structure shape was becoming too flat. Many times this determination was made on a strictly visual basis. A system for evaluating the flatness of such structures and making recommendations for remedial action based on deflection is needed. A simple method of predicting potential movement of a structure that is deflected is also needed. Two programs for accomplishing these objectives have been developed. They are MULTSPAN, which evaluates the degree of flatness, and SOILEVAL, which predicts soil movements on the basis of simplified soils information.

MULTSPAN is used to evaluate the current safety of a structure, whereas SOILEVAL is used to evaluate how much additional movement a structure can be expected to undergo. MULTSPAN uses the measurements of chords and midordinates and compares the measurements with design or previous measurements.

MULTSPAN MODEL

The MULTSPAN analysis provides recommendations for remedial action on the basis of the degree of flatness of top arcs within the structure. Most of these structures are various portions of circles. It is reasonably simple to measure chords and midordinates and compare them with design values. Design values for various types of structures are built into the MULTSPAN program, or other values can be input. The program compares the measured values with the design values (or with measured values from previous inspection) and calculates the deflection as a percentage of midordinate change. Figure 1 shows a typical arch structure and the measurements that are made with such a structure.

The measurements are entered into MULTSPAN, and the degree of flatness, defined as a percentage change of the midordinate, is computed. To project the appropriate remedial action, data concerning the actual behavior of approximately 100 corrugated metal structures in Ohio and observations of several failures were examined and statistically processed (*1*). Table 1 gives the recommendations for various degrees of deflection of top midordinates.

The behavior of a flexible structure is less sensitive to changes in shape of the sides, corners, or bottom. However, large side or corner deformations (increases or decreases in side or corner midordinates) have been found to be harmful to overall stability. The criteria in Table 2 are suggested and have been implemented in MULTSPAN for the evaluation of side or corner changes in shape.

SOILEVAL MODEL

The SOILEVAL program was developed to evaluate the potential for continued movement of a structure and to predict

Bowser-Morner Associates, Inc., 4518 Taylorsville Road, P.O. Box 51, Dayton, Ohio 45401-0051.

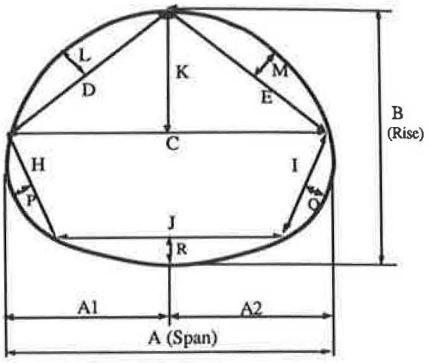

FIGURE 1 Typical measurements for a pipe-arch structure. (A through R represent dimensions to be monitored.)

a general time frame for the movement. The model is based on classical soil mechanics theory and was calibrated with actual field cases. An attempt was made to use simplified data for input to allow the program to be useful to field personnel. It is possible to use the program to evaluate an existing structure or as a design tool to evaluate the type, required width, and degree of compaction of the select backfill and the original soil.

TABLE 1 PERCENT TOP MIDORDINATE (K, L, OR M) REDUCTION AND REMEDIAL ACTION

Top Mid-Ordinate Percent Reduction	Depth of Cover (ft)	Recommended Action
<15	Any	No action required.
15 – 20	Over 6.0	No action required.
15 – 20	Under 6.0	Monitor on 6-month interval.
20 – 25	Over 6.0	Reduce legal load to 90% of H-20 and monitor on 6-month intervals.
20 – 25	Under 6.0	Reduce legal load to 75% of H-20 and monitor on 6-month intervals.
25 – 30	Over 6.0	Reduce load to 75% of H-20 and monitor on 6-month intervals.
25 – 30	3.0 – 6.0	Reduce load to 50% of H-20 and monitor on 6-month intervals.
25 – 30	Under 3.0	Reduce load to 50% of H-20 and do detailed analysis based on borings.
>30	Any	Close road until detailed analysis is done.

TABLE 2 PERCENT SIDE OR CORNER MIDORDINATE CHANGE (P AND Q IN EXAMPLE IN FIGURE 1) AND RECOMMENDED REMEDIAL ACTION

Side or Corner Mid-Ordinate Percent Reduction	Depth of Cover (ft)	Recommended Action
<30	Any	No action required
30 - 60	Any	Monitor on 6 - month interval
>60	Under 3.0	Reduce load to 50% of H-20 and perform detailed analysis, including soil borings
>60	Over 3.0	Close road until detailed analysis is done

Background

The deflection of a buried flexible structure can be predicted in accordance with the classical formula for evaluation of strain or deformation of a structural member (strain = stress/modulus of elasticity) (*2*). The equation for deflection of a flexible structure supported by backfill takes the following conceptual form:

$$\text{Structure deflection} = \frac{\text{load on structure}}{\text{structure stiffness} + \text{soil stiffness}} \quad (1)$$

Several theories to evaluate the structure-soil interaction have been proposed. Most theories for structure-soil interaction use some form of this equation.

Iowa Formula

The formula recommended by Watkins and Spangler (*3*) for predicting deflections of buried flexible pipe is

$$\Delta x = \frac{D'KW_c r^3}{EI + 0.061E'r^3} \quad (2)$$

where

Δx = horizontal deflection of the pipe (in.), considered the same as the vertical deflection;
D' = deflection lag factor, normally taken as 1;
K = a bedding constant with values between 0.08 and 0.11, depending on the bedding condition;
W_c = vertical load per unit length acting on the top of the pipe (lb/in.);
r = mean radius of the pipe (in.);
E = modulus of elasticity of the pipe material (lb/in.^{2});
I = moment of inertia per unit length of cross section of the pipe wall (in.^{4}/in.); and
E' = modulus of soil reaction (lb/in.^{2}).

The use of this formula is recommended as part of the design process for corrugated metal pipes (*4*), smooth steel pipes (*5*), polyethylene pipes (*6*), polyvinyl chloride pipes (*7*), fiberglass pipes (*8*), and generally for all buried flexible structures. Although it is confirmed that E' is not a constant but varies with depth of installation (*9*), the values suggested by Howard (*2*) are extensively used.

Other Proposed Models

Watkins et al. (*6*) summarized a number of proposed variations of the classical Iowa formula and found that all of them can be represented by a simple relationship:

$$\Delta y = \frac{\varepsilon_s (2r)}{A + BEI/(E_s r^3)} \quad (3)$$

where

ε_s = P/E_s = vertical soil strain (soil deformation),
P = $W_c(2r)$ = vertical nominal pressure acting on top of pipe (lb/in.^{2}),
E_s = soil stiffness (lb/in.^{2}), and
A and B = empirical constants.

It was found from field tests that much of the deformation process takes place as the backfill is being placed, so for pipe deflection calculations a short-term modulus should be used. However, there may be continued deformation with time because of consolidation of the sidefill (especially with cohesive backfills), so that usually ultimate soil settlement should be included in ε_s (*6*).

Several procedures for flexible pipe deformation evaluation have been developed using finite-element methods. CANDE (Culvert Analysis, Design) is a Federal Highway Administration–sponsored computer program by Katona et al. (*10*). Three levels of sophistication are available. Level 1 is based on a closed-form elasticity solution, whereas Levels 2 and 3 are based on the finite element method. The soil-culvert interaction design method by Duncan (*11*) uses design graphs and formulas based on finite-element analysis. In the program SSCOMP, Seed and Duncan (*12*) use nonlinear finite-element analysis to model soil-structure interaction, taking into account the layerwise placement of backfill and the nonlinear stress-strain soil behavior.

The finite-element evaluations are beyond most field personnel. A simplified model for a rough evaluation of flexible buried structures that could be easily used in routine evaluation of existing structures and preliminary design of new structures was desirable. The SOILEVAL model was developed to provide this simplified model. The SOILEVAL model presented in this paper uses the classical theories of soil compressibility and settlement of shallow foundations. However, some coefficients were empirically obtained by statistical processing of field measurements.

Specifics of SOILEVAL Model

The form of the equation used in SOILEVAL to evaluate soil-structure interaction is

$$\Delta y = \frac{A\,\Delta W\,\mathrm{SF}}{EI/r_a^3 + BE'} \leq \mathrm{Fs}\,\Delta W\,\mathrm{SF} \qquad (4)$$

where

Δy = maximum expected deflection at the crown of the structure (in.);
ΔW = potential horizontal movement of one side of the structure due to compression of both backfill and original soil under the stress generated by the pipe (in.);
SF = shape factor, defined as the ratio between the vertical displacement of the structure at the crown and the corresponding maximum movement on one side of the structure;
r_a = average radius of the structure (in.), equal to (span + rise)/4;
A and B = empirical coefficients statistically determined from field measurements; and
Fs = factor of safety to take into account the variability of soil properties, equal to 1.5.

All other parameters are as defined previously.

SOILEVAL incorporates the following characteristics of soil-structure interaction:

1. The compressibility index, coefficient of pressure at rest, initial void ratio, relative density, or degree of compaction of the soil supporting the structure are used in calculations instead of special defined characteristics (deformation lag factor or modulus of soil reaction).
2. Both the backfill and the original soil are considered to interact with the structure, up to a distance of about 2.5 times the rise of the structure laterally from the pipe wall.
3. The pipe stiffness is taken into account when it is large enough to provide resistance to deformation. However, for very flexible pipes, 150 percent of the average potential deformation of the surrounding soil is used to determine the maximum expected pipe deflection because of the potential variability of the soil properties.
4. A shape factor that represents the ratio between the decrease in rise and the corresponding lateral displacement on one side of the pipe is defined; the factor depends on the shape and dimensions of the pipe structure.

How each parameter is determined in the SOILEVAL model is described as follows.

Potential Horizontal Movement due to Soil Compressibility (ΔW)

Classical theory of settlement for shallow foundations has been used for calculating the potential horizontal movement. The fill at the side of the structure is considered as a soil column, loaded by the pressure created by the structure onto the fill (*13*). Figure 2 explains the meaning of the notation used.

The potential horizontal displacement of the structure due to soil compressibility (without any restriction due to structure stiffness) is obtained by summing the displacements calculated for each incremental layer on one side of the pipe. In a manner

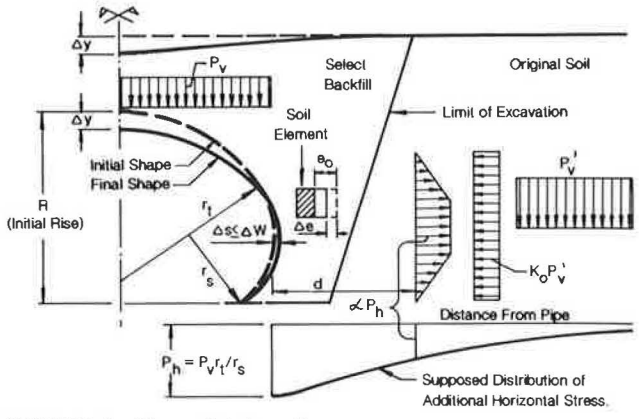

FIGURE 2 Pipe-soil interaction.

similar to the calculation of shallow foundation settlement, the summation is extended to a distance at which the additional stress in the soil generated by the pipe is less than 20 percent of the horizontal stress corresponding to the overburden pressure or to a maximum distance of 2.5 times the rise dimension, whichever is less. The following equations are used:

$$\Delta W = \Sigma[W\,\Delta e/(1 + e_o)] \tag{5}$$

$$\Delta e = C_c \log \frac{K_o P_v' + \alpha P_h}{K_o P_v'} \tag{6}$$

$$\alpha = 10^{(-0.45\ d/R)} \tag{7}$$

$$P_h = P_v\, r_t/r_s \tag{8}$$

where

W = initial width of an incremental layer (in.);
Δe = potential decrease in void ratio;
e_o = initial void ratio, not affected by the supplementary pressure induced by the structure;
C_c = compression index of the soil (backfill or original soil beyond the backfill);
K_o = the coefficient of earth pressure at rest;
P_v' = the effective overburden pressure at the level of calculation (i.e., approximately in the middle of the loaded area by the structure) (lb/in.^{2});
α = the influence of coefficient at a distance d (in.) from the structure corresponding to the middle of a given incremental layer (this parameter gives a variation of stresses close to the Boussinesq distribution for a trapezoidal loading);
P_h = the supplementary pressure on the side plates of the structure induced by the downward movement of the structure's crown (lb/in.^{2});
P_v = the total vertical pressure due to the soil dead load on the top of the structure, considered approximately equal to the product of the unit weight of the backfill and the depth of cover (lb/in.^{2});
R = rise of the structure (in.);
r_t = top radius of the structure (in.); and
r_s = side radius of the structure (in.).

A number of soil properties must be measured or estimated, both for the backfill or the original soil, including e_o, C_c, K_o, and unit weight. The SOILEVAL model gives the option of entering them as input data or estimating them on the basis of various levels of knowledge of soil condition.

Potential backfill and original soils were divided into seven categories, and the geotechnical parameters were estimated for each category. These parameters versus soil type have been built into the SOILEVAL program so that by choosing a soil category on the basis of simplified soils data, the appropriate geotechnical indexes are automatically used. If more precise data are available, the program allows direct input of the soil parameters. Table 3 gives the soil categories and the corresponding C_c values built into the model. The values are based on well-documented case histories and information given elsewhere (*14–18*).

The relative degree of compaction of the backfill (stiffness or hardness of original soil) is necessary for an evaluation of the potential movement of a structure. The SOILEVAL model

TABLE 3 COMPRESSIBILITY INDEX VALUES

CATEGORY OF SOIL	TYPE OF SOIL	ASTM D-2487 CLASS	FINES CONTENT (% < #200 SIEVE)	C_c Values For: LOOSE/SOFT MATERIAL ($C_{c,w}$)	MEDIUM ($C_{c,av}$)	DENSE/STIFF MATERIAL ($C_{c,b}$)
I	Gravel	GW,GP	<12	0.03	0.01	0.003
II	Silty/Clayey Gravel	GM,GC	12 – 50	0.05	0.02	0.008
III	Well-Graded Sand	SW	<12	0.06	0.02	0.007
IV	Poorly-Graded Sand	SP	<12	0.05	0.03	0.018
V	Silty/Clayey Sand	SM,SC	12 – 20 20.1 -30* 30.1– 50	0.06 0.16 0.33	0.03 0.08 0.17	0.015 0.040 0.088
VI	Silty Soils	ML,MH	>50	** (max 0.40)	0.007 (W_L–10) but min 0.05 and max 0.20	*** (min 0.025)
VII	Clayey Soils	CL,CH	>50	** (max 0.80)	0.007 (W_L–10) but min 0.10	*** (min 0.050)

NOTES: W_L is the liquid limit of the soil
* Default value is 30 when grain size distribution is not given
** $C_{c,w} = 2\ C_{c,av}$
*** $C_{c,b} = (C_{c,av})^2 / C_{c,w} = 0.5\ C_{c,av}$
If W_L is unknown, default values are used, which give:
$C_{c,av} = 0.10$ for Category VI soil
$C_{c,av} = 0.18$ for Category VII-a soil (lean clay)
$C_{c,av} = 0.35$ for Category VII-b soil (fat clay)

provides three approaches to estimating the average degree of compaction (denseness or hardness) of soils:

- Standard penetration test results,
- Direct measurements of soil density and moisture content, and
- Design requirements or inspection records that give the degree of compaction.

A parameter that is a measure of relative density, degree of compaction or stiffness, has been developed to allow a selection of soil parameters on the basis of the stiffness of the backfill. Figure 3 shows a relationship between various criteria that can be used in SOILEVAL for defining the denseness or the stiffness of the soil.

When the standard penetration test is used to characterize the soil condition, the equations in Table 4 are considered in the SOILEVAL program. The formulas in Table 4 are based on relationships suggested in literature (*19–22*). The equations shown in Table 4 have been built into the model to calculate P when the D_{50} and average standard penetration value N of the backfill are known.

The parameters e_o and K_o may be directly input into the model, if known. If they are not known, the model provides a value based on soil category and standard penetration values (or other parameters that given an estimate of the degree of compaction) as shown in Table 5.

Shape Factor

The shape factor establishes a relationship between movement of the crown and the movement of the sides of the structure. It is defined as the ratio between the decrease in rise (Δy) and the corresponding increase in half-span (or in half-chord at the midheight of the rise in the case of circular arches, where the span is measured at the foundation level). Simple geometrical relationships have been derived by considering small but finite deformations of the pipe when chord length may be considered a constant. The relationships are given in Table 6. A factor of 0.84 was derived empirically to correct the theoretical formula for small pipe-arches on the basis of statistical processing of more than 300 field measurements.

Empirical Constants A *and* B

The parameters A and B in Equation 4 were statistically determined from field measurements. Nine carefully monitored case histories were used to estimate these values. Table 7 gives the characteristics of the structures considered in the calibration.

The best fit between the measured settlements at the crown and the computed values was found for $A = 3.6$ psi and $B = 0.0015$. The graph in Figure 4 is drawn for the best fit so obtained.

Applicability of SOILEVAL Model

Equation 4 evaluates the deflection at the crown on the basis of three main parameters: (*a*) potential movement due to soil compressibility, (*b*) pipe stiffness, and (*c*) soil stiffness. Therefore, although the calibration is based exclusively on corrugated metal structure case histories, it is believed the model can be used for materials other than steel as well.

Case histories of pipes other than steel were not available in the literature; however, data in the literature were used to verify the applicability of the SOILEVAL model to nonmetalic structures.

Truss Pipe (*23*) makes available the results of deflection measurements on about 140 thermoplastic composite pipes used for gravity-flow sanitary sewer systems. The pipes consist of a double-wall system, with concentric inner and outer walls braced by a truss-type structure. The walls and the truss struc-

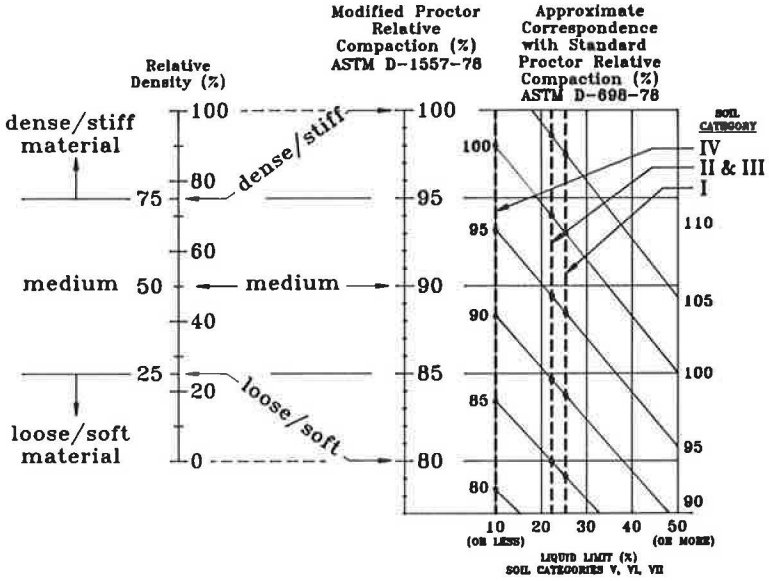

FIGURE 3 Approximate comparison between various estimates of denseness or stiffness.

TABLE 4 RELATIVE DENSITY/CONSISTENCY PARAMETER (P) FOR VARIOUS SOIL TYPES

SOIL CATEGORY	AVERAGE D_{50} (mm)	P: If P > 75, use P = 75 If P < 25, use P = 25
I	12.5	$43 \times \log [96.56 \times N \times D_{50}^{-0.284} \times (\sigma v')^{-0.56}]$
II	1.0	$43 \times \log [72.42 \times N \times D_{50}^{-0.284} \times (\sigma v')^{-0.56}]$
III	0.5	$43 \times \log [65.19 \times N \times D_{50}^{-0.284} \times (\sigma v')^{-0.56}]$
IV	0.3	$43 \times \log [60.36 \times N \times D_{50}^{-0.284} \times (\sigma v')^{-0.56}]$
V	0.15	$43 \times \log [54.32 \times N \times D_{50}^{-0.284} \times (\sigma v')^{-0.56}]$
VI	0.023	$43 \times \log [36.21 \times N \times D_{50}^{-0.284} \times (\sigma v')^{-0.56}]$
VII	0.007	$43 \times \log [24.14 \times N \times D_{50}^{-0.284} \times (\sigma v')^{-0.56}]$

Where:

- P = a parameter which is used in the same manner as the relative density for estimation of the compressibility index
- N = blows per foot in Standard Penetration Test
- D_{50} = mean diameter of soil particles (mm)
- $\sigma v'$ = effective overburden pressure at the test location (psf)

TABLE 5 INITIAL VOID RATIO FOR VARIOUS SOIL TYPES

SOIL CATEGORY	TYPE OF SOIL	ASTM D-2487 CLASS	STANDARD PENETRATION BLOW COUNT, N	VOID RATIO, e_o	K_o FOR: BACKFILL	K_o FOR: ORIGINAL SOIL
I & II	Gravels	GW,GP	≤ 10	0.6	0.4	0.4
		GM,GC	11-30	0.5	0.5	0.45
			≥ 31	0.4	0.6	0.5
III & IV	Sands	SW,SP	≤ 10	0.7	0.4	0.4
			11-30	0.55	0.5	0.45
			≥ 31	0.4	0.6	0.5
V	Silty/Clayey	SM,SC	≤ 10	0.8		
	Sand		11-30	0.6	0.6	0.5
			≥ 31	0.45		
VI	Silty Soils	ML,MH	≤ 5	0.9		
			6-15	0.7	0.6	0.5
			≥ 16	0.5		
VII-a	Clayey Soils,	CL	≤ 5	1.0		
	W_L < 50		6-10	0.8	0.7	0.6
	(Lean)		≥ 11	0.6		
VII-b	Clayey Soils,	CH	≤ 5	1.6		
	W_L ≥ 50		6-10	1.1	0.7	0.6
	(Fat)		≥ 11	0.7		

ture are formed of a single thermoplastic extrusion of either polyvinyl chloride or acrylonitrile butadiene styrene. The composite pipe stiffness defined by the ratio EI/r^3 is about 30 psi.

Although little information was available about the backfill soil condition, the trench dimensions, the degree of compaction, or the soil beyond the backfill, an estimate of the deflection using SOILEVAL was possible. The agreement between calculated and measured data was considered satisfactory (*24*).

Twenty-eight case histories of high-density polyethylene pipes reported by Chua and Petroff (*25*) were also evaluated. In almost all cases the predicted maximum deflections after complete consolidation of the soil were slightly greater than the maximum observed deflections, which also supports the validity of the model in these conditions (*26*).

TABLE 6 SUMMARY OF SHAPE FACTORS FOR VARIOUS TYPES OF PIPES

PIPE SHAPE	CHARACTERISTICS	SHAPE FACTOR	RANGE, (AVERAGE VALUE) FOR ARMCO/AISI PIPES	
Roundpipe	$S = R$	2.0		(2.0)
Superspan Pipearch	$S \geq 20$ Feet	$0.5\left(\frac{S}{R-R_T}+\frac{S}{R_T}\right)$	2.97–4.90	(4.0)
Small Pipe-Arch	$S < 20$ Feet	$0.5\left(\frac{0.84\,S}{R-R_T}+\frac{S}{R_T}\right)$	2.53–3.99	(3.3)
Underpass	$R_T > R_B$	$0.5\left(\frac{S}{R_B}+\frac{S}{R_T}\right)$	2.28–2.60	(2.4)
Multi-Plate Arch	$R<\frac{S_B}{2}$	$\sqrt{2\left(\frac{S_B}{R}\right)^2+4}-\frac{S_B}{R}$	1.42-2.72	(2.0)
Vertical Ellipse	$R > S$	$\frac{2S}{R}$	1.79-1.82	(1.8)
Horizontal Ellipse	$S > R$	$\frac{2S}{R}$	2.70-3.82	(3.1)
Low Profile Arch	$R_T \cong 0.9R$	$0.5\left(\frac{S-S_B}{R-R_T}+\frac{S}{R_T}\right)$	1.46-1.83	(1.7)
High Profile Arch	$R_T \cong 0.6R$	$0.5\left(\frac{S-S_B}{R-R_T}+\frac{S}{R_T}\right)$	1.61–1.95	(1.9)
Pear	$R_B > R_T$	$0.5\left(\frac{S}{R_B}+\frac{S}{R-R_B}\right)$	1.88–2.30	(2.1)

Notations in Table 6:

S = Span; R = Rise; S_B = Bottom Span; R_T = Top Rise; $R_B = R - R_T$ = Bottom Rise; r_t = Top Radius

TABLE 7 CHARACTERISTICS OF CORRUGATED METAL STRUCTURES CONSIDERED IN THE CALIBRATION

Case History No.	Type of Structure	Span (ft - in)	Rise (ft - in)	Gage No.	Height of Cover (ft)	Soil Category: Backfill	Soil Category: Original Soil
1	Pipearch	11' - 7"	7' - 5"	12	7.6	V	VII-a
2	Ellipse	29' - 5"	19' - 11"	5	13.5	V	N/A*
3	Pipearch	7' - 11"	5' - 7"	7	2.1	V	V
4	Pipearch	10' - 8"	6' - 11"	8	4.5	VI	V
5	Pipearch	10' - 8"	6' - 11"	10	3.7	VII-a	VII-a
6	High Profile	27' - 3"	15' - 5"	5	11.5	VII-a	Rock
7	High Profile	27' - 3"	15' - 5"	5	29.0	VII-a	Rock
8	Pipearch	10' - 8"	6' - 11"	7	9.3	V	V
9	Pipearch	10' - 8"	6' - 11"	7	9.4	V	V

*Bridge Abutments

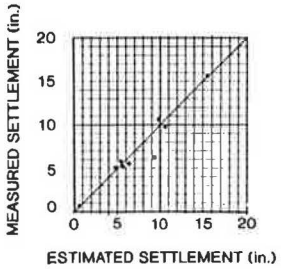

Case History Number	Measured Settlement at Crown (in)	Estimated Settlement at Crown (in)
1	7.7	8.0
2	9.8	10.1
3	1.3	1.1
4	5.0	4.9
5	5.4	7.1
6	11.3	11.0
7	16.7	16.3
8	6.1	5.3
9	5.8	5.7

FIGURE 4 Model calibration: measured versus estimated displacement at crown.

CONCLUSIONS

1. MULTSPAN provides a simplified method of evaluating structures on an annual basis so that problems can be anticipated long before they occur and remedial action can be taken.

2. SOILEVAL provides a simplified semiempirical method of predicting movement of flexible buried structures. The program has been found useful in predicting future movements of pipes that have experienced some degree of movement.

3. SOILEVAL can be used as a design tool to design the backfill or the structure given a certain type of backfill. It can also be used to design the width of the select backfill.

REFERENCES

1. *MULTSPAN-SOILEVAL Users Manual, An Analytical Program To Evaluate Corrugated Metal Pipes*. Bowser-Morner Associates, Inc., Dayton, Ohio, 1986 (revised 1990).
2. A. K. Howard. Modulus of Soil Reaction Values for Buried Flexible Pipes. *Journal of the Geotechnical Engineering Division*, ASCE, Vol. 103, No. GT1, Jan. 1977, pp. 33–43.
3. R. K. Watkins and M. G. Spangler. Some Characteristics of the Modulus of Passive Resistance of Soil: A Study in Similitude. *HRB Proc.*, Vol. 37, 1958, pp. 576–583.
4. R. K. Watkins and R. P. Moser. *The Structural Performance of Buried Corrugated Steel Pipes*. Utah State University, Logan, and American Iron and Steel Institute, Washington, D.C., 1969.
5. *Steel Pipe Design and Installation*. AWWA M11, Manual of Water Supply Practices. American Water Works Association, 1969.
6. R. K. Watkins, E. Szpak, and W. B. Allman. *Structural Design of Polyethylene Pipes Subjected to External Loads*. Engineering Experiment Station, Utah State University, Logan, 1974.
7. *Handbook of PVC Pipe Design and Construction*. Uni-Bell PVC Pipe Association, Dallas, Tex., 1983.
8. *AWWA Standard for Fiberglass Pressure Pipe*. ANSI/AWWA C 950-88. American Water Works Association, Denver, Colo., 1989.
9. J. D. Hartley and J. M. Duncan. E′ and Its Variation with Depth. *Journal of Transportation Engineering*, ASCE Vol. 113, No. 5, Sept. 1987, pp. 538–553.
10. M. G. Katona, J. M. Smith, R. S. Odello, and J. R. Allgood. *CANDE—A Modern Approach for the Structural Design and Analysis of Buried Culverts*. Report FHWA-RD-77-5. FHWA, U.S. Department of Transportation, 1976.
11. J. M. Duncan. Soil-Culvert Interaction Method for Design of Culverts. In *Transportation Research Record 678*, TRB, National Research Council, Washington, D.C., 1978, pp. 53–59.
12. R. B. Seed and J. M. Duncan. *SSCOMP: A Finite Element Analysis Program for Evaluation of Soil-Structure Interaction and Compaction Effects*. Geotechnical Engineering Research Report UCB/GT/84-02. University of California, Berkeley, 1984.
13. D. C. Cowherd, S. M. Thrasher, V. G. Perlea, and J. O. Hurd. Actual and Predicted Behavior of Large Metal Culverts. *Proc., Second International Conference on Case Histories in Geotechnical Engineering*, St. Louis, Mo., Vol. 2, 1988, pp. 1,471–1,476.
14. K. Terzaghi and R. B. Peck. *Soil Mechanics in Engineering Practice*. John Wiley and Sons, Inc., New York, 1967.
15. B. K. Hough. *Basic Soil Engineering*. Ronald Press Co., 1969.
16. D. F. McCarthy. *Essentials of Soil Mechanics and Foundations*. Reston Publishing Co., 1977.
17. R. B. Peck, W. E. Hanson, and T. H. Thornburn. *Foundation Engineering*. John Wiley and Sons, Inc. New York, 1974.
18. R. J. Bally and V. G. Perlea. *Embankment Dams and Levees on Weak Foundations Soils* (in Romanian). Ed Ceres, Bucharest, Romania, 1983.
19. J. W. Searle. The Interpretation of Begemann Friction Jacket Cone Results To Give Soil Types and Design Parameters. *Proc., Seventh European Conference on Soil Mechanics and Foundation Engineering*, Brighton, England, Vol. 2, 1979, pp. 265–270.
20. J. H. Schmertmann. Static Cone To Compute Static Settlement Over Sand. *Journal of the Soil Mechanics and Foundation Engineering Division*, ASCE , Vol. 96, No. SM3, March 1979, pp. 1,011–1,043.
21. P. K. Robertson, R. G. Campanella, and A. Wightman. SPT-CPT Correlations. *Journal of Geotechnical Engineering*, ASCE, Vol. 109, No. 11, Nov. 1983, pp. 1,449–1,459.
22. Z. V. Solymar and D. J. Reed. Comparison Between In-Situ Test Results. *Proc., ASCE Conference, Use of In-Situ Tests in Geotechnical Engineering*, Blacksburg, Va., 1986, pp. 1,236–1,248.
23. *Truss Pipe*. Contech Construction Products, Inc., Middletown, Ohio, 1988.
24. D. C. Cowherd and V. G. Perlea. A Model for Predicting Movements of Large Diameter Buried Flexible Conduits. *Proc., International Symposium on Unique Underground Structures*, Denver, Colo., Vol. 1, 1990, pp. 9-1–9-20.
25. K. M. Chua and L. J. Petroff. Predicted Performance of Large Diameter Buried Flexible Pipes: Learning from Case Histories. *Proc., Second International Conference on Case Histories in Geotechnical Engineering*, St. Louis, Mo., Vol. 2, 1988, pp. 1,417–1,420.
26. V. G. Perlea. Discussion on the Paper Predicted Performance of Large Diameter Buried Flexible Pipes: Learning from Case Histories. *Proc., Second International Conference on Case Histories in Geotechnical Engineering*, St. Louis, Mo., Vol. 3, 1988, pp. 1,779–1,780.

Publication of this paper sponsored by Committee on Culverts and Hydraulic Structures.

Evaluation of Shear Plates and Grouted Shear Key Joint Performance of a Three-Sided Precast Culvert

BRYAN E. LITTLE, THEODORE A. MIZE, AND ROBERT J. BAILEY

The effectiveness of shear plates and a grouted shear key joint system in providing load transfer across three-sided bridge sections is evaluated. Because of the flat-top culvert geometry accommodating pavement directly on top of the sections, it was important to determine the structure's response to differential deflections between adjacent sections when subjected to live loading. Prompted by research that evaluated shear plates on tongue-and-groove jointed box sections with spans up to 12 ft, the project focused on a three-sided structure with a substantially longer span (30 ft) and a grouted shear key joint system. Deflection results are presented for various combinations of shear plates and the keyed joint when subjected to simulated live loading. The results indicate that the grouted shear key joint system is an effective means of distributing the load between the precast sections. The addition of shear plates does not enhance the structural response of the grouted structures. Shear plates alone are ineffective.

In today's culvert and small bridge replacement markets, three-sided structures have been successfully installed under a variety of conditions in several parts of the country. The three-sided bridge system is a rigid frame design that incorporates a flat-top geometry (see Figure 1). By providing a flat-top structure, the system allows pavement to be placed directly on top of the structure, thereby decreasing project time, backfill requirements, and potential for differential backfill settlement. Before testing of the structure, the policy associated with the system was to provide a grouted shear key joint accompanied by shear plates (see Figure 1) when combinations of long spans (more than 16 ft) and shallow earth covers (0 to 2 ft) were encountered. In a load test on an installed structure the following two issues were investigated:

1. How does the system behave structurally when a live load is applied?
2. To what degree do grouted, keyed joints or shear plates (or both) enhance the structure with respect to resisting loads?

The design loading for this bridge was AASHTO HS20-44. For design purposes, this required less steel than for the Interstate loading. The tension steel provided in the bottom of the bridge deck (As2) was between the requirement for an HS20-44 and an Interstate load, as shown in the following (units are in.^{2}/ft):

Required for HS20-44 loading: 0.901
Provided: 0.960
Required for Interstate loading: 1.048

Therefore, the Interstate load is a more rigorous test because of the "under steel" with respect to the Interstate design.

TEST PROGRAM

A three-sided bridge structure was identified for the load test in Bloomfield Township, Michigan. The structure contained 35 linear ft (seven sections of 5 ft each) of 30-ft span × 7-ft rise with a 30-degree left forward skew. The sections were installed on two separate cast-in-place footings supplied by the contractor. The backfill was placed to the top of the structure and was ready for testing to begin. A test procedure was developed and sent to an independent licensed engineer for review.

The preliminary steps of the test procedure were as follows:

1. A hydraulic jack was calibrated to provide a chart of applied load in pounds versus gauge readings of hydraulic fluid pressure in psi.
2. Dial indicators with adjustable support rods, 8W24 beams, 2- × 10- × 20-in. wood bearings (simulated wheel loadings) and steel plates were procured.
3. The loaded truck was driven into position and deflection readings from the truck wheel loads were recorded.
4. The hydraulic jack was activated and load was applied in increments of 7,800 lb to a maximum of 31,200 lb, representing the wheel load with 30 percent impact for the Interstate alternate axle load as presented in ASTM C850. Deflection readings were taken from each of the dial indicators at each increment.
5. Steps 3 and 4 were performed for each of four test conditions.

Load Tests 1 and 2

Deflection Tests 1 and 2 were conducted with the joint conditions as described in Figure 2. In Test 1 the deflection was measured for a "butt type" joint (no grout and no shear plates). In Test 2 the deflection was measured on the same joint with the shear plates in place.

Technology Division, Price Brothers Company, 367 West Second Street, Dayton, Ohio 45402.

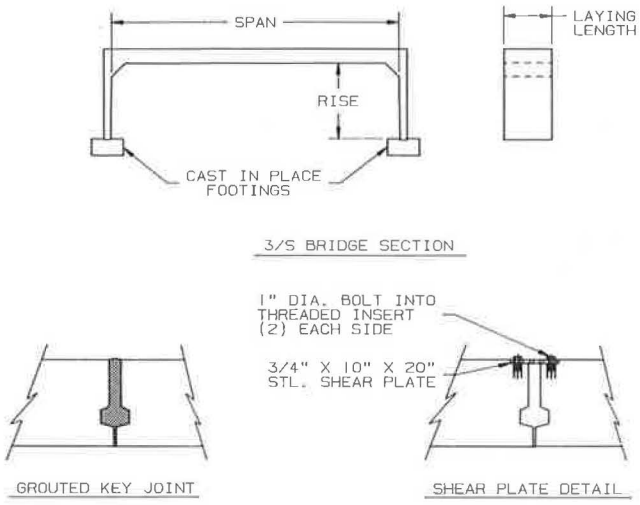

FIGURE 1 Three-sided bridge system.

The tests were set up in accordance with Figures 2 and 3. All dial indicator readings were taken before the positioning of the truck. This was the zero reading.

After the truck was in position, measurements were taken to record the location of the wheels relative to the applied test load. Figures 4 through 6 show the test arrangement for Tests 1 and 2. The load was applied according to the procedure described, and the deflections, as determined by the dial indicators, were recorded at each load increment. After Test 2 was completed both of the ungrouted joints were grouted.

Load Tests 3 and 4

Tests 3 and 4 were conducted in the same manner, except the load was positioned at the location shown in Figure 7. Test 3 was conducted with the grout and shear plates in place. Test 4 was conducted on the grouted joint without shear plates.

TEST RESULTS

Load-deflection results for the applied jack load (Figure 3) are given for the four joint conditions in Tables 1 through 4. The tables do not include the deflections due to the truck wheel loads. The deflections corresponding to the truck wheel loads were 0.028, 0.015, and 0.008 in., respectively, at Dial Indicators 1, 2, and 3 for Tests 1 and 2. For Tests 3 and 4, the corresponding deflections were 0.010, 0.012, and 0.012 in. As the load was applied by jacking the truck up, the truck wheel loads were reduced somewhat. Therefore, the deflections due to the truck wheels were reduced. The deflections due to these truck wheel loads were considered negligible in the analysis.

The load-deflection results corrected for apparent bridge settlement are shown in Figures 8 and 9. The test details are shown in Figures 4 through 6. The differential deflections across the joint versus jack load are shown in Figure 10.

DISCUSSION OF RESULTS

For each joint condition presented in Tables 1 through 4, a maximum load of 31,200 lb was applied in 7,800-lb increments. This load was applied, released, and reapplied so that deflections due to bridge settlement could be established by taking "no load" dial indicator readings after the first load cycle. In this manner dial indicator readings were corrected for apparent bridge settlement, and the results are presented in Figures 8 and 9. Analysis of Figure 8 indicates that deflections at Dial Indicator 2 (loaded side of joint) were greatest in Test 1 (ungrouted joint with no shear plates). Deflections at this dial indicator were reduced the most in Tests 3 and 4 (grouted joint with and without shear plates, respectively). Analysis of deflections at Dial Indicator 3 (unloaded side of joint) in Figure 9 indicate that deflections increased progressively from Test 1 (ungrouted and no shear plate) to Test 3 and 4 conditions. Results for Tests 3 and 4 were iden-

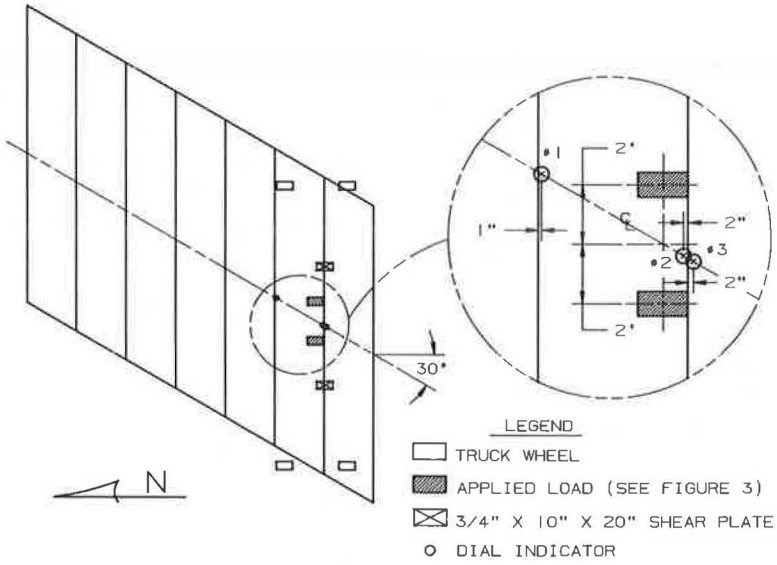

FIGURE 2 Test 1 (ungrouted without plates) and Test 2 (ungrouted with plates).

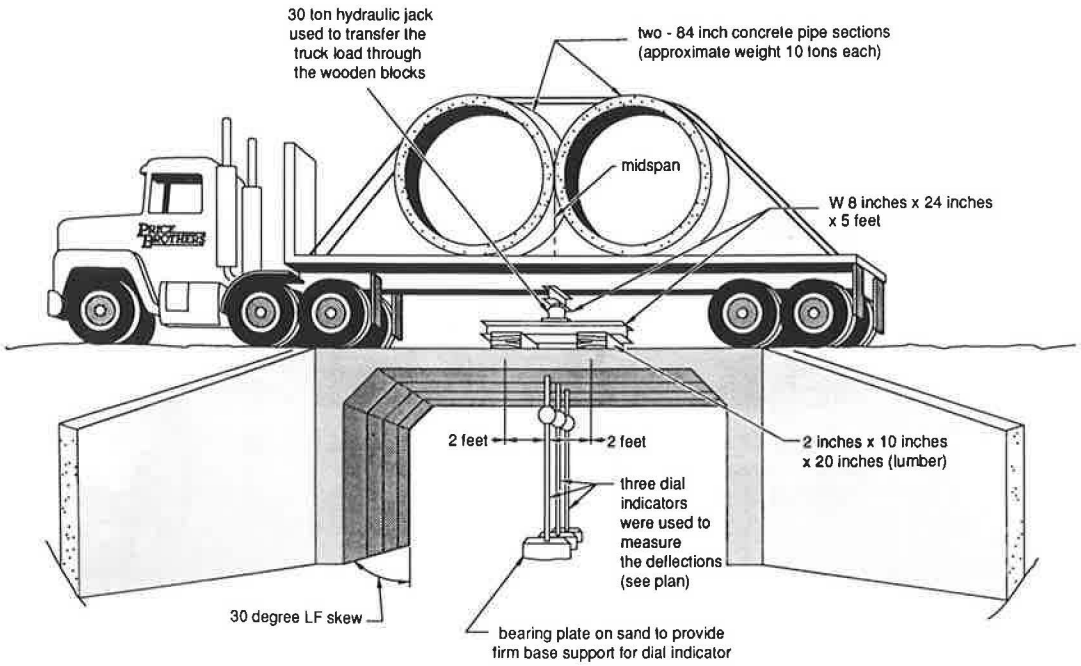

FIGURE 3 Load test arrangement—diagram.

FIGURE 4 Load-deflection test arrangement for three-sided bridge.

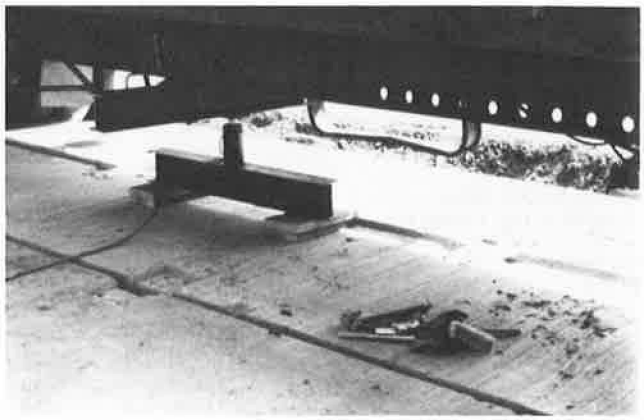

FIGURE 5 Load was applied by hydraulic jack in 7,800-lb increments to a maximum load of 31,200 lb. Load was distributed on the 10- × 20-in. bearing areas at 4-ft centers to simulate truck wheel bearing areas. The 31,200-lb load is equivalent to the ASTM C850 Interstate alternate axle loading.

FIGURE 6 Deflections were obtained by three dial indicators. Locations relative to the load points are indicated in Figures 1, 2, and 7.

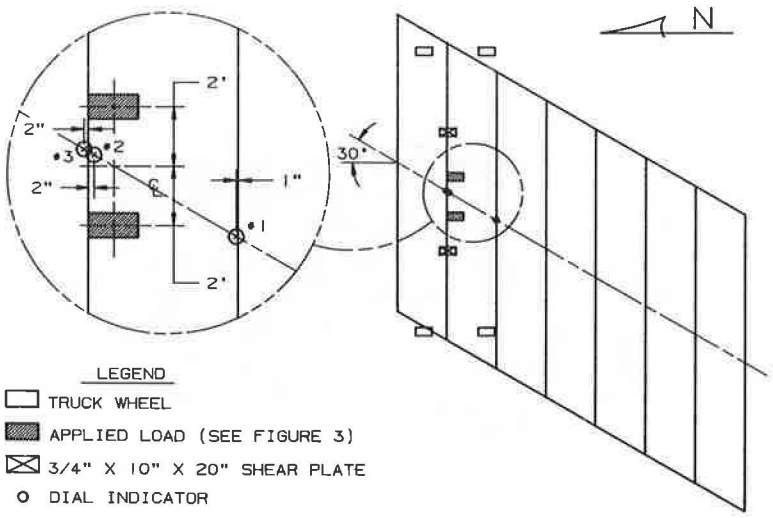

FIGURE 7 Test 3 (grouted with plates) and Test 4 (grouted without plates).

TABLE 1 THREE-SIDED BRIDGE LOAD TEST—UNGROUTED WITHOUT SHEAR PLATES (TEST 1)

Jack Load (lbs.)	Deflection (inches) Dial # 1	Dial # 2	Dial # 3
0	0	0	0
7800	.017	.030	.001
15600	.037	.065	0
23400	.074	.110	-.001
31200	.121	.166	-.001
0	.020	.017	-.003
7800	.037	.048	-.002
15600	.058	.083	-.004
23400	.085	.122	-.004
31200	.123	.170	-.004

For load and dial indicator locations, see Figures 2 & 3.

TABLE 2 THREE-SIDED BRIDGE LOAD TEST—UNGROUTED WITH SHEAR PLATES (TEST 2)

Jack Load (lbs.)	Deflection (inches) Dial # 1	Dial # 2	Dial # 3
0	0	0	0
7800	.016	.027	.004
15600	.035	.056	.008
23400	.053	.090	.012
31200	.080	.128	.016
0	0	.005	.001
7800	.019	.033	.002
15600	.036	.063	.006
23400	.055	.094	.010
31200	.079	.127	.015

For load and dial indicator locations, see Figures 2 & 3.

TABLE 3 THREE-SIDED BRIDGE LOAD TEST—GROUTED WITH SHEAR PLATES (TEST 3)

Jack Load (lbs.)	Deflection (inches) Dial # 1	Dial # 2	Dial # 3
0	0	0	0
7800	.008	.013	.013
15600	.017	.028	.027
23400	.027	.042	.041
31200	.034	.056	.054
0	0	.002	.001
7800	.009	.015	.013
15600	.018	.030	.028
23400	.027	.044	.042
31200	.035	.057	.054

For load and dial indicator locations, see Figures 3 & 7.

TABLE 4 THREE-SIDED BRIDGE LOAD TEST—GROUTED WITHOUT SHEAR PLATES (TEST 4)

Jack Load (lbs.)	Deflection (inches) Dial # 1	Dial # 2	Dial # 3
0	0	0	0
7800	.010	.014	.014
15600	.018	.028	.028
23400	.027	.042	.042
31200	.035	.055	.054
0	.001	.001	0
7800	.010	.014	.014
15600	.018	.029	.028
23400	.027	.042	.041
31200	.035	.055	.054

For load and dial indicator locations, see Figures 3 & 7.

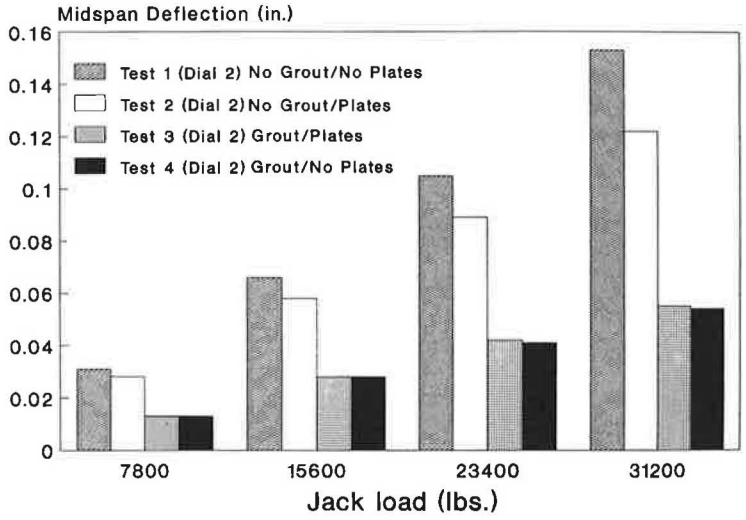

FIGURE 8 Load versus deflection (loaded side of joint).

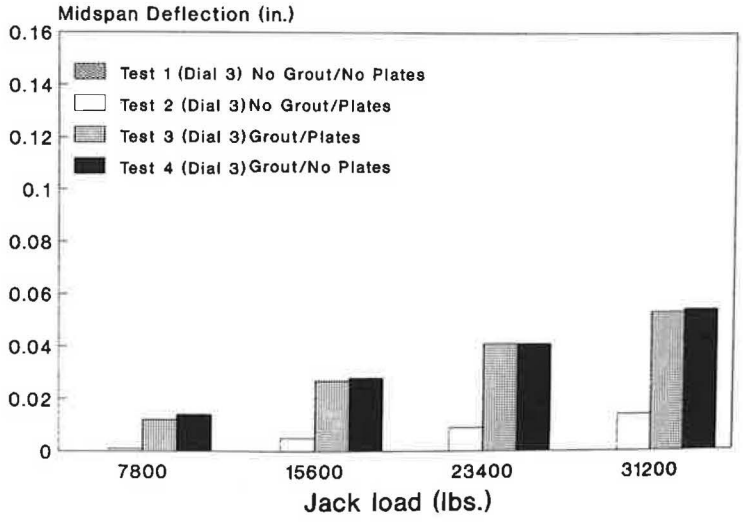

FIGURE 9 Load versus deflection (unloaded side of joint).

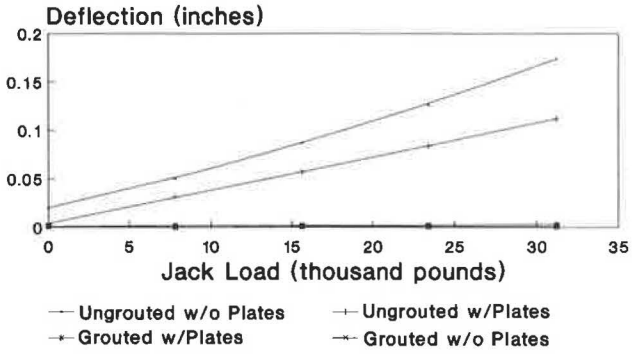

FIGURE 10 Jack load versus differential deflection across joint (differential deflection = Dial 2 − Dial 3).

tical for all practical purposes and indicated the greatest amount of distribution of load across the joint (see Figure 10). In fact, the load is completely transferred across the joint for this condition, because the deflections are the same on the loaded and unloaded side of the joint. The results of Tests 3 and 4 indicate that the grout, alone, completely transfers the load across the joint, and shear plates are redundant. In essence, the shear plates can be eliminated.

This project is typical of many in Michigan and throughout Ohio. The yardstick for total deflection used by the Ohio Department of Transportation is $L/800$. This corresponds to a deflection of 0.45 in. As indicated in Tables 1 through 4, these deflections were well under the limit of $L/800$.

CONCLUSIONS

1. The tests indicate that, both individually and combined, shear plates and the grouted keyway transfer load across the joint.
2. The grouted keyway alone provided complete load transfer across the joint.
3. Shear plates alone are ineffective because they only provided minimal load transfer.
4. By comparison, the grouted keyway was much more effective than the shear plates alone, and the difference in joint performance between the grouted joint and the grouted joint combined with shear plates was minimal.

RECOMMENDATIONS

1. The use of the grouted keyway joint should be continued to safeguard against reflective pavement cracking due to differential deflection of the bridge sections under load.
2. The use of shear plates at grouted joints should only be considered for special end treatment (headwalls, etc.) to tie the end pieces to the body of the structure.

Publication of this paper sponsored by Committee on Culverts and Hydraulic Structures.

Microcomputer-Based Culvert Ranking System

CARL E. KURT AND GARTH W. MCNICHOL

The efficient use of limited resources is a problem that faces every local government. These governments have large investments in local roadways, bridges, and culverts. No management system has been developed for culvert systems. The development of a ranking system for culverts found on local agency systems is presented. Cost models are developed to identify major contributors to user and agency costs. On the basis of the cost models, a working dBase III Plus™ microcomputer software package was developed to evaluate culvert systems of local agencies. The results of the proposed system were compared with existing culvert replacement strategies with good agreement.

Culverts are an integral part of any highway system. The enormous public investment in these structures demands that they be properly managed and receive timely and cost-effective maintenance, rehabilitation, and replacement. At present, pavement and bridge management systems have been developed for roadway and bridge systems, respectively. In most local agencies there are more culverts than bridges. However, culvert systems, by their nature, are significantly different from pavement or bridge systems. No management system has been developed for culvert systems.

A true culvert management system will be complex. It must be able to perform a complete functional evaluation of each culvert and identify the optimum options for maintenance, rehabilitation, or replacement. Significant resources will be required to advance current technologies to this level; however, the long-term savings in public costs would justify the expense.

The first step toward a comprehensive culvert management system is the development of a system to give a relative ranking to each culvert in the agency's system. The methodology for developing such a system is presented. Whereas the approaches used on existing bridge management systems are evaluated, cost models for culverts are developed to identify major contributors to user and, for some situations, agency costs. The methodology is used to develop a computer software system that uses a data base management system. To demonstrate the applicability of the data base system, microcomputer, and the ranking system, a culvert system of a local agency is evaluated. The results of the proposed system are compared with existing culvert replacement strategies.

LITERATURE REVIEW

After a review of the literature, it was determined that little information has been developed and reported for incorporation into a culvert management or ranking system. Culverts have properties similar to bridges, but they also have significant differences. Several bridge management systems have been developed. Because of the similarities between management of culverts and bridges, a brief discussion of the development of bridge management systems is presented.

A management system could be defined generally as any system or series of engineering and management functions that, taken together, result in the actions necessary to manage the system. For bridges or culverts, the actions may include evaluation of problems, selection of improvement projects, and the programming and initiation of specific projects.

Alternatively, the actions could be inventory and inspection of culverts or bridges, evaluation of priorities, selection and programming of projects, and improvement of structures.

In the United States, the approach taken to culvert or bridge management ranges from informal to formal. Most bridge management system (BMS) developers encourage development of a comprehensive system that tends toward the formal end of the spectrum. These management systems are more likely to result in sound, cost-effective decisions. They provide formal procedures to ensure consistency in the decision-making process; analytical models to evaluate needs, priorities, and options; and an adequate data base to support the analytical models. The primary objective of most management systems is to assist the program manager in setting the needs for resources and to use the resources available in a cost-effective manner while meeting current and future needs.

A bridge ranking system was developed in Kansas using a modified version of the Delphi technique (*1*), which was originally developed by the Rand Corporation in the late 1940s for arriving at a consensus of experts. The Kansas Department of Transportation (KDOT) organized a Delphi panel consisting of 25 key individuals from KDOT (average length of service of 26 years) to make the necessary assessments for development of priority-ranking formulas. This system may work well for large agencies, but a local agency usually has only one or two experts. Thus, the approach may not be applicable to the implementation of a bridge or culvert management system by a local agency.

One of the first formulations of the level-of-service concept for traffic was accomplished at North Carolina State University by Johnston and Zia (*2*) for the North Carolina Department of Transportation. The purpose of the research was to establish level-of-service requirements to evaluate the adequacy of North Carolina bridges. Level-of-service goals were set for various bridge parameters such as load capacity, deck width, and vertical clearances. The goals are target values for selected bridge characteristics. They were varied on the basis

C. E. Kurt, University of Kansas, Lawrence, Kans. 66045. G. W. McNichol, Douglas County Public Works, Lawrence, Kans. 66044.

of highway functional classification, traffic volume, and other factors. The goals were set with the recognition that widely varying traffic needs exist throughout the highway system and that many bridges on local roads can adequately serve traffic needs with lower load capacities and geometric standards than would be necessary for bridges on heavily traveled highways. The degree to which a bridge is deficient can be measured by comparing bridge characteristics with level-of-service goals. Shortfalls from the goals determine the type and extent of improvement needed. The shortfalls are useful for comparing bridge needs and setting improvement priorities.

Several versions of the early North Carolina system were reviewed, including those of Nebraska (*3*), Virginia (*4*), and Pennsylvania (*5*). These systems were essentially modifications of the North Carolina system except that each state varied weighting factors to meet its own criteria.

Several BMSs were studied before the current culvert management system—CMS—was developed. One was that of Hudson et al. (*6*), which reviewed the management needs associated with the nation's bridges and investigated practices of selected state departments of transportation in bridge management activities at the network level. This background provided the framework for a generic BMS followed by a conceptual model BMS. This system is currently being developed for bridges but not culverts.

Later versions of BMSs have begun to incorporate life cycle cost and incremental benefit-cost analysis (*7*). The objective of these analyses is to identify projects that produce benefits greatly in excess of their cost. Deterioration models are being studied to predict deterioration rates of new bridges or bridges that receive various rehabilitation or maintenance treatments (*8*). These methods may provide some advantages for determining which projects would maximize benefits; however, cost data are required for a large number of alternatives.

In conclusion, no BMS can be directly applied to culverts because BMSs do not consider the hydraulic function of culverts, most BMSs are not microcomputer oriented, and other BMSs require large resources of experienced people (e.g., Delphi) or data.

RANKING FORMULA DEVELOPMENT

A methodology is presented for developing the ranking formula for use in a culvert management system. The level-of-service goal concept, originally developed by Johnston and Zia (*2*) for BMSs, was selected as the basis for the proposed culvert management system. Level-of-service goals are set for each culvert parameter. The goals are target values used to assess culvert adequacy and may vary on the basis of highway functional classification, traffic volume, and other factors. When a culvert parameter fails to meet its service goal, a deficiency is incurred. The equation describing this relationship is

$$\text{Deficiency points} = \text{actual condition} - \text{goal condition} \quad (1)$$

Four priority-ranking formulas were developed for use in the culvert management system. Development of the formulas involved identification of factors that control user and agency costs: load capacity, hydraulic capacity, width deficiency, and maintenance costs. The factors were selected on the basis of experience and discussions with engineers and supervisors.

The objective of the priority-ranking formulas is to develop a numerical value for each culvert in the system. The priority-ranking formulas are a function of culvert parameters. The simplest have the following form:

$$\text{Deficiency points} = \sum K_i f_i(a, b, c, d) \quad (2)$$

where

K_i = weighting factors,
$f_i(a, b, c, d)$ = priority-ranking formulas, and
a, b, c, d = culvert parameters.

Before the ranking formula can be implemented, parameters must be collected for all culverts in the system. If the approach is to work, all culvert parameters must be accurate and consistent.

The weighting factors provide a means to give relative importance to each of the ranking formulas. They also provide flexibility and permit modification of the system to consider local conditions. For example, if narrow culverts are important local considerations, the weighting factor for the width deficiency ranking formula may be increased.

Before the analytical procedures used in the development of the four priority-ranking formulas are presented, the development of a traffic model must be presented. Because one of the goals of the project was to make the system applicable to local systems, the traffic profile selected was based on a traffic weight study conducted by KDOT (*9*, pp. 33–36). The data at seven rural stations were considered. The study provided data on the distribution by type and weight of all traffic measured. There were 29 combinations of loaded and empty vehicles. Operating costs were assigned to each vehicle type on the basis of estimated 1988 costs. A more detailed discussion of the traffic and cost model used is given elsewhere (*10*).

LOAD CAPACITY RANKING FORMULA

User costs are associated with a culvert with a load capacity less than the goal because the user must drive extra miles around the posted culvert. The costs occur every day that the deficiency remains. To establish the load capacity ranking formula, the cost model previously discussed was developed to relate user cost to insufficient load capacity.

A linear regression model was used to represent user costs for culvert capacities between 3 and 37 tons. The structure was assumed to be closed if the service load dropped below 3 tons. The equation defining the relationship between unit user cost (in dollars) per day-mile-ADT and insufficient load capacity is

$$\text{Cost/day-mile-ADT} = (-0.0029 * \text{SV}) + 0.1053 \quad (3)$$

When the load capacity cost model is substituted into the deficiency points equation, the load capacity ranking formula becomes

$$\text{CP} = \text{WC} * (\text{CG} - \text{SV})/345 * \text{ADT} * \text{DL} \quad (4)$$

where

CP = capacity priority,
WC = load capacity weighting factor,
CG = capacity goal (tons),
SV = single vehicle posting (tons),
ADT = average daily traffic, and
DL = detour length (mi).

CP may not be less than 0.

Hydraulic Capacity Ranking Formula

User costs are associated with the hydraulic capacity of a culvert because of the extra mileage accumulated during detour around a flooded culvert. Hydraulic-related costs occur only on flood days. A culvert with insufficient hydraulic capacity may result in recurring agency costs due to flood damage to the roadway, structure, or adjacent property. The following cost model was developed for user and agency costs due to insufficient hydraulic capacity.

The percentage of ADT affected by insufficient hydraulic capacity was established from the same vehicle data used to develop the load capacity ranking formula. In this case, if a culvert cannot support a vehicle of a particular weight, then, theoretically, the vehicle should not be affected by flooding of the culvert. In this way, each detoured vehicle is counted only once for a culvert deficiency. On the basis of this assumption, the percentage of ADT affected by insufficient hydraulic capacity is a function of load capacity.

The user costs for each vehicle type developed for the load capacity ranking formula were used to develop a cost model to describe hydraulic-related user costs. An operating cost was assigned to each type of vehicle affected. An exponential curve was developed to best fit the data and relate the unit user cost per day-mile-ADT and insufficient hydraulic capacity. The relationship is

$$\text{Cost/day-mile-ADT} = 0.062 * (SV - 3)^{0.30} \quad (5)$$

where SV is as previously defined.

Agency costs considered in this ranking formula are the cost per flood per day and the number of flood days per year. The average cost per flood is the cost, to the agency, of flood damage to the roadway, structure, and adjacent property at a particular culvert site. The number of flood days per year is the number of days each year a particular culvert site floods. When the hydraulic capacity cost model is substituted into the deficiency points equation, the hydraulic ranking formula becomes

$$HP = WH * (NF - NG)/365 * [(KF * ADT * DLh) + \$/\text{flood}] \quad (6)$$

where

HP = hydraulic priority,
WH = hydraulic capacity weighting factor,
NF = number of flood days per year,
NG = goal for number of flood days per year,
$KF = 0.062 * (SV - 3)^{0.30}$,
DLh = detour length due to flooding (mi), and
\$/flood = average damage cost per flood day.

HP may not be less than 0.

Width Deficiency Ranking Formula

User costs related to the width deficiency of a culvert result from accidents. Width-related costs occur every day until the deficiency is corrected. Narrow culverts contribute to single-vehicle collisions involving pedestrians or the culvert structure and to multiple-vehicle collisions involving approaching or passing vehicles. Resulting user costs include property damage, injury, and loss of life. Agency costs include repair of structural damage and higher insurance premiums. To establish the width deficiency ranking formula, a cost model was developed to relate cost to insufficient culvert width.

The first step was to establish a relationship between culvert with deficiency and related accidents. A study of bridge width and safety (*11*) provided information to derive a relationship between the number of accidents per million vehicles and the relative bridge width. The relative bridge width is the difference between the traveled-way width and the bridge width. It was believed that this best represents the situations found at narrow, rural culvert sites. The equation is

$$\text{Number of accidents per million vehicles} = (0.0022 * WD^2) - (0.061 * WD) + 0.5 \quad (7)$$

where WD is the relative bridge width (ft).

The traveled-way width is the combined width of the lanes only crossing the structure (shoulders are not included). If the culvert is wider than the traveled way, the relative culvert width is a positive value. If the culvert is narrower than the traveled way, the relative culvert width is a negative value.

The second step in the development of the cost model was to establish an appropriate cost per accident. A cost of \$48,430 was chosen on the basis of 1985 nationwide accident cost data (*12*). That was the value for rural non-federal-aid systems, and it best represents a rural local agency road system. The value was verified by using another technique given elsewhere (*13*). The equation defining the relationship between unit user cost per day-ft-ADT and insufficient culvert width is

$$\text{Cost/day-ft-ADT} = 0.048430 * ADT * [(0.0022 * WD^2) - (0.061 * WD) + 0.5] \quad (8)$$

When the width deficiency cost model is substituted into the deficiency points equation, the width deficiency ranking formula becomes

$$WP = WW * [(WD^2 - WDG^2)/9{,}380 - (WD - WDG)/338] * ADT \quad (9)$$

where

WP = width priority,

WW = width deficiency weighting factor, and
WDG = relative culvert width goal (ft).

WP may not be less than 0.

Maintenance Ranking Formula

Agency costs related to maintenance of a culvert result from blockage of a waterway by debris and sediment. Routine maintenance for culverts consists primarily of the removal of obstructions and the repair of erosion and scour. Prevention of joint leakage may be critical in culverts bedded in pipeable soils to prevent undermining and loss of support. The maintenance cost model was based on yearly maintenance costs incurred by the agency for each structure. When the maintenance cost model is substituted into the deficiency points equation, the maintenance ranking formula becomes

$$MP = WM * (MC - MG)/365 \quad (10)$$

where

MP = maintenance priority,
WM = maintenance weighting factor,
MC = maintenance cost ($/year), and
MG = maintenance goal ($/year).

MP may not be less than 0.

The ranking formulas developed for this culvert management system were assembled into a deficiency points equation. The equation represents the total combined user-agency cost per day for a given culvert. For each culvert, the deficiency points (DP) are the sum of four culvert ranking formulas: load capacity, hydraulic capacity, width deficiency, and maintenance. The deficiency points are calculated on the basis of the following formula:

$$DP = CP + HP + WP + MP \quad (11)$$

Weighting Factors

Weighting factors allow the user to change the relative importance of the various ranking formulas. Since the ranking formulas are all based on estimated costs, the recommended value for all weighting factors is 1.0. If specific local considerations are important, the weighting factor may be increased or decreased. However, the weighting factors should not be changed indiscriminately. Because the basis of the formulas are user and agency costs, a change in the weighting factors has the effect of reducing or increasing the costs associated with each priority formula. For example, it could be argued that load capacity is not important because culverts in the agency are not posted. However, there is a risk to the public and the agency in case of structural failure of some culverts. Therefore, the weighting factor for LC should be set equal to zero for this extreme case.

Culvert Parameters

The proposed deficiency points ranking formula contains four weighting factors, four ranking formulas, and eight basic culvert parameters. The culvert parameters are posted weight (tons), ADT, relative width (ft), detour length, flood detour length, flood days per year, average cost per day per flood, and maintenance costs per year.

The development of such a system is a series of compromises. If every conceivable culvert parameter were used in the priority-ranking formulas, the data collection effort would become significant. Even for smaller culvert systems, this approach could become an unwise use of limited resources. Because the objective of the culvert management system is to set priorities and get a relative ranking of the system's culverts, a more logical approach is to minimize the number of culvert parameters collected.

The number of deficiency points for each culvert is always greater than or equal to zero. Obviously, the worst culvert in the system will have the largest number of deficiency points, and the best culverts in the system will have no deficiency points.

SOFTWARE

To assist in verifying that the proposed system works, a comprehensive data base software system was developed. Written in dBASE III™, CMS provides for the creation of the required data bases, conducts certain hydraulic analyses, calculates the deficiency points for each culvert, and provides for output in several formats.

Before CMS will work, three data bases must be created. The first contains the culvert parameters, the second defines the level-of-service goals, and the third defines the weighting factors. For first-time users, default data bases are provided.

CMS is a menu-driven system. Step-by-step execution of individual menu items gives the user full control of program flow and analysis. The user reaches the appropriate module by working through the menu structure shown in Figure 1. The numbers above each box are the responses the user should make to get to the desired menu. The user may always move to the previous menu by returning to any menu and pressing 9.

By selecting the create option, the user may add data to the culvert, level-of-service goal, or weighting factor data base. By selecting the merge/modify option, the user may merge an existing culvert data base or modify existing data in the culvert, level-of-service goals, or weighting factor data bases. By selecting the culvert ranking option, the user may rank all culverts in the system. Obviously, before culverts are ranked, data for the culverts must be collected and entered into the culvert data base. The culvert ranking results may be viewed on the screen or sent to the printer using the output results option.

The user may select the hydraulics option to perform simple hydraulic analysis of existing culverts. Two analysis procedures are supported by CMS. The rational method permits the user to input respective land use areas and their corresponding runoff coefficients. After the rainfall intensity is entered, the peak flow rate for the drainage basin is calculated. The second analysis procedure is based on U.S. Geological Survey data for calculating the peak flow rates on unregulated streams in Kansas (*14*). A regression equation based on return period, drainage area, 24-hr rainfall depth, and main channel slope was implemented in the software.

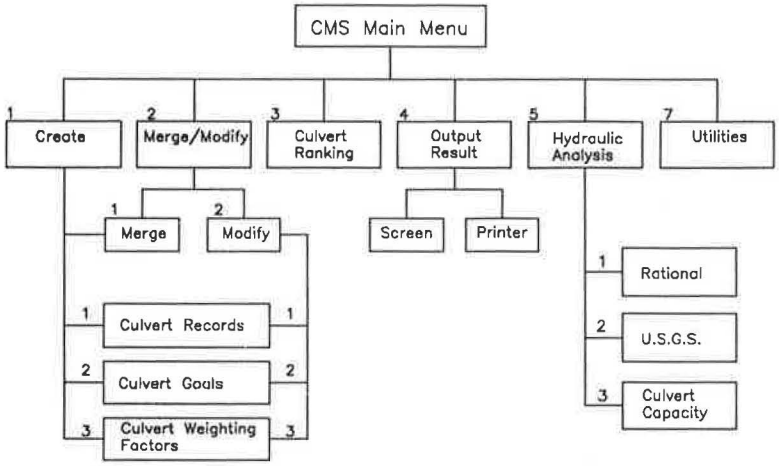

FIGURE 1 CMS menu structure.

A simple culvert capacity calculator is also supported in the hydraulics option. This determines the culvert capacity by multiplying the open end area by an average velocity. The coefficients required to conduct any of the hydraulics options are automatically stored in the culvert data base.

The utilities option may be selected to configure CMS and to designate specific data base file names, agency name, and paper width for printer output.

APPLICATION TO A LOCAL CULVERT SYSTEM

To illustrate the application of the proposed system to a local agency culvert system, the culverts of a local county were evaluated. The county, in Kansas, is located near a growing major metropolitan area. However, many of the county culverts are on rural roads.

To provide a feel for the county's culvert system status at time of evaluation the following description is provided. There were 1,459 culverts in the system. The distribution of culverts by type is as follows: 77 were corrugated metal arch, 676 were corrugated metal pipe, 94 were concrete arch, 346 were reinforced concrete box, 96 were reinforced concrete pipe, 89 were simple span, 69 were stone arch, 1 was stone box, and 11 were of an unknown variety.

The agency had previously developed a good data base for its culvert system. However, some additional assumptions and modifications were needed to evaluate the system. Forty-four culverts had been load rated. Because CMS requires a load rating for each culvert, a load rating was assigned to all other culverts on the basis of the agency's structural condition rating system. New culverts and older culverts with no problems were rated at 16 tons. Culverts with minor structural problems were rated at 13 tons, those with intermediate structural problems were rated at 8 tons, those with major structural problems were rated at 3 tons, and failed culverts were rated at 0 tons. Fifteen culverts were closed but were included in the totals.

Four hundred seventy culverts were not adequate to handle the flow requirements of their particular drainage basin. Estimates for the number of flood days per year and cost per flood for each culvert were made on the basis of agency data. If the culvert's hydraulic capacity was adequate to handle the flow, the number of flood days per year was set equal to zero. If the flow capacity was inadequate, 1 flood day per year was assigned at cost of $1,000 per flood. In the case of structures being replaced by structures with twice the capacity, 2 flood days per year were assigned at a cost of $1,000 per flood. Two hundred eighty-seven culverts were narrower than the traveled roadway. The relative culvert width ranged from 0 to −10 ft. The average relative culvert width was −0.6 ft.

One hundred forty-two culverts required major maintenance. Estimates of the yearly cost of maintenance for each culvert were made using agency data. Culverts requiring no, minor, medium, or major maintenance were assigned maintenance costs of $0, $200, $400, or $600 per year, respectively.

The highway classifications, at time of evaluation, were not available. All highway classifications were assumed to be "local." The ADT counts varied from 0 to 4,107. Ninety percent of the ADTs were below 1,000. The average ADT was 376.

Weighting Factors and Level-of-Service Goals

Whereas any number of highway function classifications could be defined, all classifications for this system were defined as "local." For all ADT ranges, the load capacity goal was set at 16 tons, the hydraulic capacity goal was set at 0 flood days per year, the relative width goal was set at 0 ft, and the maintenance goal was set at $0 per year. All weighting factors used in this application were set equal to 1.0.

Results

The 1,459 culverts were evaluated using a 12 MHz 80286 microcomputer. The analysis took approximately 20 min, including the calculation of all deficiency points and placement of the culverts in descending order on the basis of the deficiency points. Because most local agency culvert systems are approximately this size, a microcomputer with the software developed in this project can handle culvert systems of this size.

For all culverts, the number of deficiency points ranged from 0 to 244. Five hundred forty-five culverts had no deficiency points. The maximum number of deficiency points (for

a culvert with the highest ADT totally deficient in load capacity, hydraulic capacity, relative width, and maintenance) would have been approximately 520.

For culverts with relatively low load capacity values, culverts with high ADTs had the higher number of deficiency points. The 10 culverts with the highest number of deficiency points had high ADTs. The ADTs varied between 724 and 2,207. The operating rating of these culverts varied between 0 and 8 tons. Six out of the top 10 culverts were hydraulically inadequate. The relative culvert widths of the first 10 culverts varied between 0 and 10 ft. Seven of the first 10 culverts had maintenance problems.

The results were then compared with the local agency's previously developed comprehensive culvert replacement program. In this program two agency persons (APs) independently ranked the culvert system. AP1 is an engineer familiar with the technical aspects of the system, whereas AP2 is an engineer familiar with management responsibilities for the system. CMS identified 32 of AP1's 50 top culverts (see Figure 2). The diagonal line is where data points would lie if the CMS ranking agreed perfectly with the agency ranking. Data points above the diagonal line represent culverts rated more critical by CMS than by AP1, and vice versa. The data points along the top of Figure 2 represent culverts ranked by CMS in the top 50 but ranked greater than 50 by AP1. The culverts that were not in the top 50 of AP1's ranking but were ranked critical by CMS tended to have reduced load capacity. Because the load capacity for these culverts was arbitrarily assigned and may be inaccurate, it is recommended that they be load rated. If it is assumed that these culverts drop out of the top 50 when properly load rated, a better correlation between CMS results and AP1 occurs (see Figure 3).

CMS identified only 23 of the top 50 culverts identified by AP2 (see Figure 4). AP2's ranking appears to place more importance on relative culvert width. This may reflect the safety concerns of a system manager. If AP2 had assigned more importance to load capacity, the correlation between the rankings by CMS and AP2 would have been better. If an actual load rating could be done for all culverts, a better correlation between CMS and AP2 would occur. Figure 5 shows the correlation if all culverts ranked high by CMS were determined adequate when load rated. Except for specific instances, the culverts chosen by CMS were scheduled for early replacement, were under construction, or were replaced.

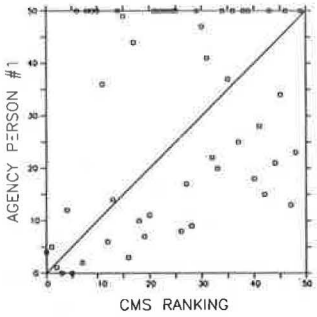

FIGURE 2 CMS compared with AP1 ranking of top 50 culverts.

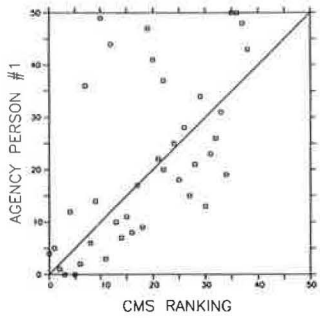

FIGURE 3 Removal of AP1's noncritical culverts improves correlation with CMS.

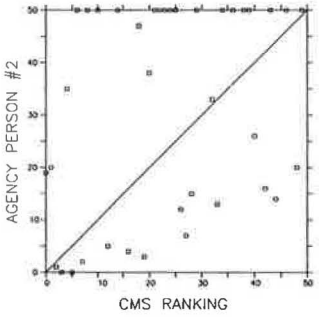

FIGURE 4 CMS compared with AP2 ranking of top 50 culverts.

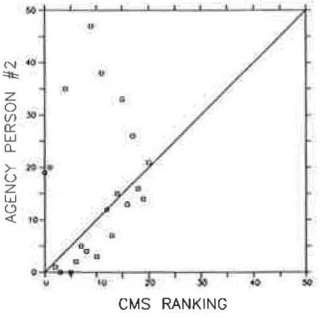

FIGURE 5 Correlation of CMS and AP2 rankings if all culverts ranked high by CMS were determined adequate when load rated.

Because 1,459 culverts were considered in the system, remarkable correlation occurred between the CMS system and the independent ranking by local APs. Several observations can be made. The need for accurate data is imperative. Errors in culvert data may cause obvious discrepancies. The cost model developed appears to give reasonable results when compared with the existing construction program. Because CMS is cost based, system administrators can evaluate the total system over a period of time. In 5 years, a lower average number of deficiency points would indicate an overall improvement of the system.

SUMMARY AND CONCLUSIONS

A ranking system for culverts found on local agency road systems was developed. Cost models were developed to identify major contributors to user and agency costs. A working dBase III Plus™ microcomputer program was developed using this cost model information. The program was used to evaluate a culvert system of a local county. The results of the proposed system were compared with existing culvert replacement strategies.

The results of the culvert management system studies support the following conclusions:

1. A culvert management system based on a cost approach is practical and gives good rankings of a local culvert system.
2. Important cost factors, in order of importance, were load capacity, relative width deficiency, hydraulic capacity, and maintenance.
3. Microcomputers can analyze local culvert systems. A working dBase™ microcomputer program was developed using cost model information. The time required to develop a culvert replacement program with the use of a culvert management system was significantly lower than with the manual selection process.
4. The system developed provides flexibility to local agencies by permitting local definition of level-of-service goals and weighting factors.
5. A measure of the system's capability is a steady decline of a system's average deficiency points.

To fully implement a culvert management system, it will be necessary to evaluate life cycle costs, deterioration models for each culvert type, and effects of further maintenance strategies. With this more comprehensive management approach, better selection of culvert maintenance projects may occur, and maintenance engineers may be able to evaluate the consequences of resource allocation during the budgeting process.

ACKNOWLEDGMENTS

The authors recognize the support provided by the Nebraska Technology Transfer Center and the Johnson County Public Works Department that made this project possible.

REFERENCES

1. *Development of a Highway Improvement Priority System for Kansas*. Division of Planning and Development, Office of Analysis and Evaluation, Kansas Department of Transportation, Topeka, 1984.
2. D. W. Johnson and P. Zia. Level-of-Service System for Bridge Evaluation. In *Transportation Research Record 962*, TRB, National Research Council, Washington, D.C., 1984.
3. *Interim Report on Bridge Maintenance, Rehabilitation and Replacement Procedures*. Nebraska Department of Roads, Lincoln, 1986.
4. W. T. McKeel, Jr., and J. E. Andrews. *Establishing a Priority of Funding for Deficient Bridges*. Virginia Department of Highways and Transportation, Richmond, 1985.
5. *The Pennsylvania Bridge Management System*. Draft final report. Bureau of Bridge and Roadway Technology, Pennsylvania Department of Transportation, Harrisburg, 1987.
6. S. W. Hudson, W. R. Hudson, and R. F. Carmichael. *A Model Bridge Management System*. Draft report. ARE Inc., Austin, Tex., 1988.
7. F. Farid, D. W. Johnston, C. C.-J. Chen, M. A. Laverde, and B. S. Rihani. *Feasibility of Incremental Benefit-Cost Analysis for Optimal Allocation of Limited Budgets to Maintenance, Rehabilitation and Replacement of Bridges*. Report FHWA-DP-71-02. North Carolina State University, Raleigh, 1988.
8. *Bridge Management Systems*. Draft report. FHWA-DP-71-01. FHWA, U.S. Department of Transportation, 1987.
9. *Kansas Truck Weight and Volume Study*. Kansas Department of Transportation, Topeka, 1985.
10. G. W. McNichol. *Development of a Microcomputer Based Culvert Management System*. Department of Civil Engineering, University of Kansas, Lawrence, 1989.
11. K. K. Mak. *Effect of Bridge Width on Highway Safety*. In *State-of-the-Art Report 6*, TRB, National Research Council, Washington, D.C., 1987.
12. A. G. Bailey. *Accident Costs—Are We Using Them Correctly?* Technical advisory attachment. FHWA, Albany, N.Y., 1988.
13. P. H. Wright and R. J. Pasquette. *Accident Rates by Road Type*. In *Highway Engineering* (4th ed.), John Wiley and Sons, N.Y., 1979.
14. R. W. Clement, *Floods in Kansas and Techniques for Estimating Their Magnitude and Frequency in Unregulated Streams*. Water-Resources Investigations Report 89-4008. U.S. Geological Survey, Lawrence, Kans., 1987.

Publication of this paper sponsored by Committee on Culverts and Hydraulic Structures.

Economic Considerations When Using Controlled Low-Strength Material (CLSM-CDF) as Backfill

WILLIAM E. BREWER AND JOHN O. HURD

Controlled low-strength material (CLSM) is defined by the American Concrete Institute as having a 28-day compressive strength less than 1,200 psi. Its primary ingredients are portland cement, fly ash, and filler aggregate. Although CLSMs have been in use for a number of years, confusion about their construction benefits and economic savings remains. The principal use of CLSM has been as a controlled-density fill (CDF) in place of conventionally placed backfill. A method for determining the cost of CLSM-CDF and how it can affect a contractor's total construction costs is described. General technical information for the manufacture and testing of CLSM in the laboratory and in the field is cited. A small sample of ready-mixed concrete producers indicates the need for dissemination of information about CLSM.

The conventional backfilling technique for all types of excavations has supposedly been the placement of granular material into the excavation in layers with tamping to achieve the desired compaction (density). In many cases, the material was dumped into the trench but never tamped or adequately compacted.

In the early 1970s engineers started examining alternatives to conventional backfilling materials and methods (*1*). One alternative was a material designated as K-Krete (CDF) (CDF stood for controlled density fill), a low-strength material (in terms of concrete) with a 28-day compressive strength of about 100 psi. This was a patented material process developed by the Detroit Edison Co., Detroit, Michigan, and Kuhlman Corp., Toldeo, Ohio. The material is still sold under the name K-Krete through trademark holders. Because of the material's success, similar materials have been developed and sold under a variety of trade names: M-Crete, S-Crete, Flowable Fill, Flash Fill, Flowable Grout, Flowable Mortar, One-Sack Mix, and so on.

By 1980 it was evident to the early developers of low-strength materials that technical information about this product was not being properly developed or transferred to the public. Some information was being published in trade magazines, but not on a consistent basis. An American Concrete Institute (ACI) committee 229 was formed to correct these deficiencies. The ACI 229 committee is designated as Controlled Low-Strength Material (CLSM). The committee defined low strength to be a material with a 28-day compressive strength of less than 1,200 psi.

W. E. Brewer, Brewer & Associates, P.O. Box 8, Maumee, Ohio 43537. J. O. Hurd, Ohio Department of Transportation, 25 South Front Street, Room 620, Columbus, Ohio 43215.

The creation of the ACI 229 committee gave publicity to CLSM. In recent years ready-mixed concrete trade associations have published numerous articles on CSLM uses (*2–4*). Even with this extended publicity, CLSM uses were confined because of misunderstandings about construction applications and a realistic pricing structure.

Although this paper primarily addresses backfilling with CLSM-CDF, CLSM is really a family of possible mixtures with a variety of uses: pavement base, structural fill, thermal fill, anticorrosion fill, high- or low-permeability fill, and so on. Each mixture is designated by a three-letter acronym, such as CPB (controlled pavement base), CSF (controlled structural fill), and CTF (controlled thermal fill).

OBJECTIVE AND SCOPE

One reason for using, or not using, CLSM-CDF has been its cost compared with that of conventional backfill. Construction costs for both conventional backfill and CLSM-CDF are investigated, and ways to reduce CLSM-CDF costs are suggested.

Information used in this paper has been gathered over the past 20 years and is the result of both laboratory and field research projects (*5–8*). Comparisons of conventional backfill and CLSM-CDF construction costs are reviewed. The review includes related topics for materials, manufacturing, transporting, placing, testing, OSHA regulations, and pricing.

CLSM AND RELATED BACKFILL PROPERTIES

Background

The basic components of CLSM are portland cement, fine aggregate, fly ash, and water. For backfilling operations the material must possess four properties: flowability, removability, strength, and a competitive price. Competitive price is the main theme of this paper. It is semidependent on the other three properties. To provide a better understanding of each property and its effect on price, each property is reviewed.

Flowability

The CLSM must be able to flow into the trench, thereby eliminating all labor requirements for placing. Several tests

have been developed for laboratory determination of adequate flow. Early researchers developed the open-ended, 3-in.-diameter × 6-in.-long cylinder test. The open-ended cylinder is placed on a level surface, and the CLSM is poured into the cylinder. The cylinder is then lifted, vertically, to allow the material to flow out on the level surface. Good flowability requires no material segregation and a spread of approximately 8 in. in diameter.

Removability

Removability must be considered if the backfilled trench may be excavated in the future. In most projects removability is a property that is requested. To ensure removability, the unconfined compressive strength should be less than 100 psi. Concrete-oriented personnel have difficulty in understanding this low strength requirement, because they usually work in the range of 3,000 to 5,000 psi. Hardened CLSM is more directly related to soils than to concrete. For easy removability, the worst thing a manufacturer can do is to put extra cement into the mixture. In one case the material achieved a reported strength of 3,000 psi in 1 year.

Strength

Compressive strength testing of CLSM has been conducted using various size cylinders and 2-in. cubes. The resulting compressive strength depends on the materials used and their respective proportions in the mixture. For standard backfilling operations, considering flowability and removability, 100 psi or less is recommended. Different materials, types, and sources can drastically change the compressive strength. It is recommended that laboratory tests be run on initial mixtures and for any changes in the mixtures. Monitoring of materials during CLSM manufacture is strongly recommended. See Table 1 for referenced CLSM laboratory mixture.

These weights provide a starting point for laboratory determination of flowability and compressive strength. Type C fly ash is now being considered or used in several locations in the United States. Laboratory and field test comparisons are being conducted for Type F and Type C fly ashes. Initial tests indicate that higher strengths are being achieved with Type C fly ash. If removability is required, the use of Type C fly ash should be closely examined.

In most cases the fill aggregate has been concrete sand (ASTM C33). It provides an excellent CLSM backfill when properly designed and manufactured. Less expensive materials can also be used for the aggregate filler. In some cases bottom ash has been successfully used. Each geographic area contains inexpensive aggregate filler material that could be used in the manufacture of CLSM.

Yield of Mixture

There are two yield considerations for CLSM mixtures: the plastic, or wet, yield and the hardened, or subsided, yield. The absolute volume of the wet mixture is calculated in the same manner as for concrete. Because of the high water content, a significant amount of water bleeds off the placed CLSM mixture. Therefore, the hardened volume is less than the initial wet volume. A typical subsided yield would have volume reduced by approximately 6 to 8 percent. The reduced hardened volume must be reflected in both price and volume

TABLE 1 CLSM LABORATORY MIXTURE AND DETERMINATION OF WET ABSOLUTE VOLUME

CLSM LABORATORY MIXTURE

Material	Weight (lb)/Cubic Yard
Portland Cement, ASTM C150 (Type I)	100
Fly Ash, ASTM C618 (Type F)	300
Filler, ASTM C33 (Aggregate)	2560
Water	600

DETERMINATION WET ABSOLUTE VOLUME

Material	S.G.	Weight	Calculated Wet Abs. Volume		
Cement	3.15	100	100/(62.4 * 3.15)	=	0.51
Fly Ash	2.47	300	300/(62.4 * 2.47)	=	1.95
Filler	2.65	2560	2560/(62.4 * 2.65)	=	15.48
Water	1.00	600	600/62.4	=	9.62
			Total (cu.ft.)	=	27.56

requirements. The specific gravity of the components will affect the final hardened volume. See Table 1 for an example of determining the wet absolute volume of a typical 1-yd³ CLSM mixture.

The wet overyield (0.56 ft³) could be adjusted by reducing the aggregate filler as long as proper flowability is maintained. Another consideration is that the higher wet yield increases the subsided volume. A volume reduction of 6 to 8 percent would result in a final subsided volume of 26.0 to 25.5 ft³.

MATERIAL COSTS

To determine a proper pricing structure for a CLSM-CDF, a knowledge of material costs is required. Material costs generally vary with geographic locations. Time of year, competition, and the amount of work within the geographical area can affect costs. Costs for CLSM-CDF in a surveyed area of Ohio are shown in Table 2.

The cost of the fill material has the greatest significance in determining the cost of a CLSM-CDF mixture. Material for possible aggregate filler use should be investigated. It can be a nonstandard material that can satisfy CLSM mixture requirements. The Hatfield Station project (Pennsylvania) is one place where bottom ash was used as the filler material (*9*).

MANUFACTURING EQUIPMENT

Ready-mixed concrete equipment has generally been used to manufacture CLSM mixtures. This is not to say that other types of equipment and mixing procedures have not or could not be just as effective. Because the early CLSM concepts were developed by ready-mixed concrete producers, it was natural for ready-mixed concrete equipment to be used.

The important thing to remember is the proper mixing of the CLSM components. Flow, removability, and strength will not be controlled without proper mixing.

TRANSPORTATION AND PLACING COSTS

The usual method for transporting CLSM-CDF mixtures to the project has been by ready-mixed concrete trucks. With the advent of CLSM-CDF mixtures, the ready-mixed concrete trucks should now be referred to as material mixing and transporting trucks. The CLSM-CDF mixture is usually placed by pouring directly from the truck into the trench or excavation. For this paper, and in general, the transportation costs for concrete are used for the transportation costs of CLSM-CDF mixtures.

Technically, the CLSM-CDF supplier should consider less wear on equipment (blades) and faster placing times. Because most CLSM-CDF mixtures contain smaller-sized aggregate than concrete, blade wear is greatly reduced. Because CLSM requires no vibration or work after placing, placement time is reduced from the usual 10 min/yd³ for concrete to 10 min or less for the entire CLSM-CDF load. Placement of CLSM-CDF mixtures can significantly decrease equipment turnaround time for trucks.

CONSTRUCTION CONSIDERATIONS AND BACKFILLING

When considering total CLSM-CDF costs, the contractor must consider related construction requirements. Related construction requirements include trench width, Occupational Safety and Health Administration (OSHA) requirements, and speed of backfill placement.

Trench widths can be reduced with the use of CLSM-CDF, because a wider trench is not required to achieve adequate compaction around the conduit. The reduction in trench width also reduces excavation costs and the amount of backfill material required.

OSHA requires sloping sides for trench excavations [29 CFR 1926.652 (7/1/89 ed.)]. For conduit placement, with a "steel box" and CLSM-CDF backfilling, sloping sides could be eliminated because no one is required to be in the trench during backfilling.

TABLE 2 CLSM CDF COST SURVEY, OHIO

COMPANY REFERENCE	MATERIAL REFERENCE	STRENGTH @ 28 DAYS PSI	COST ($/CY.YD.)
A	3 bag grout	?	52.00
B	K-Krete-CDF	100	29.50
C	Low Strength	500-1000	31.50
D	Fill Crete	?	36.75
E	Flowable Fill	500	30.00
F	U-Crete	500	30.00

? Means that producer had no information about the 28 day compressive strength.

All producers made claims about easy removability.

Backfilling is faster with the use of CLSM-CDF. There are no delays for compaction testing in the trench. Backfilling is as fast as the CLSM-CDF material can be poured into the trench, as long as conduit flotation can be controlled. A faster backfilling operation reduces total project construction time.

QUALITY CONTROL AND FIELD TESTING

The quality control and testing of CLSM-CDF mixtures are similar to construction controls for concrete and soils. The suggested controls and field-testing procedures apply to the end use of the mixture. The tests consist of the following ASTM standards and test procedures: ASTM C138, test for unit weight; ASTM C39, modified test for compressive strength; and flow test (no ASTM designation).

The cylinder size and rodding requirements of ASTM C39 have been modified. The cylinder size can be either 4 × 8 in. or 3 × 6 in. Naturally, 6 × 12 in. cylinders can be used, but smaller cylinders yield satisfactory results. To simulate field placement, no rodding should be done after placing the mix in the cylinder. The cylinders should be allowed to stand undisturbed for at least 48 hr.

COMPETITIVE PRICE

The price per cubic yard of a CLSM-CDF mixture, as manufactured by the ready-mixed concrete producer, is governed by the cost of its components, the cost of competitive products, and the construction method. For this paper, material cost survey form sheets were developed along with a material cost determination procedure to be used by a ready-mixed concrete producer (see Figure 1 for cost form sheet). Five ready-mixed concrete producers in Ohio participated in the cost survey. Each producer was interviewed about possible uses of CLSM-CDF in its operation. Material cost and mix information received from the producers interviewed is given in Tables 3 and 4.

The material cost information was then used to calculate the cost of a standard CLSM-CDF mixture using ASTM C33 concrete sand as the filler. The CLSM-CDF costs include transportation and placement times. They were calculated using the same transportation and placement time costs as for concrete mixtures (see Table 5 for determination of CLSM-CDF mixture costs for material, transportation, and placement times).

The largest cost in a six-sack concrete mix is the cement (61 percent). Figure 2 shows a cost comparison for a six-sack concrete mix. The largest cost for CLSM-CDF, on the basis of average and minimum survey values, is the aggregate filler, 59 percent and 60 percent, respectively. See Figures 3 and 4 for cost comparisons for CLSM-CDF using average and minimum survey values. The filler material in a CLSM-CDF mixture greatly influences the final cost. On the average, for every 10-cent reduction in filler costs per ton, the resulting CLSM-CDF material cost reduction is 1 percent/yd^3.

Cost reductions for CLSM could be made to adjust for less equipment wear and faster placement times. The CLSM-CDF

Estimated Costs (Work Sheet Information)

Supplier:_____ **Date:**_____

Item Reference	P. C. Concrete	CLSM-CDF
Materials:		
Cement		
Fine Aggre. (lb)		
Coarse Aggre. (lb)		
Water (lb)		
Fly Ash (lb)		
Trucking:		
Travel (time)		
Unloading (time)		
Yields: (c.f.)		

FIGURE 1 Survey form for CLSM-CDF costs.

TABLE 3 CLSM-CDF COST INFORMATION, OHIO

MATERIAL	COMPANY SURVEY REFERENCE				
REFERENCE	1	2	3	4	5
	(Cost per Ton...$/T)				
Cement (Type 1)	60.00	57.00	57.00	62.00	60.00
Fine Aggr. (C33)	6.00	5.80	4.85	6.50	7.50
Coarse Aggr. (C33)	7.85	7.95	8.60	5.95	5.45
Fly Ash (F)	23.00	9.00	26.50	13.00	11.50
Unloading Time (con)	60 min.	60 min.	60 min.	10_3min./ yd^3	10_3min./ yd^3
Cost 6 Sack Mix	50.00	48.00	42.00	47.50	49.50

	Minimum	Maximum	Average
	(Cost per Ton...$/T.)		
Cement (Type 1)	57.00	62.00	59.20
Fine Aggr. (C33)	4.85	7.50	6.23
Coarse Aggr. (C33)	5.45	8.60	7.16
Fly Ash (F)	9.00	26.50	16.60
Cost 6 Sack Mix (con)	42.00	50.00	47.40

TABLE 4 CONCRETE MIX INFORMATION, OHIO

MATERIAL	COMPANY SURVEY REFERENCE				
REFERENCE	1	2	3	4	5
	(Pounds/Cubic Yard For 6 Sack Mix)				
Cement (Type 1)	564	564	564	564	564
Fine Aggr. (C33)	1320	1380	1380	1508	1500
Coarse Aggr. (C33)	1680	1765	1730	1735	1725
Cost 6 Sack Mix	50.00	48.00	42.00	47.50	49.50

	Minimum	Maximum	Average
	(Pounds/Cubic Yard For 6 Sack Mix)		
Cement (Type 1)	564	564	564
Fine Aggr. (C33)	1320	1380	1418
Coarse Aggr. (C33)	1680	1765	1727
Cost 6 Sack Mix (con)	42.00	50.00	47.40

TABLE 5 DETERMINATION OF CLSM-CDF COST

6 Sack Concrete Mix

Material Reference	Weight/ Cu.Yd.(lb)	Cost ($/T)	Matl.Cost ($/Cu.Yd.)	% Cost
Cement	564	59.20	16.69	61
Fine Aggr.	1418	6.23	4.42	16
Coar.Aggr.	1727	7.16	6.18	23
			27.29	100

Cost for 6 sack concrete mix including material, transportation and overhead...$ 47.40.

Therefore cost for transportation and overhead would equal...
$ 47.40 - 27.29 = **$ 20.11/cy.**

CLSM-CDF MIXTURE (Based on Average Values)

Material Reference	Weight/ Cu.Yd.(lb)	Cost ($/T)	Matl.Cost ($/Cu.Yd.)	% Cost
Cement	100	59.20	2.96	22
Fine Aggr.	2550	6.23	7.79	59
Fly Ash	300	16.60	2.49	19
			13.24	100

Add in transportation and overhead costs...
$ 20.11 + 13.24 = $ 33.35/cy.

Adjust for under yield...$ 33.35/1.06 = **$ 31.46/cy.**

CLSM-CDF MIXTURE (Based on Minimum Values)

Material Reference	Weight/ Cu.Yd.(lb)	Cost ($/T)	Matl.Cost ($/Cu.Yd.)	% Cost
Cement	100	57.00	2.85	27
Fine Aggr.	2550	4.85	6.18	60
Fly Ash	300	16.60	1.35	13
			10.38	100

Add in transportation and overhead costs...
$ 20.11 + 10.38 = $ 30.49/cy.

Adjust for under yield...$ 30.49/1.06 = **$ 28.76/cy.**

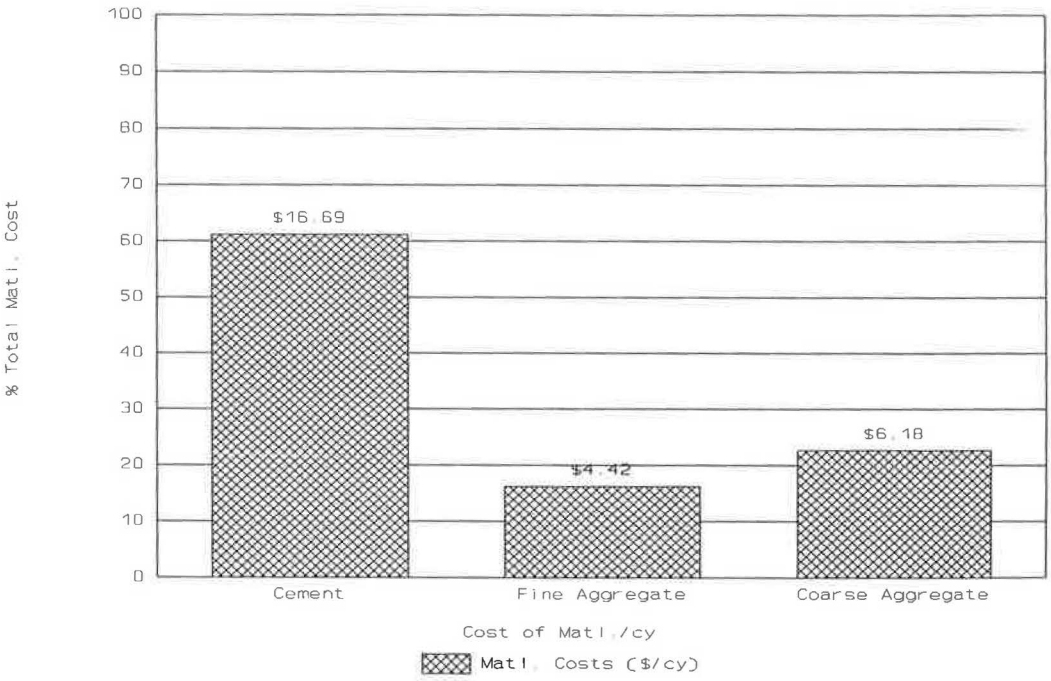

FIGURE 2 Concrete material cost comparisons.

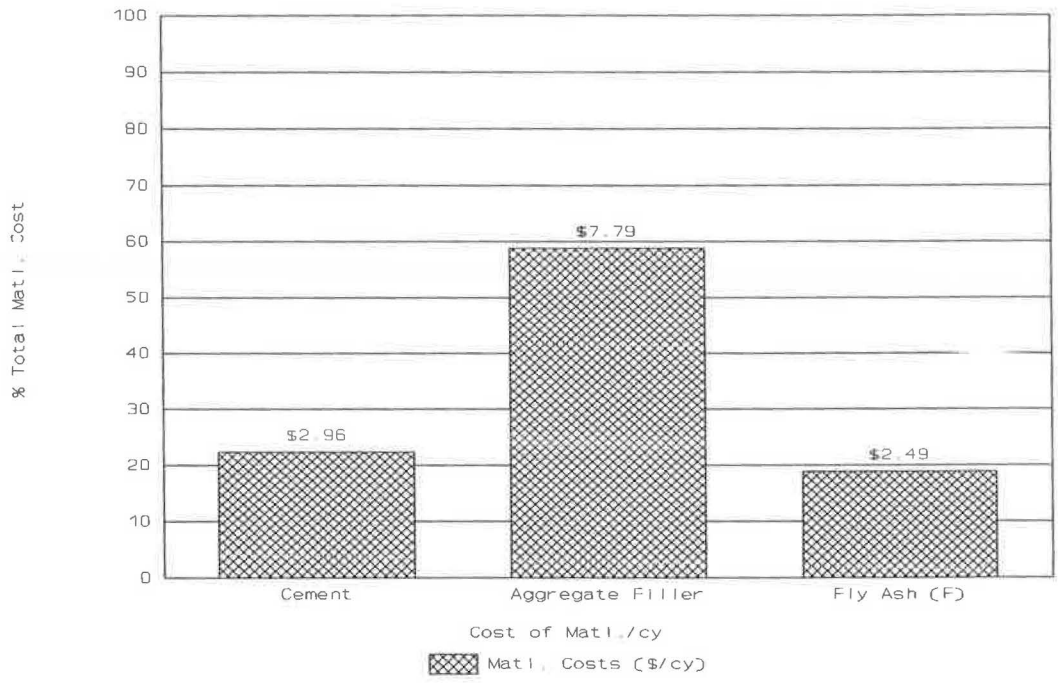

FIGURE 3 CLSM-CDF material cost comparisons (average).

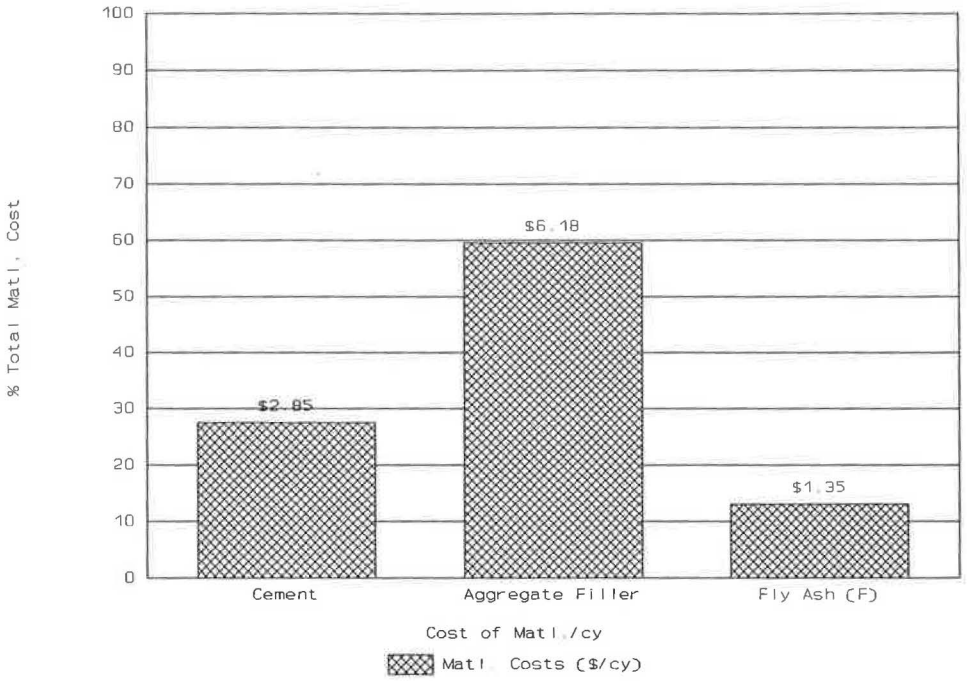

FIGURE 4 CLSM-CDF material cost comparisons (minimum).

TABLE 6 COST COMPARISONS—CLSM-CDF VERSUS CONVENTIONAL BACKFILL

Description	Quantity (Cu.Yd.)	Labor ($/Cu.Yd.)	Material ($/Cu.Yd.)	Total ($)
Granular Backfill - Air Tamped				
Material & Labor	26.67	14.00	8.00	586.74
Testing 6" lifts		($ 250/day...1 day)		250.00
Total Cost				836.74
CLSM-CDF				
Material	26.67	(no labor)	28.76	767.03
Testing		(Flat fee - 2 cylinders)		100.00
Total Cost				867.03

Note: Quantities based on a trench 3' wide, 6' deep, and 40' long.

Every 1' reduction in trench with, in this example, would represent a backfill cost reduction of $ 255.64 when using CLSM-CDF. The trench width reduction would be possible because conventional compaction requires additional access width around the conduit.

estimated costs shown in Table 5 do not reflect any adjustments for these reductions.

CLSM-CDF COSTS COMPARED WITH THOSE OF CONVENTIONAL BACKFILL

The cost of using CLSM-CDF in place of conventional backfill has been debated by many CLSM-CDF producers and contractors. The economy of using CLSM-CDF depends on the specification enforcement of the conventional backfill method and the cost of backfill materials. Using the costs for CLSM-CDF given in Table 5, an illustrative comparison between conventional backfill and CLSM-CDF will be made.

Consider a roadway trench with the following dimensions: width, 3 ft; depth, 6 ft; and length, 40 ft. The total backfill material requirement is 26.67 yd^3 less the pipe's displaced volume. Cost comparisons are given in Table 6, which indicates that CLSM-CDF is comparable with conventional backfill costs where compaction in lifts is required. Conventional backfill unit costs in Table 6 were supplied by the Area Paving Council, Toledo, Ohio. An additional cost advantage would be realized for CLSM-CDF if the contractor considered OSHA regulations and total construction project time. Naturally, any reduction in trench width due to backfilling around and under a conduit would also favor the use of CLSM-CDF. For example, every 1-ft reduction in trench width in this example represents a backfill cost reduction of $255.64 when using CLSM-CDF. The trench width reduction is possible because conventional compaction requires additional access width around the conduit.

RESPONSE TO TELEPHONE SURVEY

After the contact with the initial 5 ready-mixed concrete producers, who assisted in providing material costs information,

TABLE 7 CLSM-CDF SURVEY RESULTS

Company Reference	Survey Response
1	Company is now under new ownership and never heard of controlled low strength material.
2	Didn't know about controlled low strength material but recommended 3 bag grout. Had no idea about removability.
3	Didn't know about controlled low strength material, recommended using 4000 psi concrete.
4	Didn't have such a product.
5	"The product we sell is called K-Krete. Need strength of 100 psi or less for removability."
6	"Can sell you low strength fill. You'll need strengths of 500 to 1000 psi for removability."
7	"We have a product called Fill Crete. Can't tell you about strength, but you shouldn't drive on it."
8	"We don't have such a product." Suggested I call company referenced as "5".
9	"We have flowable fill but can't tell you anything about compressive strength...call back later."
10	"Yes, we can supply. You'll need at least 500 psi strength. Our product is called U-Crete."

Note: Same question asked of each ready mixed concrete producer.

"Do you have a product to backfill a washed out area under a floor? I've heard of a flowable, controlled low strength material that could be used. If so what would be the estimated 28 day compressive strength?"

another 10 ready-mixed concrete producers in Ohio were contacted. The second group was from a different area in Ohio. The 10 producers all sold to the same market area. The survey results are given in Table 7 and indicate the need for the dissemination of information about CLSM.

SUMMARY

The purpose of this paper was to furnish a cost determination method for CLSM mixtures. During its preparation, other problems were discovered:

- Lack of general knowledge about all CLSM mixtures by ready-mixed concrete producers,
- Misunderstanding by contractors about how a CLSM mixture could help reduce construction costs,
- Unrealistic pricing of CLSM mixtures by ready-mixed concrete producers, and
- Limited knowledge in the construction industry about the use of fly ash in various construction materials.

The cost determination method provided should help establish a realistic and competitive price for all CLSM mixtures. The major cost factor for CLSM is the aggregate filler. The finding of a suitable, less expensive, nonstandard aggregate filler material can result in a satisfactory product at a low cost while conserving other building materials.

ACKNOWLEDGMENT

The authors acknowledge the ready-mixed concrete and fly ash industries for their assistance in the preparation of this paper. They specially thank the surveyed ready-mixed concrete companies that provided insight into the determination of economical CLSM mixtures.

REFERENCES

1. W. E. Brewer. The End of the Backfill Problem. *Concrete Construction Magazine*, Oct. 1975.
2. G. Hewitt. If It Plays in Peoria It Will Do So Everywhere. *Illinois Ready Mixed Concrete Newsletter*, Feb. 1989.
3. W. E. Brewer. Controlled Low Strength Material (CLSM) & the Ready Mixed Producer. *Tennessee Concrete*, Vol. 2, No.2, 1988.
4. CDF Expedites Subdivision Development. *Ohio Paver*, Feb. 1988.
5. W. E. Brewer et al. *Method of Building Embankments and Structure Supports of Backfilling.* U.S. Patent 4,050,258, Sept. 27, 1977.
6. W. E. Brewer et al. *Method of Backfilling*. U.S. Patent 4,050,261, Sept. 27, 1977.
7. W. E. Brewer et al. *Controlled Density Fill Material Containing Fly Ash*. U.S. Patent 4,050,950, Dec. 13, 1977.
8. W. E. Brewer et al. *Method of Bedding a Conduit Using Controlled Density Fill Material.* U.S. Patent 4,062,195, Dec. 13, 1977.
9. Slurry Fills Ease Big Pipe Setting. *ENR*, Nov. 11, 1976.

Publication of this paper sponsored by Committee on Culverts and Hydraulic Structures.

Development of an Impact Cone Penetration Device for Backfill Evaluation

A. P. S. Selvadurai and B. Bakht

The results of a series of preliminary studies that were conducted to develop a penetration device to be used in the assessment of the in situ condition of backfill materials behind the conduit wall of soil-steel structures and in other buried conduits are described. In particular, the methodologies associated with the design of an impact cone device and the results of a series of preliminary tests conducted on dense sand and loose granular soils are discussed.

Large-span metallic soil-steel structures and buried flexible conduits are used extensively as alternatives to conventional bridge structures for highway and rail overpasses. These structures are composed of corrugated metal and can occupy spans of up to 45 ft (*1–4*). The corrugated metal plate sections are typically ⅛ to ¼ in. thick, depending on the size of the arch, with 6- × 2-in. corrugations. The mechanical response of these structures in situ is dominated by the interaction between the flexible corrugated metal and the relatively compressible compacted soil placed adjacent to it. The soil medium is designed and placed to provide the relative stiffness necessary to generate full capacity of the soil-steel structure predominantly through shell action. Although the backfill material is usually placed to a given compaction specification, during the lifetime of the structure it can experience either compaction or loosening because of additional nonuniform surcharge imposed by compaction equipment or traffic loads. In addition, processes such as groundwater flow, frost action, and the attendant removal of fine particles can lead to reductions in the density of the backfill. In certain older soil-steel structures, inadequate material specification or compaction control has led to in situ backfill with loose regions of both cohesive and granular soils. The changes in the condition of the backfill can have a significant influence on the interaction behavior of an embedded flexible soil-steel structure. In extreme situations, reduction in deformability characteristics of the backfill has led to excessive deflections of the soil-steel structure, causing loss of serviceability or collapse of the structure by buckling (*5*). Evaluation of the in situ condition of the backfill adjacent to flexible soil-steel structures is therefore of fundamental importance to the assessment of the integrity of such structures.

Because of the cohesionless nature of conventional backfill materials and their free-draining granular particulate structure (e.g., dense sands, crushed granular A aggregate, etc.), it is not possible to retrieve samples for purposes of laboratory testing. Conventional testing philosophies (*6–9*) strongly advocate the use of in situ testing techniques for evaluation of in situ properties of granular materials such as backfill. Four types of in situ testing techniques, applicable predominantly to granular soils, are cone penetration testing, flat plate dilatometer testing, screw plate testing, and pressuremeter testing.

Cone penetration devices have been successfully used in geotechnical engineering practice for the evaluation of in situ properties of granular soils (*10–16*). In cone penetration methods static or dynamic testing techniques are used to evaluate either elementary in situ properties, such as relative density and void ratio, or, through empirical correlations and theoretical developments, the deformability and shear strength characteristics of granular materials. Both dynamic and static cone penetration techniques have been successfully used in the in situ measurement of properties of dry granular soils, cohesive soils, and frozen soils. No attempt is made herein to provide a complete bibliography on the subject of penetration testing. Other sources (*10–16*) and, where relevant, the conferences associated with them cite in excess of 500 further sources dealing with penetration testing. Extensions of conventional cone penetration testing are achieved through the piezocone test (*17*).

Pressuremeter testing techniques (*18–20*) have also been successfully applied to determine the deformability and shear strength characteristics of granular soils such as sands, silty sands, and, on certain occasions, sandy gravels. Pressuremeter testing techniques [either full displacement (*21*) or self-boring (*18*)] are expensive and are considered nonroutine. Furthermore, the relative particle sizes associated with granular backfill compacted adjacent to a soil-steel structure (the ratio of the diameter of a pressuremeter to largest particle size can be of the order of 3 to 5) are such that conventional pressuremeter testing would be of limited reliability. For this reason pressuremeter testing can be advocated for situations where the backfill consists of fine granular materials such as sandy silt or sandy clay.

In recent years flat plate dilatometer testing has gained popularity in connection with in situ testing of both granular and cohesive soils. The details of this test procedure are given elsewhere (*22,23*). In the flat plate dilatometer test, a highly flexible diaphragm is activated by internal pressurization of the device. The deflections of the membrane are then interpreted to estimate parameters such as relative density, void ratio, deformability characteristics, and so forth. Despite the highly speculative nature of the interpretation schemes, the device would be of limited practical use in in situ testing of backfill. The reliability of the membranes and their deformations would be limited in tests of granular materials con-

A. P. S. Selvadurai, Department of Civil Engineering, Carleton University, Ottawa, Ontario, Canada K1S 5B6. B. Bakht, Research and Development Branch, Ministry of Transportation, Downsview, Ontario, Canada M3M 1J8.

taining relatively large particles with dimensions on the order of the diameter of the flexible diaphragm used in the test device.

The screw plate test is versatile and has been used extensively for determination of the in situ strength and deformability characteristics of both granular and cohesive soils (*24–30*). The device involves the insertion of a helical plate into the soil with a minimum of soil disturbance and its subsequent load testing. Here again, the granular structure of a typical backfill restricts the application of screw plate testing to situations in which mechanical devices (e.g., power augers) are available for the insertion of the screw plate and appropriate reaction devices (e.g., anchorages) are available for the application of the loads.

Owing to the preceding factors, in situ testing of backfill material has to be performed in such a way that the condition of the backfill can be determined at a variety of locations adjacent to a soil-steel structure with relative ease. As a preliminary study toward achieving this objective, the adaptability of in situ penetration testing techniques for the evaluation of the backfill condition adjacent to soil-steel structures was investigated. The objective of the laboratory testing program was to develop a procedure whereby the relative density of the backfill could be evaluated by performing a penetration test. It is assumed that with a knowledge of the in situ relative density characteristics of a backfill, its strength and deformability characteristics can be estimated through laboratory tests on samples of the granular material that are compacted to the measured relative density. The stages in the development of the laboratory device for impact penetration testing are summarized. The dynamics of projectiles penetrating geological media has attracted the attention of engineers and scientists for almost the past three centuries (*31–35*). Certain preliminary results of impact penetration tests conducted on moist dense sand and loosely placed crushed granular A aggregate are presented.

EXPERIMENTAL INVESTIGATIONS

The primary objective of the study was to develop a relatively simple testing technique wherein a cone penetration device is inserted into a compacted granular soil adjacent to a rigid or flexible structural boundary. The boundary represents the conduit wall of a soil-steel structure. The constraints imposed on the penetration testing methodology were the following: (*a*) the orientation of the penetration device should be approximately normal to the plane of the rigid boundary, (*b*) the penetration device should be driven without the aid of a reaction frame, and (*c*) the energy imparted to the penetration device should be standardized and controllable. Two types of penetration tests were performed with these constraints in mind. The test procedures are outlined in the ensuing sections.

Cone Penetration Device

A number of cone penetration devices are used in in situ testing of both granular and cohesive soils. The devices are characterized in relation to the angle of the cone device, which can range from 30 to 60 degrees. In this investigation, the cone angle was set at 60 degrees, and the diameter of the cone device was 1.4 in. Details of the stainless steel cone penetration device are shown in Figure 1. The cone section of the device was attached to a load cell to measure loads applied to the cone tip during an experiment. In this series of preliminary tests, however, no attempt was made to measure the loads induced at the conical tip of the penetrometer. The device has appropriate couplings that allow the connection to loading devices.

Loading Procedures

Two types of horizontal cone penetration tests were conducted with the device. In the first type of test, the cone penetration device was attached to a horizontally mounted MTS servo-controlled hydraulically driven actuator, which can apply a constant rate of penetration of 0.1 in./min. Details of the experimental procedure are shown in Figure 2. In this loading procedure a load cell attached to the actuator is used to measure the total load acting on the cone penetration device. The tests were carried out in a concrete test tank 60 in. long, 36 in. wide, and 48 in. deep (Figure 2). The reaction frames required for the application of the loads were attached to the test tank. The second series of tests involved the application of an impact load to the penetration device. The device used for the application of the impact load was a Low

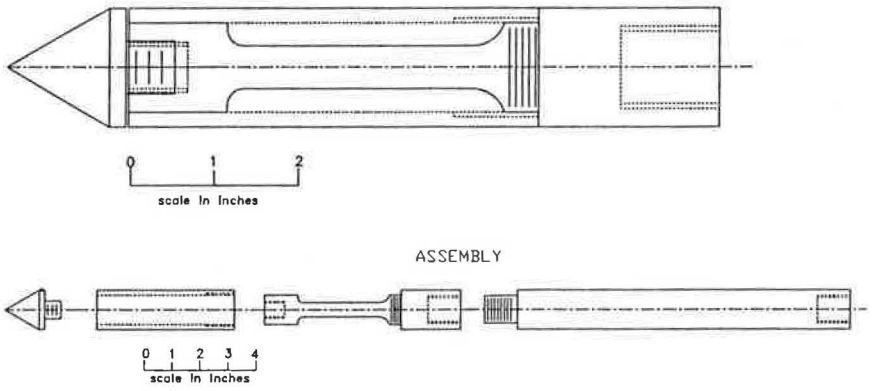

FIGURE 1 Details of the cone penetration device.

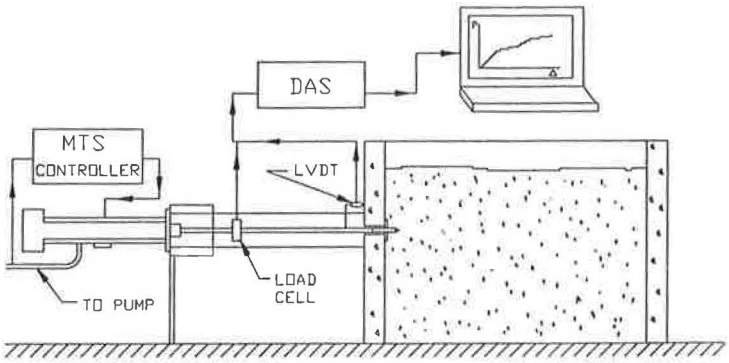

FIGURE 2 Penetration testing facility: constant rate of penetration of the cone device.

Velocity Powder Actuated Tool (HILTI Model DX 36M). The energy input to an impact was controlled by the selection of a charge type (HILTI Cartridge #2; Brown Extra Light; No. 000502906 CAL. 27 Short). Special couplings were designed to guide the energy of the impact to the penetration device. Figures 3 and 4, respectively, show the facilities and the stages in the application of the impact load to the cone penetration device.

Testing Facilities

The quasi-static penetration tests that used the MTS device were performed in the test facility shown in Figure 2. The inside of the tank was lined with stainless steel sheets, and a metal plate was incorporated at the region where the cone penetration tests were performed. The entry point for the cone penetration device was cut out in the metal plate, and an aluminum foil barrier was installed. To prevent extrusion of the soil through the aluminium foil barrier during compaction, a solid cap was installed flush with the inner face of the metal plate. Using this procedure, adequate compaction of the soil was achieved in the vicinity of the rigid plate without damage to the soil retention barrier and the attendant loosening of the soil in the cone penetration zone. The impact cone penetration tests were performed in a test tank measuring approximately 95 × 83 in. in plan area and 72 in. in depth. The details of the test facility are shown in Figure 5. The end sections of the facility were fabricated of steel channel sections. A channel section near the base of the test tank was provided with circular cutouts for conducting the cone penetration tests. Altogether three slots were provided on each side of the test tank. The locations of the penetration test are shown in Figure 5. Here again, the apertures in the channels were provided with the metal foil–metal plate restraining system to allow retention of the soil during compaction and penetration testing. In the impact cone penetration tests, the cone device was guided through a teflon-lined aluminum housing. The housing was directly attached to the end-channel sections of the test tank.

Material Preparation

Two types of granular materials were used in the investigations. The first was classified as a mortar sand (D_{10} = 0.01 in., C_u = 3, and C_c = 0.95). The mortar sand was used in both test tanks shown in Figures 2 and 5. Because of the small dimensions of the tank shown in Figure 2, it was not feasible to use mechanical methods for the compaction of the sand. The sand was compacted manually using a tamper weighing 12 lb and a standard number of impacts applied by a free fall from a height of approximately 6 to 9 in. This compaction scheme has been used effectively in other experiments, and the resulting density can be controlled reasonably accurately (*36,37*). In the experiments involving constant rate of penetration of the cone penetration device, the mortar sand was compacted to a bulk unit weight of 170 lb/ft^3 at a moisture content of approximately 4.5 percent. The density of the compacted mortar sand was measured using a nuclear density meter (TROXLER 3401). The compaction of the sand in the larger test tank was carried out by using a vibratory plate compactor (Vibroplate MIKASA 52G), which makes it possible to attain good compaction of the moist sand at the end regions of the test tank, where the cone penetration tests will be conducted. Using the vibratory plate compactor, the moist sand was compacted to a bulk unit weight of 117 lb/ft^3. Again in this case the nuclear density meter was used to ascertain the in situ density of the compacted moist sand. A crushed granular A material (D_{10} = 0.008 in., C_u = 50, and C_c = 3.1) was also used in this series of preliminary investigations. The material was placed in a loose state and manually compacted with a tamper. Because of the loose placement of the crushed granular A material, it was not possible to attain good control of density within the compacted regions. The bulk unit weight of the granular A material varied from approximately 107 to 112 lb/ft^3. These two extreme density variations were observed at the end regions of the test tank, the locations for the penetration tests.

EXPERIMENTAL RESULTS AND DISCUSSION

Three experiments were performed in which cone penetration into the compacted sand was achieved at a constant rate of 0.1 in./min. Figure 6 shows the variation of the load-displacement response for the cone penetration device. The penetration resistance has a characteristic shape indicated by a near-bilinear form. The first linear portion roughly corresponds to the complete penetration of the conical part of the device into the compacted sand. The second linear portion of the load-displacement curve is indicative of the frictional resistance

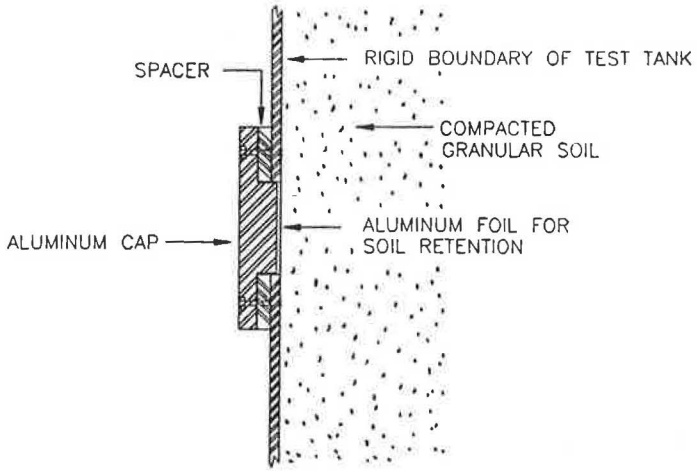

(A) APERTURE IN BOUNDARY OF TEST TANK AND SOIL ARRANGEMENT FOR SOIL RETENTION

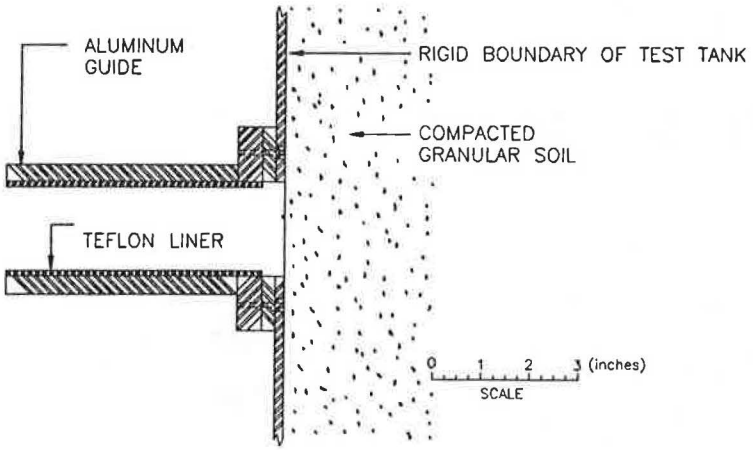

(B) TEFLON LINED GUIDE FOR POSITIONING OF CONE PENETRATION DEVICE

FIGURE 3 Entry point arrangement in the impact cone penetration testing.

generated along the cylindrical portion of the penetrating device. The maximum load measured in the test was about 1,600 lb and occurred at a penetration of approximately $4D$, where D is the diameter of the cone.

The results of the impact cone penetration tests conducted on both dense moist sand and loosely placed granular A material are shown in Figure 7. The results for the normalized penetration values are plotted as a function of the number of impacts applied to the device. The results derived from tests conducted on compacted mortar sand indicate a great deal of uniformity. In these tests the maximum cone penetration for tests conducted in dense sand was about $2D$, and for tests conducted in loosely placed granular A it was about $3.8D$.

CONCLUSIONS

The evaluation of the condition of a backfill behind the conduit wall of a soil-steel structure is an important consideration in the assessment of the load-carrying capacity of the soil-steel structure. Accurate assessment of the backfill condition can lead to an improved estimate of the integrity of the soil-steel structure system. In situ testing techniques offer the most reliable means for estimating the condition of the backfill. The most convenient method for evaluating the condition of the backfill nearest the conduit is to introduce the testing device through the conduit wall. The alternative method of introducing the testing device through the top of the embankment is both time-consuming and expensive. Furthermore, the interpretation of such a test must take into consideration the influence of a flexible soil-steel structure. The technique of introducing the testing device through the conduit wall limits the use of many of the conventional methods of in situ testing, such as the pressuremeter, screw plate, flat plate dilatometer, and so forth.

Cone penetration tests offer a suitable alternative to the aforementioned in situ tests. The conventional modes of cone

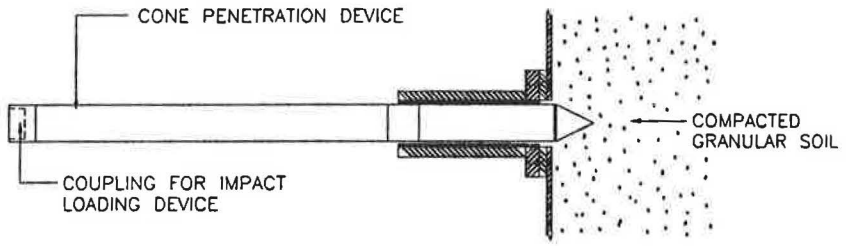

(A) INITIAL POSITIONING OF CONE PENETRATION DEVICE IN GUIDE

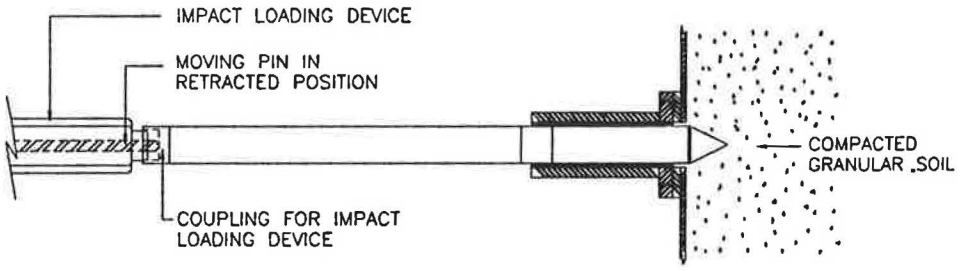

(B) LOCATION OF LOADING DEVICE IN COUPLING PRIOR TO APPLICATION OF IMPACT LOAD

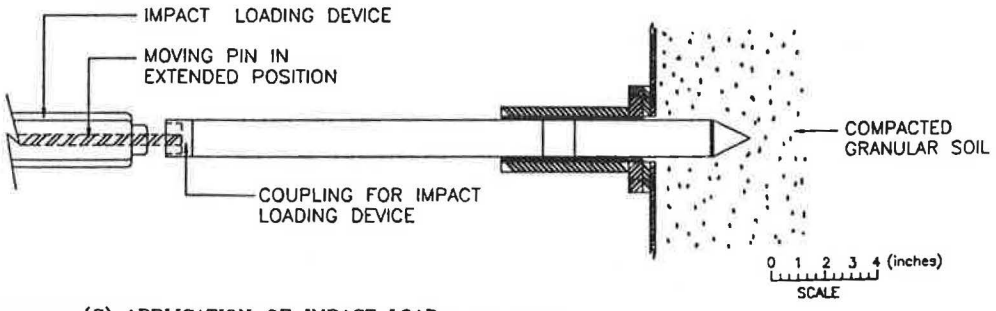

(C) APPLICATION OF IMPACT LOAD

FIGURE 4 Stages in the impact cone penetration testing.

penetration testing invariably focus on techniques in which the cone penetration is vertical and suitable reaction frames are available for the application of the loads. With regard to backfill testing through the conduit wall of the soil-steel structure, these procedures are of limited applicability. Furthermore, the constraints of ease of use and portability of testing equipment necessitate development of an impact cone testing device. The primary objective is to ascertain the condition of the backfill by correlating the penetration resistance of an impact cone device with the relative density of the backfill. The stages in the develpment of an impact cone penetration device tested under laboratory conditions have been documented. The laboratory studies included the design of a cone penetration device and the identification of a method of applying impact loads to the cone device. The results of the preliminary laboratory studies indicate that the impact penetration resistance, as indicated by the penetration ratio Δ/D (where Δ is the penetration and D is the diameter), at impacts in excess of 20 exhibit a reasonably linear variation, and the slope of the plot of Δ/D versus N can be used as an indicator or penetration resistance index for the relative density of the granular material.

As emphasized previously, the impact penetration testing scheme described is a preliminary laboratory investigation that requires further laboratory study and field verification. The future research program could include the following:

1. Development and standardization of the dimensions of the cone and its materials,
2. Standardization of the impact energy input to the cone penetration device and the evaluation of the rate of energy input by force-velocity measurements,

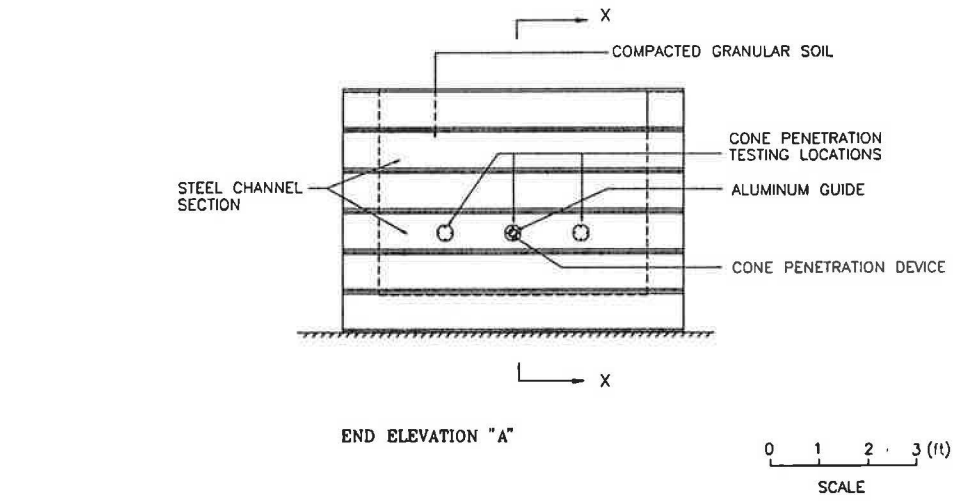

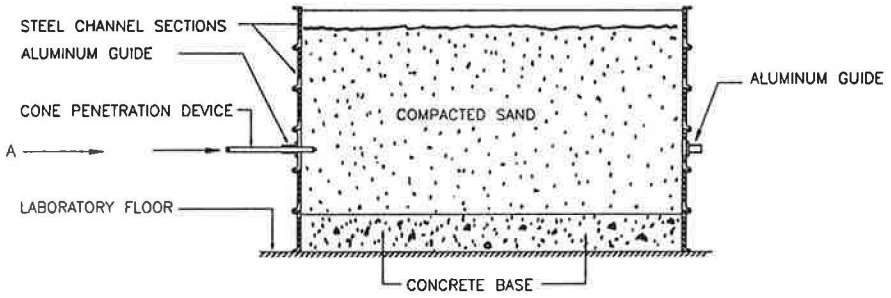

FIGURE 5 Penetration testing facility: impact penetration of the cone device.

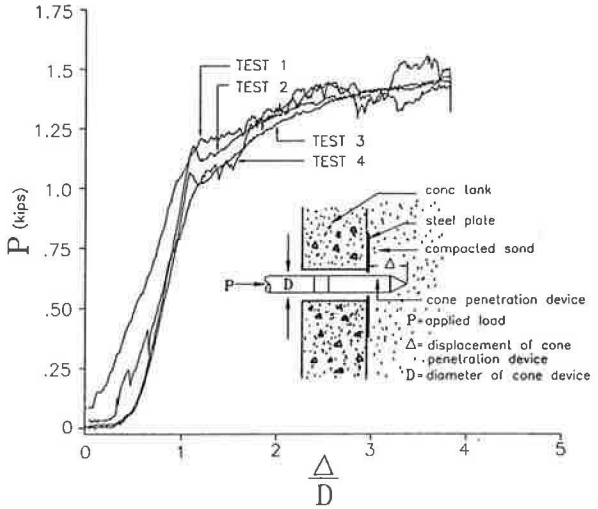

FIGURE 6 Load-penetration data for constant rate of penetration tests conducted on compacted sand.

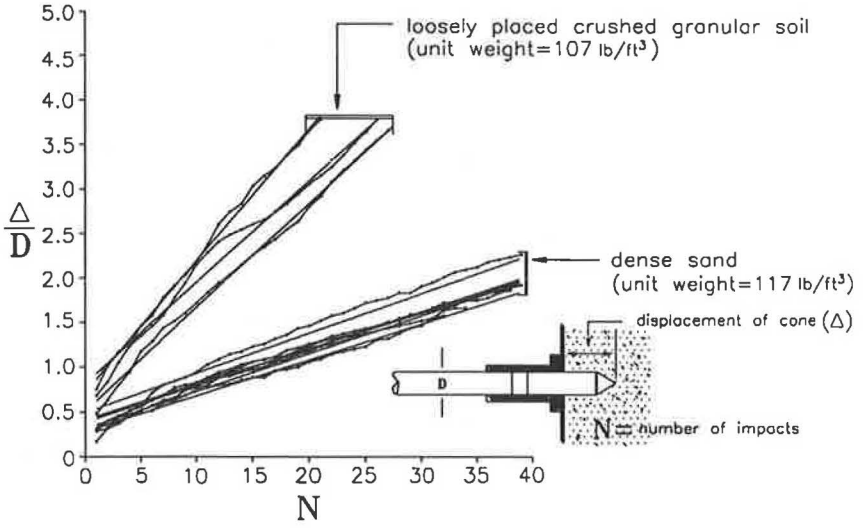

FIGURE 7 Penetration-impact number data for penetration tests conducted on densely compacted sand and loosely placed crushed granular A.

3. Extensive laboratory studies involving sand and crushed gravel that are compacted to specified densities at known moisture contents,
4. The development of correlation between relative density and penetration resistance for various granular backfill materials,
5. Extension of the studies to include poor-quality backfill materials,
6. Adaptation of the impact cone penetration device for in situ use,
7. Field trials involving the impact cone penetration device and existing and newly constructed soil-steel structures, and
8. Theoretical evaluation of the penetration mechanics of the impact cone penetration device.

ACKNOWLEDGMENTS

The work described in this paper was supported in part by a research contract awarded by the Ministry of Transportation of Ontario, Downsview, Ontario. The author appreciates the valuable advice and assistance given by K. C. McMartin of Carleton University and L. Fearn, L. McLeod, and Yue Sheng.

REFERENCES

1. *Transportation Research Record 878*, TRB, National Research Council, Washington, D.C., 1982 (entire issue).
2. J. M. Duncan. Behavior and Design of Long-Span Metal Culverts. *Journal of the Geotechnical Engineering Division*, ASCE, Vol. 105, 1979, pp. 399–418.
3. B. Bakht. Soil-Steel Structure Response to Live Loads. *Journal of the Geotechnical Engineering Division*, ASCE, Vol. 107, 1981, pp. 779–798.
4. J. M. Duncan and J. K. Jeyapalan. Deflection of Flexible Culverts due to Backfill Compaction. In *Transportation Research Record 878*, TRB, National Research Council, Washington, D.C., 1982, pp. 10–17.
5. B. Bakht and A. C. Agarwal. On Distress in Pipe-Arches. *Canadian Journal of Civil Engineering*, Vol. 15, 1988, pp. 589–595.
6. In Situ Measurement of Soil Properties. *Proceedings of the ASCE Special Conference*, Vols. 1 and 2, Raleigh, N.C., 1975.
7. M. C. Ervin (ed.). In Situ Testing for Geotechnical Investigations. *Proceedings of the Extension Course*, Sydney, Australia, A. A. Balkema, Rotterdam, the Netherlands, 1983.
8. A. S. Balasubramaniam, S. Chandra, and D. T. Bergado (eds.). Recent Developments in Laboratory and Field Tests and Analysis of Geotechnical Problems. *Proceedings of the International Symposium*, Bangkok, Thailand, A. A. Balkema, Rotterdam, the Netherlands, 1986.
9. J. H. Schmertmann. *Guidelines for Cone Penetration Test Performance and Design. FHWA, Report FHWA-TS-78-209*. U.S. Department of Transportation, 1978.
10. A. Verruijt, F. L. Beringen, and E. H. de Leeuw (eds.). Penetration Testing. *Proceedings of the 2nd European Symposium on Penetration Testing*, Amsterdam, Vols. 1 and 2, A. A. Balkema, Rotterdam, the Netherlands, 1982.
11. C. P. Wroth, The Interpretation of In Situ Soil Tests, 24th Rankine Lecture. *Geotechnique*, Vol. 34, 1984, pp. 449–489.
12. A. W. Skempton. Standard Penetration Test Procedures and the Effect in Sands of Overburden Pressure, Relative Density, Particle Size, Ageing and Overconsolidation. *Geotechnique*, Vol. 36, 1986, pp. 425–447.
13. J. K. Mitchell. New Developments in Penetration Tests and Equipment. *Proceedings of the International Symposium on Penetration Testing I*, Vol. 1, 1988, pp. 245–261.
14. C. P. Wroth. Penetration Testing—A More Rigorous Approach to Interpretation. *Proceedings of Penetration Testing*, ISOPT, Orlando, Fla., Vol. 1, 1988, pp. 303–311.
15. M. Jamiolkowski and P. K. Robertson. Future Trends for Penetration Testing. *Proceedings of the Geotechnology Conference on Penetration Testing*, Birmingham, United Kingdom, Thomas Telford, 1988, pp. 321–342.
16. D. A. Ardus (ed.). Offshore Site Investigation. *Proceedings of a Conference*, Graham and Trottman, London, 1980.
17. J. M. Konrad and K. T. Law. Undrained Shear Strength from Piezocone Tests. *Canadian Geotechnical Journal*, Vol. 24, 1984, pp. 392–405.
18. D. Windle and C. P. Wroth. In Situ Measurement of the Properties of Stiff Clays with Self-Boring Instrument. *Proceedings of the 9th International Conference Soil Mechanics and Foundation Engineering*, Tokyo, Vol. 1, 1977, pp. 347–352.
19. F. Baguelin, J. F. Jezequel, and D. H. Shields. *The Pressuremeter and Foundation Engineering*, Trans Tech Publications, Clausthal, 1978.
20. A. P. S. Selvadurai. Large Strain and Dilatancy Effects in a

Pressuremeter. *Journal of Geotechnical Engineering*, ASCE, Vol. 110, 1984, pp. 431–436.
21. J. M. O. Hughes and P. K. Robertson. Full Displacement Pressuremeter Testing in Sand. *Canadian Geotechnical Journal*, Vol. 22, 1985, pp. 298–307.
22. S. Marchetti. In Situ Tests by Flat Plate Dilatometer. *Journal of the Geotechnical Engineering Division*, ASCE, Vol. 106, 1980, pp. 299–321.
23. A. J. Lutenegger. Current Status of the Marchetti Dilatometer Test. *Proc. International Symposium on Penetration Testing*, Vol. 1, 1988, pp. 137–155.
24. O. Kummeneje and O. Eide. Investigation of Loose Sand Deposits by Blasting. *Proc., 5th International Conference on Soil Mechanics and Foundation Engineering*, Paris, Vol. 2, 1961, pp. 491–497.
25. R. Dahlberg. *Settlement Characteristics of Preconsolidated Natural Sands*. Report ISBN 91-540-2410-2. National Swedish Institute for Building Research, Stockholm, Sweden, 1975.
26. A. P. S. Selvadurai and T. J. Nicholas. A Theoretical Assessment of the Screw Plate Test. *Proc. International Conference on Numerical Methods in Geomechanics*, Aachen, Germany, Vol. 3, 1979, pp.1,245–1252.
27. A. P. S. Selvadurai, G. E. Bauer, and T. J. Nicholas. Screw Plate Testing of a Soft Clay. *Canadian Geotechnical Journal*, Vol. 17, 1980, pp. 465–472.
28. A. P. S. Selvadurai. On the Screw Plate and Auger Testing of Soft Clay. *Proc. International Symposium on Soil and Rock Investigation by In Situ Testing*, Paris, Vol. 2, 1982, pp. 379–384.
29. A. P. S. Selvadurai. The Use of Auger-Type Devices for the In Situ Testing of Soft Sensitive Clays. *Geotechnical Engineering*, Vol. 15, 1984, pp. 59–70.
30. A. P. S. Selvadurai and K. R. Gopal. Consolidation Analysis of the Screw Plate Test. *Proc. 39th Canadian Geotechnical Conference*, 1986, pp. 167–178.
31. L. Euler. *Neue Grundsatze der Artillerie*. Berlin. Reprinted as *Euler's Opera Omnig*. Druck und Verlag von B. G. Teubner, Berlin, 1922.
32. B. Robins. *New Principles of Gunnery*. London, 1742.
33. W. A. Allen, E. B. Mayfield, and H. L. Morrison. Dynamics of a Projectile Penetrating Sand. *Journal of Applied Physics*, Vol. 28, 1957.
34. M. E. Backman and W. Goldsmith. The Mechanics of Penetration of Projectiles into Targets. *International Journal of Engineering Science*, Vol. 16, 1978, pp. 1–99.
35. M. J. Forrestal. Penetration into Dry Porous Rock. *International Journal of Solids and Structures*, Vol. 22, 1986, pp. 1,485–1,500.
36. A. P. S. Selvadurai. The Enhancement of the Uplift Capacity of Buried Pipelines by the Use of Geogrids. *Journal of Geotechnical Testing*, ASTM, Vol. 12, 1989, pp. 211–216.
37. A. P. S. Selvadurai and C. T. Gnanendran. An Experimental Study of a Footing Located on Sloped Fill; Influence of a Soil Reinforcement Layer. *Canadian Geotechnical Journal*, Vol. 26, 1989, pp. 467–473.

Publication of this paper sponsored by Committee on Subsurface Soil-Structure Interactions.

Structural Performance of an Aluminum Box Culvert

J. O. HURD, S. M. SARGAND, G. A. HAZEN, AND S. R. SUHARDJO

Corrugated metal box-type culverts are increasingly used as replacements for short-span bridges. Their lightness, relatively easy and quick transportation and construction procedures, and lower cost make them attractive in many instances for short-span bridges. Because they are flexible, the flexural stiffness and moment capacity of the structural plates are increased with stiffeners placed along the length of the culvert. A corrugated box culvert carries most of its load through interaction between the culvert and the surrounding backfill. Results of field tests performed on an aluminum low-profile, box culvert during the construction sequence and live load application are evaluated, experimental results are compared with results obtained from the CANDE finite element computer program solutions, stress disruption at bolts is evaluated, and the composite action between rib and plate is determined.

The soil-structure interaction problem involves complex nonlinearity that is due to the contact between the culvert and the backfill materials and the stress-strain behavior of geologic media surrounding the culvert. The performance of corrugated box-type culverts is influenced by several factors, such as geometry, construction sequences, structural joint slippage, type of backfill material, and degree of compaction (*1*). Several previous investigations have contributed to the analysis of box culverts.

Duncan et al. (*2*) performed finite element analysis to develop design equations for crown and haunch moment capacities. Their analysis was performed on aluminum box-type culverts with different spans and rises when subjected to varying cover depths and live loads. They conducted a full-scale field test on a stiffened box-type culvert, and results were compared with finite element analysis. On the basis of this study, a simplified design method for determining the bending moments at the haunch and crown region for different spans, cover depths, and vehicle loads was proposed.

Hurd and Sargand (*3*) measured the geometry of various sizes and shapes of culverts in service for many years. They analyzed the culverts with the CANDE program and concluded that the variation between design and true geometry has a significant effect on deflection, moment, and thrust.

Beal (*4*) instrumented a corrugated aluminum culvert at 16 locations spaced around the structure's circumference at midspan. Corrugated aluminum plate with reinforcing ribs was also tested in the laboratory. From the field and laboratory tests and analytical results, Beal concluded that for deeply buried culverts (*a*) backfill placement sequence results in distortion of culvert shape; (*b*) live load stresses were small compared with dead load stresses; and (*c*) computed design estimates of thrusts were greater than measured values, and computed design estimates of moments were less than measured values. Curvature was measured to determine plate moments, because thrust was assumed to be negligible.

Seed and Ou (*5*) concluded that a higher degree of compaction significantly improves the agreement between field measurements and finite element analysis. Moreover, finite element analysis that does not model compaction greatly underestimates culvert deformations, stresses, and axial thrusts.

J. O. Hurd, Ohio Department of Transportation, 25 South Front Street, Room 620, Columbus, Ohio 43215. S. M. Sargand, G. A. Hazen, and S. R. Suhardjo, Department of Civil Engineering, Ohio University, Athens, Ohio.

FIELD STUDY

The aluminum box culvert selected for testing has a span of 14 ft 10 in., a rise of 4 ft 10 in., and a length of 42 ft. The crown and the sides were constructed of corrugated aluminum plates 0.2 and 0.175 in. thick, respectively. The corrugation has a 9-in. pitch and a 2.5-in. depth with Type IV bulb-angle stiffening ribs located every 18 in. at the crown and Type II stiffening ribs every 27 in. at the side. All the ribs were bolted on the outside plate only. The ends of the structural plate were anchored into a 3- × 3-ft reinforced concrete strip footing on either side.

Six sections were chosen across the mid-length to measure strains, as shown in Figure 1. It was assumed that bending and normal stresses on the rib occur in the direction of its length, because the culvert is flexible transverse to this axis. The structural plate is characterized by a biaxial strain field. At each section, two biaxial strain gauges were attached to the inside corrugated plate, and two uniaxial gauges were attached to the outer rib, as shown in Figure 2.

The strain gauge rosette patterns were installed near three bolt holes, as shown in Figure 3, to evaluate the stress concentration around the bolts. A total of 30 rosette gauges were mounted. At each of the bolt hole locations, the strain gauge rosettes were installed at 0-, 45-, and 90-degree planes clockwise with respect to the horizontal culvert axis across the corrugation where the rib is attached. Five vibrating wire strain gauges were cemented on the inside plate, and four more were cemented on the outer rib. Two horizontal rod extensometers at the springline of both sides of the culvert and two more 6 in. above the crown in the soil cover were installed to monitor soil movements.

Eleven points were established around the culvert periphery as shown in Figure 4 to measure deflections. Measurements were made using a tape extensometer with respect to

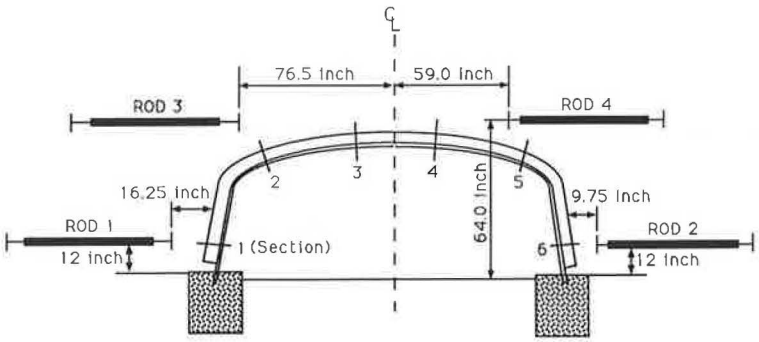

FIGURE 1 Location of measuring instruments.

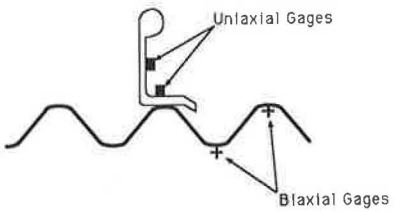

FIGURE 2 Typical location of strain gauges.

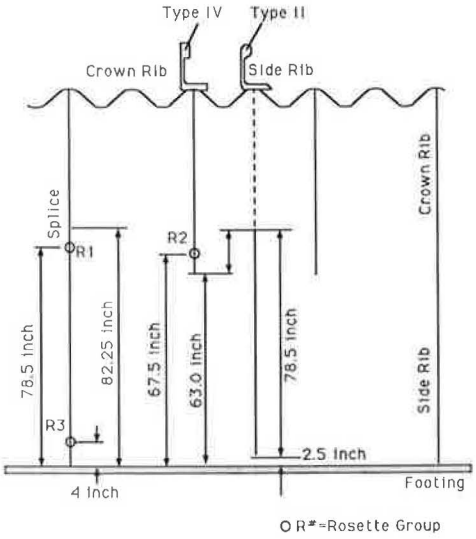

FIGURE 3 Location of rosette group.

two reference points located in the streambed. The movements of these reference points were monitored by level circuit surveying.

The initial readings for all measurements were taken when the fill height and the footing were at the same level. A gravelling sand backfill material was placed in about 6- to 12-in. lifts, alternately, on both sides of the culvert. Each lift was watered and then compacted with vibratory plate compactors. The density was monitored with a Troxler nuclear density gauge; at least 95 percent of the standard Proctor maximum dry density was required to continue backfill placement. Readings of strain, displacement, and soil deformation were monitored simultaneously for each backfill lift. When the backfill reached 68 in. above the footing or 10 in. above the top crown, 9 in. of subgrade was placed in two lifts of 4 in. and 5 in. each. This was followed by 1 ft of asphalt pavement in three lifts. Only the first two lifts of 4 in. and 5 in. were monitored. The whole process, from backfilling to paving, was completed in 11 days. Eight days after the final pavement was placed, static live load tests were conducted at five positions to establish the critical loading conditions (see Figure 5). A series of live loads consisting of 16, 32, and 42 kips was applied to the culvert-soil system by means of a dump truck loaded on its rear with crushed limestone. The truck was positioned so that its rear axle was centered at the five positions. The middle axle tires on both sides were deflated before any measurements were made.

RESULTS AND DISCUSSION

The crown moved upward during the early stages of backfilling. The upward movement was due to the lateral inward

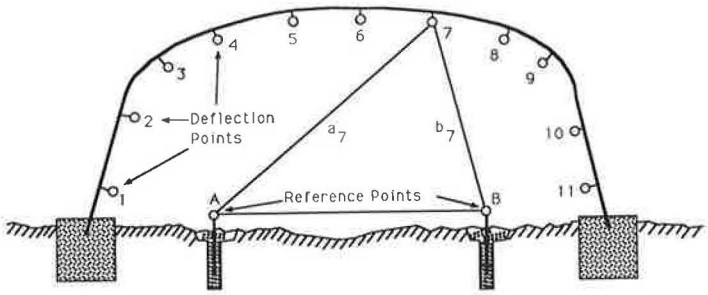

FIGURE 4 Deflection measurement circuit.

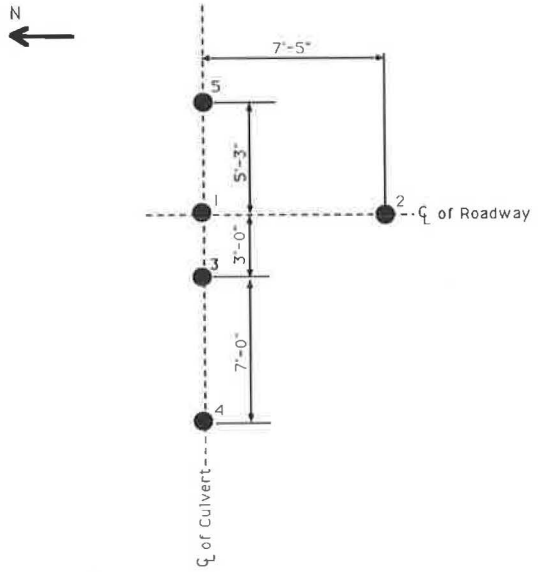

FIGURE 5 Live load application positions.

pressure of the compacted backfill. As the fill height approached the crown, the crown began to move downward. The downward deflection increased with the height of backfill. Figure 6 shows the downward movement.

Tables 1 and 2 give the soil displacements during backfill and live load, respectively. It is clear that Rod Extensometers 1 and 2 extended in length during the early stages of backfill. This trend agreed with deflection results of the sidewall of culvert, which verified that the sides of the culvert experienced inward deflection during early stages of backfill. As backfill material was placed above the crown, Rod Extensometers 3 and 4 also contracted. The results verified that the sides of the culvert deflected outward after backfill above the crown level.

During the application of live load, all of the rod extensometers except Rod Extensometer 1 contracted. In addition, live load position did not have much effect on rod displacements.

Through the backfill process, the culvert was shifted laterally. The lateral shift might be the result of the imbalance in backfilling procedure and the degree of flexibility of the culvert structure. The deflections caused by live load alone

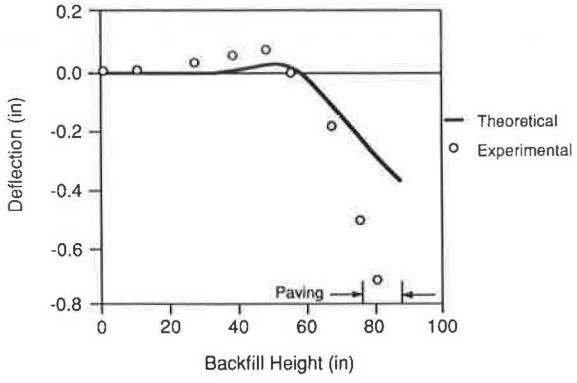

FIGURE 6 Vertical crown deflection during backfilling and paving.

TABLE 1 SOIL DISPLACEMENT DURING BACKFILL

Backfill Height (inch)	North Spring Line (Rod 1)	South Spring Line (Rod 2)	North Spring Line (Rod 3)	South Spring Line (Rod 4)
20	0.0000	0.0000	-	-
28	-0.0002	-0.0107	-	-
34	-0.0017	-0.0417	-	-
42	-0.0022	-0.0522	-	-
48	-0.0070	-0.0597	-	-
52	-0.0113	-0.0662	-	-
60	-0.0172	-0.0785	-	-
68	-0.0140	-0.0717	0.0217	0.0183
72	-0.0087	-0.0698	0.0250	0.0150
77	0.0005	-0.0650	0.0300	0.0250
81	0.0038	-0.0558	0.0233	0.0603
86	0.0102	-0.0483	0.0655	0.0748

Note: The symbol dash (-) indicates that the data copuld not be obtained since Rods 3 & 4 were installed when the backfill height reached 68 inches.

TABLE 2 SOIL DISPLACEMENT DUE TO LIVE LOAD

Live Load and Position		North Spring Line (Rod 1)	South Spring Line (Rod 2)	North Spring Line (Rod 3)	South Spring Line (Rod 4)
16 kip	1	-0.0100	0.1733	0.0900	0.0967
	2	-0.0100	0.1733	0.0883	0.1000
	3	-0.0120	0.1667	0.0867	0.0833
	4	-0.0100	0.1717	0.0867	0.0967
	5	-0.0100	0.1733	0.0883	0.0967
32 kip	1	-0.0067	0.1767	0.0950	0.1050
	2	-0.0067	0.1783	0.0933	0.0917
	3	-0.0067	0.1783	0.0950	0.1050
	4	-0.0083	0.1767	0.0900	0.1017
	5	-0.0083	0.1750	0.0900	0.0967
42 kip	1	-0.0005	0.1800	0.1033	0.1200
	2	-0.0005	0.1850	0.1000	0.0967
	3	0.0000	0.1850	0.1017	0.1133
	4	-0.0016	0.1800	0.0950	0.1100
	5	-0.0016	0.1800	0.0967	0.0733

were considerably lower than those caused by the construction sequence. Several loading positions were examined. Position 1 gave the maximum crown deflection due to live loads of 16, 32, and 42 kips, as shown in Figure 7. Deflections are within design tolerance.

A comparison was made between composite and noncomposite values of moment and thrust. After comparing the results and observing disagreement between the composite and noncomposite values, it was decided to base the analysis on noncomposite values.

The results of the bending moment due to backfill and live load in all five positions are given in Tables 3 and 4, respectively. The moment at the crown changed sign from negative before the fill reached the crown to positive after the fill covered the crown. At the haunch the moments increased in magnitude with constant negative signs. At the springline the moment values were small.

Moments are not significant when the backfill is at the haunch level. Moment is not symmetric during construction. This may be due to a shift in the culvert during asymmetric placement of backfill. Moments measured in the sides and crowns were of approximately the same magnitude. Maximum moment was observed during asphalt paving. It was found that the maximum moment occurred during live load appli-

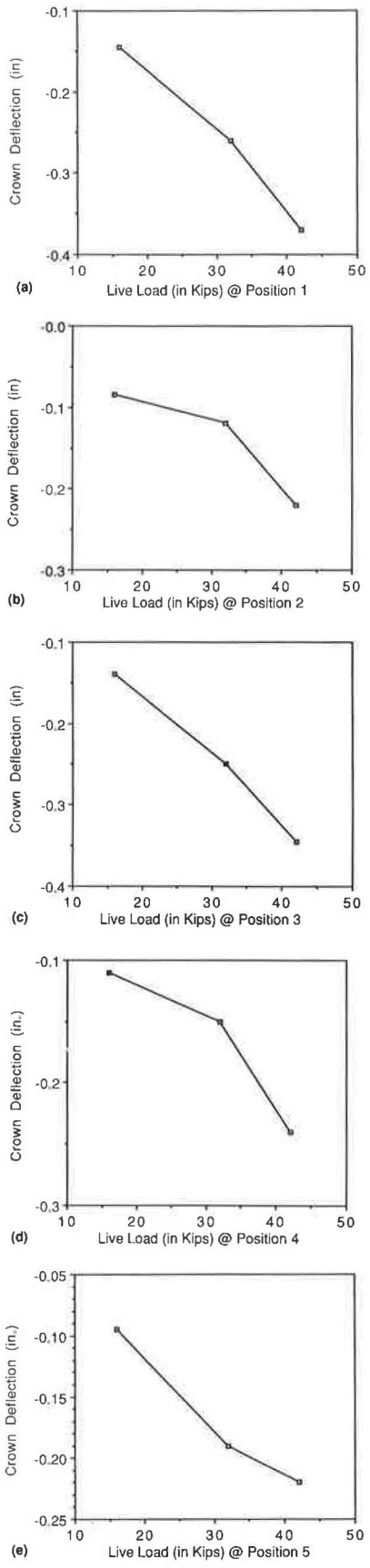

FIGURE 7 Vertical crown deflections under live load application.

TABLE 3 BENDING MOMENT DURING BACKFILL

Backfill Height (inch)	Bending Moment (kip-ft./ft.) @ Section : 1	2	3	4	5	6
12	-0.030	-0.116	-0.193	-0.093	0.036	0.124
20	-0.001	-0.103	-0.307	-0.158	0.033	0.164
28	-0.008	-0.387	-0.263	-0.505	0.012	0.322
34	-0.010	-0.421	-0.167	-0.690	0.067	0.351
40	0.024	-0.464	-0.312	-0.667	0.071	0.365
48	0.067	-0.486	-0.065	-0.740	0.043	0.361
52	0.219	-0.463	-0.005	-0.778	-0.071	-0.019
60	0.240	-0.446	-0.124	-0.807	-0.042	0.023
68	0.201	-0.689	-0.079	-0.121	-0.103	0.085
72	0.110	-0.831	0.052	0.592	-0.192	0.040
77	0.084	-0.912	0.687	0.700	-0.493	0.049
81	-0.044	-1.415	1.135	1.339	-0.861	0.052
86	-0.070	-1.541	1.545	1.364	-0.967	0.014

TABLE 4 BENDING MOMENT DUE TO LIVE LOAD

Live Load and Position		Bending Moment (kip-ft./ft.) @ Section : 1	2	3	4	5	6
16 kip	1	-0.023	-0.219	0.220	0.164	-0.145	0.096
	2	-0.007	-0.040	-0.100	0.143	-0.031	0.085
	3	-0.050	-0.185	0.173	0.200	-0.130	0.094
	4	-0.038	-0.109	0.061	0.121	-0.076	0.095
	5	-0.032	-0.040	-0.041	-0.002	-0.081	0.150
32 kip	1	-0.082	-0.568	0.661	0.216	-0.330	0.100
	2	-0.033	-0.128	-0.254	0.253	-0.152	0.022
	3	-0.143	-0.479	0.561	0.360	-0.342	0.037
	4	-0.118	-0.229	0.243	0.120	-0.188	0.087
	5	-0.083	-0.104	-0.029	0.146	-0.107	0.061
42 kip	1	-0.138	-0.885	0.529	0.768	-0.697	0.066
	2	-0.077	-0.275	-0.391	0.619	-0.404	-0.046
	3	-0.260	-0.654	0.680	0.328	-0.530	0.023
	4	-0.195	-0.485	0.290	0.165	-0.436	0.009
	5	-0.137	-0.219	-0.032	0.119	-0.234	-0.016

cation at Position 1. For the live load of 42 kips the moment was close to the maximum backfill moment.

Thrust results obtained during backfill and live load applications are given in Tables 5 and 6, respectively. For the crown region, except during the early stages of backfill, thrusts were always compressive, and their magnitude increased with the backfill height. At the haunch region, thrusts were negative and small compared with the crown. At the springline, in the

TABLE 5 AXIAL THRUST DURING BACKFILL

Backfill Height (inch)	Axial Thrust (kip/ft.) @ Section : 1	2	3	4	5	6
12	1.70	1.46	1.73	0.60	1.34	0.26
20	1.38	1.75	1.74	0.61	1.48	0.45
28	-0.38	5.03	0.05	0.20	2.69	0.87
34	-0.48	6.46	0.64	0.03	3.80	0.95
40	-0.79	3.06	0.67	0.46	3.98	-1.04
48	-2.07	6.63	-1.34	-0.31	3.60	-0.60
52	-1.56	6.39	-1.15	-0.76	2.88	-3.56
60	-1.39	6.24	-1.30	-0.82	2.97	-3.22
68	-4.83	5.90	-2.37	-2.41	3.05	-3.10
72	-4.76	5.92	-5.93	-9.22	3.13	-3.69
77	-5.17	6.34	-12.62	-12.66	2.50	-3.51
81	-6.46	5.63	-14.32	-16.06	1.78	-4.19
86	-7.19	5.64	-17.44	-18.17	0.85	-4.61

TABLE 6 AXIAL THRUST DUE TO LIVE LOAD

Live Load and Position		Axial Thrust (kip/ft.) @ Section : 1	2	3	4	5	6
16 kip	1	-0.562	-1.496	-1.597	-1.775	-1.229	-0.606
	2	-0.133	-0.304	-0.725	-1.342	-0.649	-1.470
	3	-0.754	-1.017	-0.578	-0.871	-0.982	-0.858
	4	-0.376	-0.411	0.039	-0.266	-0.681	0.680
	5	0.167	0.050	0.214	-0.679	-0.394	-0.943
32 kip	1	-0.580	-2.709	-5.578	-3.758	-2.363	-0.526
	2	0.450	-0.278	-2.646	-2.602	-1.342	-1.910
	3	-1.239	-1.756	-1.701	-0.908	-1.418	-0.807
	4	-0.644	-0.055	-0.146	0.106	-0.925	-0.294
	5	0.349	0.313	0.524	0.537	-0.115	-0.491
42 kip	1	-1.435	-3.884	-6.737	-5.782	-3.088	-0.037
	2	-0.008	-0.793	-3.534	-4.205	-2.439	-2.311
	3	-2.004	-1.838	-1.789	-0.920	-2.040	-0.216
	4	-0.798	-0.843	-0.797	0.375	-1.575	-0.055
	5	0.634	-0.170	0.325	1.421	-2.005	1.414

early backfill stage, negative thrusts developed and became positive as backfill material height reached 34 in. Thrusts were found to be largest at Position 3 because of live load application. Thrust in the culvert was measured under live loads of 16, 32, and 42 kips. In this culvert, values of thrust vary from 3 to 12 kips under a live load of 42 kips.

Figure 8 shows the transverse and longitudinal stress distributions at the location of Rosette Group 1 (haunch) with 16-kip live load applied at Position 1. Rosette Group 1 is located at the last bolt hole of the side rib near the splice that joined the rib with the crown rib at about 78.5 in. measured

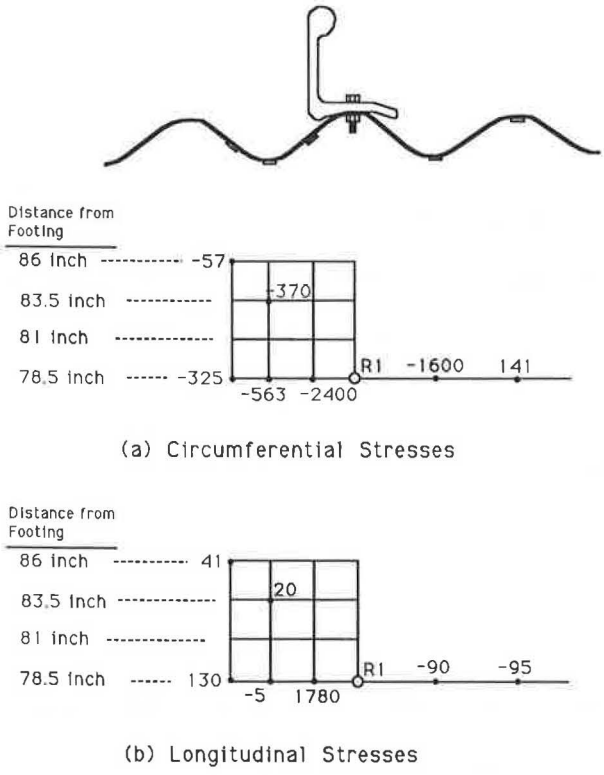

FIGURE 8 Circumferential and longitudinal stresses in Rosette Group 1 (haunch) with 16-kip live load applied at Position 1.

along the curvature from the footing. Rosettes were mounted at 0-, 45-, and 90-degree planes with respect to the longitudinal direction of the culvert, three rosettes on each plane.

The shear transfer from the rib to the plate is noticeable as normal stresses diminish in magnitude away from the bolt hole. That the circumferential stresses were compressive and decreased in magnitude away from the bolt hole indicates that the presence of bolt was disrupting the local stress distribution. Under live loads of 32 and 42 kips applied at Position 1, magnifications of the same trend result.

Hazen et al. (*6*) conducted a laboratory simulation of the bolted aluminum box culvert and duplicated the local effect of the bolted connection that was measured in the field. Their laboratory test results also indicated the presence of stress concentrations and local distortion at the bolt location.

FINITE ELEMENT ANALYSIS

The CANDE finite element program was used to predict the behavior of the structure during backfilling and under live load application. The Duncan soil model was employed for in situ soil and backfill material. A total of 11 contruction increments were used in the simulation of backfill. A 9-in. layer of subgrade and a 12-in. layer of asphalt pavement, respectively, were the 12th and the 13th increments. No interface elements were used between the soil and structure.

The equivalent load for analysis was determined from the Duncan method. A small variation in the geometry of a box culvert has a significant effect on moment and thrust (*3*). In this study the true initial shape of the culvert was calculated from deflection measurement data before the placement of backfill material. Because the design shape can be fully determined at every point (as opposed to 11 measured points only), for modeling purposes the design shape was adjusted to fit the measured shape. Backfill soil parameters were determined from multiaxial and triaxial tests and are given in Table 7. The parameters were incorporated into the CANDE analysis.

Final deflection was calculated to be only one-half as large as measured (as shown in Figure 6). Overall, the CANDE finite element program predicted the deflection of the box-type culvert tested with reasonable accuracy when the load is applied in a monotonically increasing manner, but the accuracy of simulation of loading and unloading conditions is questionable.

The culverts experienced permanent deformation during construction and usage, causing variation in the response of the culvert during the application of live load. Consequently, there was a negative impact on the load capacity of these soil structures. Finite element analysis gives a symmetric result, so a shifting of the flexible culvert during backfill, which takes place in the field, is not duplicated. Maximum moment and thrusts are recorded at places different from those predicted by the finite element solution.

The finite element solution for bending moment compares favorably with the experimental results for the later stages of fill and when subjected to live load, as shown in Figures 9 and 10. Because the culvert responds noncompositely in the early stages, it is difficult to compare experimental and composite responses accurately.

TABLE 7 PARAMETERS FOR DUNCAN'S HYPERBOLIC SOIL MODEL—BACKFILL MATERIAL

Parameter	Symbol	General Value	CTE Value
Friction angle	ϕ_o	39 degs.	39 degs.
Reduction in friction angle	$\Delta\phi$	3.0 degs.	5.5 degs.
Cohesion intercept	c	0	0
Modulus number	K	1200	450
Modulus exponent	n	1.1	0.35
Failure ratio	R_f	0.70	0.60
Bulk modulus number	K_b	350	300
Bulk modulus exponent	m	0.25	0.30

Tangent Young's Modulus (E_t):

$$E_t = KP_a\left[\frac{\sigma_3}{P_a}\right]^n\left[1-\frac{R_f(1-Sin\phi)(\sigma_1-\sigma_3)}{2cCos\phi+2\sigma_3 Sin\phi}\right]^2$$

Tangent Bulk Modulus (B):

$$B = K_b P_a\left[\frac{\sigma_3}{P_a}\right]^m$$

Angle of Internal Friction (ϕ):

$$\phi = \phi_o - \Delta\phi \log_{10}\left(\frac{\sigma_3}{P_a}\right)$$

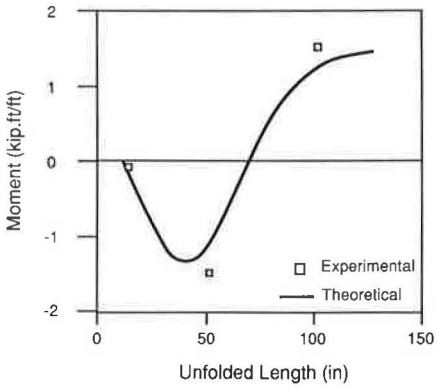

FIGURE 9 Bending moment due to backfill.

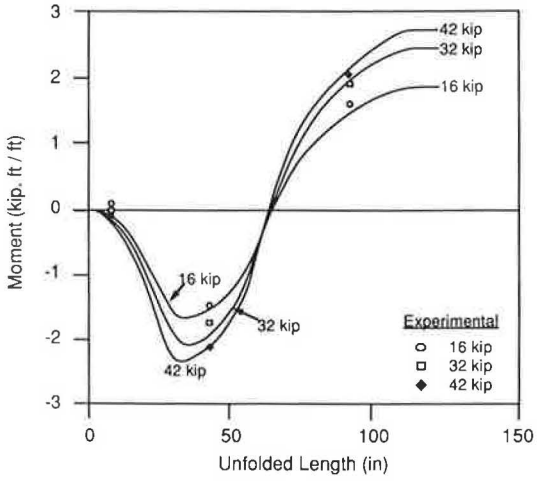

FIGURE 10 Bending moment due to live loads.

Measured thrusts, when compared with calculated values, are inconsistent, as shown in Figures 11 and 12. This results from the tendency of ribs to be primarily compressive members and the plate to be in tension while resisting moment with a couple action. Thus, moment is only piecewise continuous between bolts. In addition, the soil frictional forces act to resist thrusts.

CONCLUSIONS

Overall, the culvert's performance was satisfactory, and finite element analysis can be used with confidence to analyze and design these types of structures. However, special consideration should be given to the determination of the geometry of the culvert, backfill procedures, and true backfill and pavement materials. Several other conclusions that can be drawn from this study are as follows:

- Crown deflections during backfill were slightly underestimated by CANDE.
- Bending moments during backfill were underestimated by CANDE.
- Thrust predictions during backfill did not match at all. The experimental thrusts were scattered, whereas CANDE predicts only slight variation.

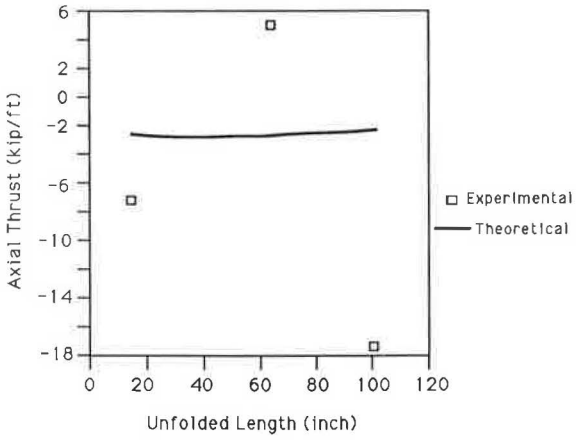

FIGURE 11 Axial thrust at the end of paving.

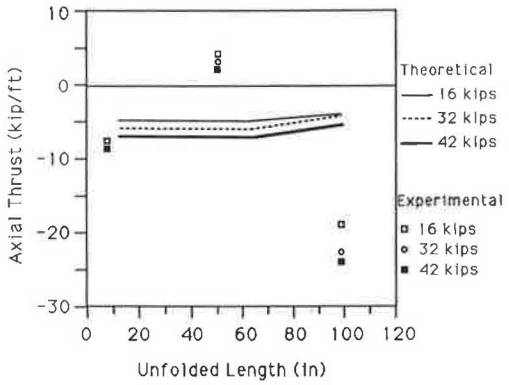

FIGURE 12 Axial thrust-unfolded length curves under live loads.

- Live load Position 1 was critical with respect to crown and haunch moments.
- During live load, the crown deflection was underestimated by CANDE. At Position 1, the CANDE prediction was close to the experimental value, and the CANDE prediction at Position 2 was significantly less than observed.
- Incremental moments due to the live load at Position 1 were adequately predicted by CANDE for the composite and noncomposite cases. On the other hand, the effects of the live load at Position 2 were underestimated by CANDE.
- CANDE underestimated the thrusts for the live load except at the north haunch. The prediction for the haunch region was better than for the crown region.

REFERENCES

1. G. A. Hazen and S. M. Sargand. *Structural Analysis of Corrugated Metal Box-Type Culverts*. Draft final report (Project 4302). Ohio University, Athens, 1990.
2. J. M. Duncan, R. B. Seed, and R. H. Drawsky. Design of Corrugated Metal Box Culverts. In *Transportation Research Record 1008*, TRB, National Research Council, Washington, D.C., 1985, pp. 33–41.
3. J. O. Hurd and S. M. Sargand. Field Performance of Corrugated Metal Box Culverts. In *Transportation Research Record 1191*, TRB, National Research Council, Washington, D.C., 1988.
4. D. B. Beal. *Behavior of an Aluminum Structural Plate Culvert*. Report RR-81-90. FHWA, U.S. Department of Transportation, 1981.
5. R. B. Seed and C. Y. Ou. Measurement and Analysis of Compaction Effects on a Long-Span Culvert. In *Transportation Research Record 1087*, TRB, National Research Council, Washington, D.C., 1986, pp. 37–45.
6. G. A. Hazen, S. M. Sargand, J. X. Zhao, and J. O. Hurd. Bolted Connections of Rib-Plate Structures. In *Transportation Research Record 1219*, TRB, National Research Council, Washington, D.C., 1989.

Publication of this paper sponsored by Committee on Subsurface Soil-Structure Interaction.

Field Performance of Precast Reinforced Concrete Box Culverts

JOHN OWEN HURD

A visual inspection was undertaken to determine to what extent, if any, durability problems exist in precast reinforced concrete box culvert exterior top slabs and joints between box sections and what measures have been or could be successful in preventing the problems. From September 1988 through January 1990 133 culverts were inspected throughout Ohio. On the basis of the results, it is recommended that external joint wrap be provided on precast concrete box culvert joints, through-bolted guardrail post connections to box culverts not be permitted, ½-in. cover be provided over longitudinal reinforcing at mating surfaces at joints, and top surfaces of box culverts be sealed.

Within the past decade large prefabricated culvert structures have become economical alternatives to conventional bridges and cast-in-place box culverts for the replacement of deteriorating small bridges. Prefabricated culvert structures include reinforced concrete arches, three-sided concrete box structures, four-sided concrete box culverts, corrugated metal long-span structures, and metal box culverts. The field performance of four-sided precast reinforced concrete box culverts is addressed.

From 1979 to the time of this study the Ohio Department of Transportation (ODOT) had installed 256 precast reinforced concrete box culverts ranging in size from 6- to 12-ft spans. The locations of these structures are shown in Figure 1.

Invert durability of precast reinforced concrete pipe has not been a problem in Ohio (*1–3*). Therefore, the invert durability of precast reinforced concrete box culverts was not expected to be a problem when they were first used. The flow in box culverts is less confined, and any corrosive effects from surface mining or other causes are generally less severe because of dilution from greater dry weather flow from larger drainage basins.

Previous work on metal box culverts (*4*) and structural plate pipe arches (*5*) indicates a potential for corrosion at seams on the top of these shallow structures. This is primarily due to exposure to water containing deicing salts. Furthermore, ODOT maintenance experience with cast-in-place concrete box culverts indicated the existence of reinforcing steel corrosion at joints or cracks. Therefore, questions arose concerning the durability of precast reinforced concrete box culvert external top surfaces and joints between box sections.

This study was undertaken to determine to what extent, if any, durability problems exist in precast reinforced concrete box culvert exterior top slabs and joints between box sections and what measures have been or could be successful in preventing the problems.

Ohio Department of Transportation, 25 South Front Street, Room 620, Columbus, Ohio 43215.

DATA COLLECTION

An inventory of precast reinforced concrete box culverts was prepared from bid-letting pamphlets for contract installations and from maintenance records of ODOT force account or purchase order installations. The following information was obtained from contract plans and maintenance records and was verified during field inspection.

- Culvert location: The county, route, and section mile mark were recorded and the culverts plotted on a highway map.
- Culvert size: The span and rise of the culvert in feet were recorded. The culvert spans ranged from 6 to 12 ft.
- Box type: Either ASTM C850 for culverts with less than 2 ft of cover or ASTM C789 for culverts with 2 or more ft of cover were recorded.
- Cover: The height of cover in feet over the top surface of the box culvert was recorded. The height of cover over the box culverts inspected ranged from 0.5 to 12 ft.
- Joint material: ODOT specifications allow the use of either bituminous plastic cement (mastic) joint filler or preformed butyl rubber joint material for concrete pipe culvert joints. Joint material for some of the concrete box culverts studied was limited to butyl rubber. The type of joint material specified was recorded. The exterior joint gap on the top of all precast reinforced concrete box culvert joints is filled with portland cement mortar.
- External joint wrap–surface treatment: The type of treatment used on the top exterior of the box culverts included complete field-applied membrane waterproofing of the top surface with multiple layers of asphalt-saturated fabric, 9-in.-wide external joint wrap meeting ASTM C877 with or without an application of a clear concrete sealant on the exterior top surface, or no treatment at all. Membrane waterproofing extended 1 ft down the sides of the culverts. The ASTM C877 joint wrap extended down to the base of the culvert to provide anchorage. The clear sealant was applied to the tops and 1 ft down the sides and joints of the box sections.
- Shear connectors: Although ODOT no longer requires shear connectors on concrete box culverts (*6,7*), some early installations of C-850 boxes had shear connectors at culvert joints. The presence of shear connectors was recorded.

From September 1988 through January 1990, 133 culverts were inspected. The culvert locations are shown in Figure 2. Inspection trip itineraries were selected to provide reasonable coverage of the state while maximizing the number of in-

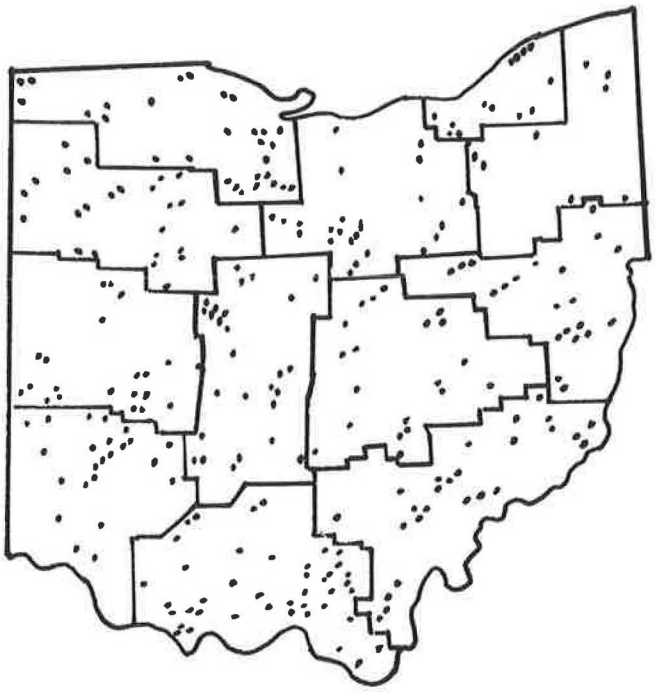

FIGURE 1 Locations of precast reinforced concrete box culverts installed by ODOT.

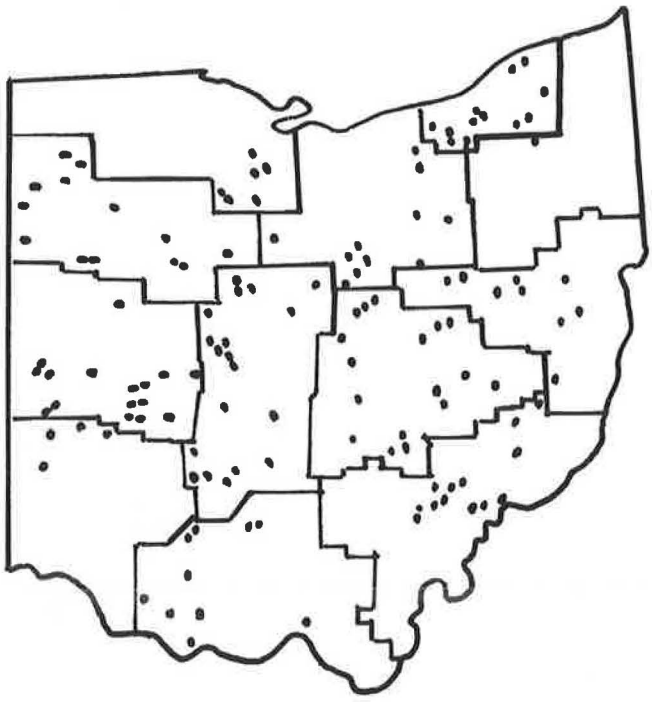

FIGURE 2 Locations of inspected culverts.

spections per trip. Inspections were conducted until it appeared that as many culverts with varying joint-surface treatments and site conditions as necessary had been inspected to allow reasonable conclusions to be drawn. The following information was obtained from field inspections:

- Joint configuration: Specific joint configurations for tongue and groove joints for precast reinforced concrete box culvert sections are not given in either ASTM C789 or ASTM C850. Therefore, joint dimensions for each culvert were recorded on a sketch similar to Figure 3.
- Guardrail connections: Where guardrail posts were connected to the culvert top slab, the type of connection, either inset bolts or through-bolting, was recorded. Connections to culvert top slabs are used on shallow culverts where no other mounting method has been proved impact safe by crash tests.
- Joint gap: The typical joint gap between the mating surfaces of the box sections was recorded. Any significant difference in box dimensions at the joint for abutting box sections was also noted.
- Steel exposure: Any exposed reinforcing steel on the mating surfaces of joints or on internal surfaces of the box was noted. The specified minimum cover over all reinforcement for internal surfaces is ⅝ in. The specified minimum cover for circumferential wires on mating surfaces is ½ in. Ends of longitudinal wires may be exposed at mating surfaces. Ends of spacers and stirrups used to position reinforcement may also be exposed.
- Manufacturer: Box culvert size, design data, manufacturer, and so forth are required to be marked on the culvert. If this marking was on the interior surface, the manufacturer was recorded. In many instances, however, the information was missing or marked on the external surface.
- Lift hole and guardrail bolt holes: The condition of the concrete around the bottoms of lift holes and guardrail bolt holes where through-bolting was used was noted. Any damage to the concrete was recorded and later subjectively rated as slight, significant, or severe. Serious spalling around guardrail bolt holes is shown in Figure 4.
- Joint leakage and corrosion: The evidence of any joint leakage, road salt deposition, or corrosion of steel was noted

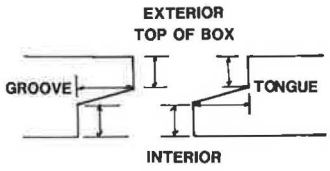

FIGURE 3 Joint configuration of precast reinforced concrete box culverts.

FIGURE 4 Spalling of concrete around guardrail bolt holes.

and recorded. On the basis of ODOT's experience with bridge deck and cast-in-place box culvert deterioration, there was concern that joint deterioration might cause progressive deterioration of the culvert tops and affect the condition of the highway fill or the road surface, or both. Joint leakage was later rated from photographs and descriptions as slight, significant, or severe. Severe joint leakage, salt deposits, and corrosion are shown in Figure 5.

- Leakage and corrosion at lift holes and guardrail bolt holes: The same information taken at joints was taken for lift holes and guardrail bolt holes.
- Condition of exposed top surface: The condition of exposed box culvert top surfaces outside the pavement or backfill was observed. Any spalling or other deterioration or damage was noted. Spalling on the unprotected top surface of one box culvert is shown in Figure 6.
- Additional information: Other observations, such as cracks in box sections, knocked-out pieces of concrete at joints, poor-quality concrete, and so forth, were also recorded.

Observation of the joints on many box culverts was difficult because additional bituminous plastic cement joint filler had been spread around the exposed interior joint gap (see Figure 7). Some ODOT district construction personnel interpret the ODOT specifications as requiring this application, whereas others do not. This not only prevents adequate inspection of the joint but also may trap moisture and salt in the joint and induce or aggravate deterioration.

FIGURE 5 Serious joint leakage, salt deposits, and corrosion.

FIGURE 6 Spalling on top surface of box culvert.

FIGURE 7 Joint material spread on inside of joint.

ANALYSES OF DATA

Because the data compiled were qualitative in nature and did not involve precise numerical measurements, statistical analyses (such as analysis of variance or convariance and regression analysis) were not performed. Instead chi-square contingency tests of grouped data were used to determine the statistical significance of relationships between culvert and site parameters and culvert performance.

The severity of joint leakage was related to box culvert manufacturer, culvert type, joint configuration, joint fit, type of specified joint material, type of joint wrap, culvert location, culvert age, height of cover, and so forth. The only significant relation observed was that between the severity of joint leakage and the type of joint wrap provided. Table 1 indicates that use of an external joint wrap (total membrane waterproofing or ASTM C877 joint wrap) prevented significant joint leakage. In all cases where leakage was observed on culverts with wrapped joints, it was limited to one spot on 1 or 2 joints out of approximately 10 joints per culvert.

Unwrapped joints sealed only with mastic or butyl joint material were ineffective in preventing leakage. This was true regardless of joint material, joint configuration, or joint fit. Leakage, salt deposition, and corrosion observed on joints were limited to the top of the box culvert and did not appear on the sides. The absence of any relationship between leakage severity and culvert age is probably due to a combination of the small age range of the culverts inspected and the ineffectiveness of the internal joint material in preventing leakage.

TABLE 1 JOINT LEAKAGE BY TYPE OF JOINT WRAP

	Joint Leakage			
Joint Wrap	None	Slight	Significant	Severe
Membrane	62	5	0	0
ASTM C-877	8	4	0	0
None	11	15	18	4

Joint leakage on unwrapped box culvert joints was significantly worse in northeastern Ohio and grew progressively less severe toward northwest, southwest, and southeast Ohio, in that order. Figure 8 shows district groupings used in the comparisons given in Table 2. Winter weather (both precipitation and temperature) decreases in severity from northeast Ohio in the same counterclockwise direction. No other site parameter affected the severity of joint leakage on culverts with unwrapped joints. No significant infiltration of backfill was observed on any culverts. It appears that the mastic and butyl joint seals were effective in this regard.

Leakage at lift holes and guardrail bolt holes was also compared with various culvert and site parameters. Full membrane waterproofing prevented leakage through lift holes, whereas some slight leakage at lift holes was observed on approximately one-third of the culverts without full membrane waterproofing. No particular factor affecting lift hole leakage on the culverts without membrane waterproofing could be identified. It appears that the care used in plugging the lift hole after the culvert had been set was the sole factor in determining whether leakage occurred.

Membrane waterproofing did not prevent leakage through guardrail bolt holes on those culverts with through-bolting of guardrail posts. More than one-half of the culverts with through-bolted guardrail post connections experienced leakage through the bolt hole. As with lift hole leakage, no particular factor affecting leakage could be identified.

FIGURE 8 District groupings.

TABLE 2 JOINT LEAKAGE ON CULVERTS WITH UNWRAPPED JOINTS BY ODOT DISTRICT

	Joint Leakage			
ODOT District	None	Slight	Significant	Severe
3·4·12	1	2	7	2
1·2	1	3	3	1
6·7·8·9	1	8	4	1
5·10·11	8	2	4	0

The presence of road salt deposits and evidence of reinforcing steel corrosion on those culverts having joint, lift hole, or guardrail bolt hole leakage were compared with various culvert and site parameters. Although the presence of salt deposits became slightly more severe with age, no culvert or site parameter could be identified that affected these conditions. As with metal box culverts (*4*), it did not appear that an increase in depth of cover significantly reduced the severity of road salt deposits or corrosion at joints. Strangely, the severity of salt deposition and corrosion at joints did not significantly decrease from the northeast area of Ohio counterclockwise as did leakage, even though salt usage in Ohio decreases dramatically from north to south.

The severity of salt deposits and corrosion on culverts with joint, lift hole, or guardrail bolt hole leakage is summarized in Tables 3 and 4. The evidence of corrosion at the joints is probably due to exposed longitudinal reinforcement, which is allowed by the ASTM specifications for precast concrete box culverts. Approximately 20 percent of the culverts observed had longitudinal steel exposed on the end box section. This percentage is a minimum estimate of occurrence on all culvert joints, because observation was based on the end sections that could be observed. Several end sections were covered by end treatment such as headwalls and wingwalls.

Corrosion at guardrail bolt holes is in part due to exposure of steel at the side of the hole. However, more severe corrosion occurs when a large part of the inner reinforcing cage is exposed by spalling of concrete, as shown in Figure 4. Seventeen of the 23 culverts with through-bolted guardrail connections had spalling rated severe or significant around the bottom of the bolt holes. This is thought to be caused by the impact of the drill striking the inner cage of reinforcement.

Some spalling was observed in nineteen culverts around the lift holes, which was probably caused by contact with lifting devices. However, this spalling was not nearly as severe as that around the guardrail bolt holes, and it did not expose the inner reinforcing cage.

TABLE 3 SALT DEPOSITS ON CULVERTS WITH LEAKAGE AT JOINTS, LIFT HOLES, AND GUARDRAIL BOLT HOLES

	Severity of Salt Deposits			
Location	None	Slight	Significant	Severe
Joint	9	12	13	3
Lift hole	7	8	2	0
GR bolt hole	5	3	4	1

TABLE 4 CORROSION ON CULVERTS WITH LEAKAGE AT JOINTS, LIFT HOLES, AND GUARDRAIL BOLT HOLES

	Severity of Corrosion			
Location	None	Slight	Significant	Severe
Joint	20	9	8	0
Lift hole	14	2	1	0
GR bolt hole	8	4	0	1

ADDITIONAL OBSERVATIONS

Some additional observations concerning general culvert conditions made during the inspections are given in this section.

Surface deterioration of the top slab of the end sections on nine culverts was observed (see Figure 6). To date this has been limited to culverts without clear sealant or membrane waterproofing and with total earth and pavement cover less than or equal to 3 ft. The deterioration is probably due in part to exposure to roadway deicing salts. Air entrainment was suggested as a remedy for the surface deterioration. However, maintenance of consistent levels of air in the precasting process has been difficult for other precast structures.

The condition of all culvert inverts was excellent. No deterioration due to flow was observed.

Longitudinal hairline cracks were observed on the interior top slab of one or two sections on seven culverts. These cracks were much smaller than a 0.01-in. crack used as a structural design basis for round concrete pipe. In only one case did it appear that leakage from a joint progressed down the crack. These cracks did not appear to pose a top slab durability problem.

To date no problems with progressive top slab deterioration or highway fill and road surface condition have been observed on any of the culverts with joint problems. Therefore, no specific remedial action has been programmed for the immediate future. Large culverts are inspected annually, and repairs will be scheduled when it appears that joint deterioration poses a threat to the rest of the box culvert top or to the highway itself.

RECOMMENDATIONS

On the basis of the observations and data analyses performed, the following recommendations are presented:

1. External joint wrap should be required on the tops and sides of precast reinforced concrete box culvert joints. If full membrane waterproofing of the top is provided, it need only extend 1 ft down the sides of the culvert.
2. A surface sealer (either full membrane waterproofing or clear sealant) should be required on the external top slab of precast reinforced concrete box culverts, especially those with less than 3 ft of cover. The sealer should extend approximately 1 ft down the sides of the culvert.
3. A minimum cover of ½ in. over both circumferential and longitudinal reinforcement should be required at the mating surfaces of precast reinforced concrete box culvert joints.
4. Lift holes should not be permitted unless full membrane waterproofing is provided over the precast box sections or approved joint wrap material is applied over the lift hole.
5. Where guardrail posts must be mounted to the precast box culvert tops, through-bolting should not be permitted.
6. Additional joint material should not be placed in the inside of the joint on the top and sides of the box culvert.
7. The manufacturer's name and required product information should be placed on the inside of the precast box culvert section within the top half of the culvert.

REFERENCES

1. D. G. Meacham, J. O. Hurd, and W. W. Shisler. *Ohio Culvert Durability Study*. ODOT/L&D/82-1. Ohio Department of Transportation, Columbus, 1982.
2. J. O. Hurd. Field Performance of Concrete Pipe at Acidic Flow Sites in Ohio. In *Transportation Research Record 1008*, TRB, National Research Council, Washington, D.C., 1985.
3. J. O. Hurd. Service Life Model Verification for Concrete Pipe Culverts in Ohio. In *Transportation Research Record 1191*, TRB, National Research Council, Washington, D.C., 1988.
4. J. O. Hurd and S. Sargand. Field Performance of Corrugated Metal Box Culverts. In *Transportation Research Record 1191*, TRB, National Research Council, Washington, D.C., 1988.
5. G. H. Degler, D. C. Cowherd, and J. O. Hurd. An Analysis of Visual Field Inspection of 900 Pipe-Arch Structures. In *Transportation Research Record 1191*, TRB, National Research Council, Washington, D.C., 1988.
6. J. O. Hurd. Research Pays Off: Eliminating Shear Connectors Slashes Culvert Cost. *TR News 138*, 1988.
7. G. R. Frederick, B. Koo, and C. V. Ardis. *Evaluation of Shear Connectors on Precast Reinforced Concrete Box Sections*. Ohio DOT Project 3612. University of Toledo, Toledo, Ohio, 1984.

This study was funded by the Ohio Department of Transportation. The findings and opinions expressed herein are those of the author and do not constitute a standard or specification.

Publication of this paper sponsored by Committee on Subsurface Soil-Structure Interaction.

New Method of Time-Dependent Analysis for Interaction of Soil and Large-Diameter Flexible Pipe

KOON MENG CHUA AND ROBERT L. LYTTON

Design equations have been developed to predict the pre-yield deflections, stresses, and strains in buried flexible plastic pipes over time. The solutions consider the effects of creep in the pipe material and the surrounding soil and backfill, the water table, arching, and variable bedding conditions. These equations are obtained by regression analysis, and results are generated using a finite element program. The design equations predict pipe deflections that are consistent with those obtained in the field over a period of time. It is shown that the arching of soil surounding a pipe can be quantified to further appreciate its cause and effects. The ratio of the pipe's vertical deflection to its horizontal deflection is shown to be an ambiguous way of defining the structural integrity of nonrigid pipes. Strain level may be a better indicator of the structural integrity of the pipe than pipe deflection, because it considers both the bending moments and the thrust in the pipe wall and can be measured against the allowable strain for that particular pipe material. Vertical pipe deflections predicted by the design equations for different depths of cover as well as for different time periods are shown to match field measurements well.

Modern cities require underground pipelines to provide essential utilities, such as wastewater disposal, potable water, and gas. In recent years there has been a steady increase in the use of flexible pipes as buried conduits despite the fact that much is not understood of soil-pipe interaction, especially their time-dependent behavior. The most common type of flexible pipe is plastic pipe.

Plastic pipes can generally be classified as thermosetting plastic or thermoplastic. The first type uses materials such as glass or sand embedded in a plastic binder. Examples are reinforced thermosetting resin (RTR) pipe, commonly called FRP or GRP (fiber-reinforced plastic or glass-reinforced plastic pipe), and reinforced plastic mortar (RPM) pipe. Thermoplastic pipes are made from materials such as polyvinyl chloride (PVC), high density polyethylene (HDPE), and acrylonitrile butadiene styrene (ABS).

All materials are known to experience a reduction in stiffness with time under an applied load. The reduction in stiffness is usually referred to as relaxation. This property is pronounced for plastic pipe, although it is less obvious in concrete and most metallic pipes. Hence in the design and use of plastic pipes, the ability to predict the effects of relaxation of the pipe and soil on the soil-pipe system is an important consideration.

K. M. Chua, Department of Civil Engineering, University of New Mexico, Albuquerque, N.Mex. 87131. R. L. Lytton, Department of Civil Engineering, Texas A&M University, College Station, Tex. 77843.

The use of flexible pipes toward the middle of the century prompted the development of design procedures. One of the most widely used is Spangler's equation (*1*, pp. 368–369). Time-dependent solutions were attempted rather crudely by using a lag factor to increase deflection with time. A new design procedure that has been developed to predict preyield deflections, stresses, and strains in buried flexible pipes over time is presented. The design equations are obtained by regression analysis, and results are generated by a nonlinear finite element program and are shown to match measured field data well.

ENGINEERING PRACTICE AND CONSIDERATIONS

Background

The soil supports the load above a flexible pipe when it is allowed to deflect and hence generate enough thrust in the soil elements to form an arch. However, a rigid pipe bears more of the load itself as the soil relaxes around it. In the study of soil-pipe interaction, especially soil interaction with flexible plastic pipe, an understanding of the factors influencing the arching of the soil surrounding the pipe is a major objective.

Modeling the Soil-Pipe System

The various ways of modeling the three major components of a soil-pipe system are the following:

1. Trench model: Flexible pipes are usually buried in properly prepared trenches. In a design analysis, there are three distinct soil zones: the in situ soil, which remains undisturbed; the embedment soil of selected and properly compacted fill, which is in contact with the pipe and includes the bedding; and the backfill, which is the disturbed or remolded native soil dumped and nominally compacted above the pipe. Figure 1 shows a typical configuration of a trench. In a proper analysis, each soil zone should be assigned its distinctly different soil properties.
2. Soil model: Design procedures currently in use have linearly elastic soils, nonlinearly elastic soils, and viscoelastic soils. For elastic soils, it is assumed that the stress state will return to the initial state on unloading. In the case of linear elasticity, a linear path is assumed. A nonlinear elastic model

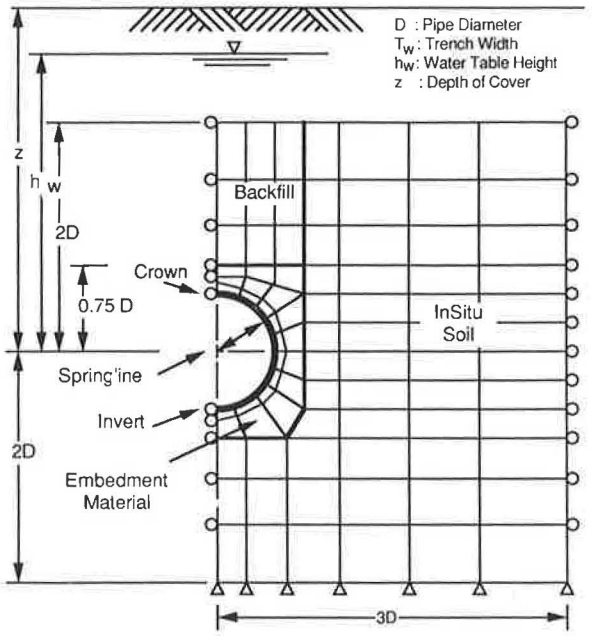

FIGURE 1 Typical configuration of a pipe trench.

that is normally used is the hyperbolic stress-strain model, as reported by Kondner (*2*) and Janbu (*3*) and subsequently used extensively in engineering applications by Duncan et al. (*4*). The use of a nonlinear elastic model allows an unloading-reloading stress path to differ from the loading stress path, hence creating a different soil modulus for a soil that has been remolded and loaded and an undisturbed soil that has undergone unloading and then reloading. In view of this, for a pipe buried in a trench, one should consider assigning the undisturbed in situ soil a larger soil modulus than the disturbed backfill when it is used in an analysis. A viscoelastic model allows properties such as the soil modulus to be time and stress-history dependent.

3. Pipe model: Buried pipes are available with smooth-wall or profile-wall cross sections. The purpose of profile-wall pipes is to achieve a higher stiffness-to-weight ratio than that of smooth-wall pipes. In modeling the material modulus of the pipe, the usual approach is to assume a linearly elastic model. However, because most flexible pipe materials are polymeric, the viscoelastic approach is more appropriate.

FORMULATION OF THE DESIGN EQUATIONS

The design equations were developed for the analysis of a flexible pipe buried in a trench of any width, with or without the presence of groundwater. The hyperbolic stress-strain model was assumed for soils in the three zones (see Figure 1). The design solutions were obtained from a factorial study using CANDE (*5*) (a nonlinear finite element code) to generate a data base of some 720 cases. Before the factorial analysis, the more influential parameters and variables in the soil-pipe system were determined. They were pipe stiffness, which takes into account the size and the material properties of the pipe; the properties of the embedment, the backfill, and the native soil; the depth of cover; soil arching; trench width; and the presence of groundwater. Subsequently, the design equations obtained from the regression analysis were verified by using several sets of field measurements supplied by a pipe manufacturer (*6*) and from the literature (*7*). Predictions that can be obtained using the design equations include (*a*) the pipe vertical deflection with or without groundwater; (*b*) the ratio of the pipe vertical deflection to its horizontal deflection; (*c*) the soil vertical and lateral stress at the springline; (*d*) the soil support modulus, which is assumed to be represented by the soil modulus taken at the springline; (*e*) the bending moment of the pipe wall at the crown; (*f*) the thrust in the pipe wall at the crown; and (*g*) the strain in the pipe wall at the crown, which can be reasonably assumed to be the maximum pipe strain. The elastic design equations were then transformed into a viscoelastic form, which gives these results as a function of time as well.

The following sections present the design equations, which are also used in a microcomputer program called TAMPIPE (*Texas A&M PIPE*).

DESIGN EQUATIONS

Pipe Vertical Deflection

It was initially thought that the equation for the pipe vertical deflection would take the form of Hoeg's equation (*8*). The pipe vertical deflection expressed as a ratio to the average pipe diameter is given by Hoeg as

$$\frac{\Delta D}{D} = \frac{\dfrac{1 - \nu_e}{3(3 - 4\nu_e)} w(1 - k)}{\dfrac{8E_pI_p}{(1 - \nu_p^2)D^3} + \dfrac{(3 - 2\nu_e)(1 - 2\nu_e)E'}{12(3 - 4\nu_e)(1 - \nu_e)}} \tag{1}$$

where

w = uniformly distributed load above the pipe,
k = ratio of the lateral to the vertical loading,
ν_e = Poisson's ratio of the elastic medium,
ν_p = Poisson's ratio of the pipe,
E_p = the elastic modulus,
I_p = the moment of inertia of the pipe wall,
D = the pipe diameter, and
E' = the soil modulus.

It is interesting to note that if the Poisson's ratio of the soil, ν_e, is taken to be 0.315, and the pipe is assumed to have a Poisson's ratio of 0.0, the equation becomes

$$\frac{\Delta D}{D} = \frac{0.131w(1 - k)}{8E_pI_p/D^3 + 0.061E'} \tag{2}$$

which is almost Spangler's equation without the lag factor. It appears that the soil used to obtain Spangler's empirical values had a Poisson's ratio of 0.315 and that the bedding constant in the numerator may well be a function of the Poisson's ratio of the soil. The exclusion of a Poisson's ratio for the pipe material may explain why Spangler's equation is inadequate in modeling buried pipes with very low stiffnesses.

The design equation that has been developed to describe the pipe vertical deflection follows the same form as Equation 1:

$$\frac{\Delta D}{D} = \frac{\frac{(1 - \nu_e)}{3(3 - 4\nu_e)}(1 - A_f)\gamma z W_f}{\frac{8E_pI_p}{(1 - \nu_p^2)D^3} + \frac{(3 - 2\nu_e)(1 - 2\nu_e)E'}{12(3 - 4\nu_e)(1 - \nu_e)}} \quad (3)$$

where

A_f = factor representing the amount of arching,
γ = the unit weight of the soil,
z = the depth of cover to the springline, and
W_f = a factor to correct for the presence of a water table.

This is the form of the model found in TAMPIPE. The soil support modulus E' is the secant modulus of the embedment soil at the springline, given by

$$E' = \left[1 - \frac{R_{fe}(1 - \sin\phi_e)\sigma_x}{(2c_e\cos\phi_e + 2\sigma_x\sin\phi_e)}\right]K_eP_a\left[\frac{(\sigma_y)}{P_a}\right]^{n_e} \quad (4)$$

where

c_e = cohesion of the embedment soil,
ϕ_e = angle of shearing resistance of the embedment soil,
K_e = soil modulus number (*4*),
n_e = modulus exponent (*4*),
R_{fe} = failure ratio (*4*),
σ_x = horizontal earth pressure at the springline, and
σ_y = vertical earth pressure at the springline and is approximately equal to the minor principal stress, σ_3.

This stress is represented by the unit weight of the backfill and the embedment soil above the pipe; the depth of cover measured to the springline; the pore water pressure; the pipe stiffness; and the modulus number of the backfill, the embedment, and the native soil. This value can be expressed by

$$\sigma_y = \frac{\gamma z/(144 \times 12)}{C_{f1} \cdot C_{f2} \cdot C_{f3}} \quad (5)$$

where

$$C_{f1} = 1.2 + (5.8 \times 10^{-2} + 4.58 \times 10^{-3} \times 8E_pI_p/D^3 \times \exp[(4.3 \times 10^{-4} - 9.0 \times 10^{-6} \times 8E_pI_p/D^3) \times 14.7K_r]$$

and

$$C_{f1} \geq 1.2$$
$$C_{f2} = 1 + 1.5p_w^{1.42}$$

p_w = pore water pressure

$$C_{f3} = 1.7588 \times \exp(-1.75 \times 10^{-3}K_r) \times 6.9453 \times \exp(2.10 \times 10^{-3}K_r) \times K_e^{-0.41 \times \exp(6.91 \times 10^{-4}K_r)}$$

In this case, K_r refers to a representative soil exponent number that takes into consideration the surrounding soil zones and the trench width and is given by

$$K_r = K_r'[1.0 + (T_w/D - 1.5)(1.1082 + .0016K_e)]$$

$$K_r \geq 0 \quad (6)$$

where

$$K_r' = -128.7675 + 1.004K_b + 42K_i/K_b$$
$$K_r' \geq 0$$

σ_x is the lateral earth pressure at the springline and is approximately equal to the major principal stress, σ_1. This value is obtained by multiplying σ_y by a lateral earth pressure coefficient, K_o, which again is a function of the modulus numbers of the soils in the three zones, the pipe stiffness, and the pore water pressure:

$$K_o = (1 - 2.96 \times 10^{-2}K_r^{0.47}p_w) \times (9.3488K_e^{-0.44}K_r^2) \times (1.0122 + 7.11 \times 10^{-4}K_r - 3.4 \times 10^{-7}K_r^2) \times \exp[8E_pI_p/D^3 \times (-0.019048 + 2.28 \times 10^{-5}K_r - 1.14 \times 10^{-8}K_r^2)] \quad (7)$$

Factors Influencing Pipe Deflection

This section indicates how the design equations can be used to analyze installation cases and how the variables affect pipe deflections, using high-density polyethylene pipes as examples.

Pipe Stiffness

This term ($PS = 8E_pI_p/D^3$) is a function of the elastic modulus or relaxation modulus, the diameter of the pipe, and the moment of inertia of the pipe wall. Figure 2 shows the reduction in pipe deflection when the stiffness of a 48-in.-diameter pipe is increased from 1.2 to 4.0 psi. The deflection of an 18-in.-diameter pipe (PS = 11.9 psi) is also shown. The three pipes were installed in a soft native soil [modulus number (K) equal to 68] with the embedment soil compacted to 85 percent Proctor.

Soil Stiffness

Because the soil modulus (E') is stress dependent, the knowledge of the state of stress of the soil around the pipe is of

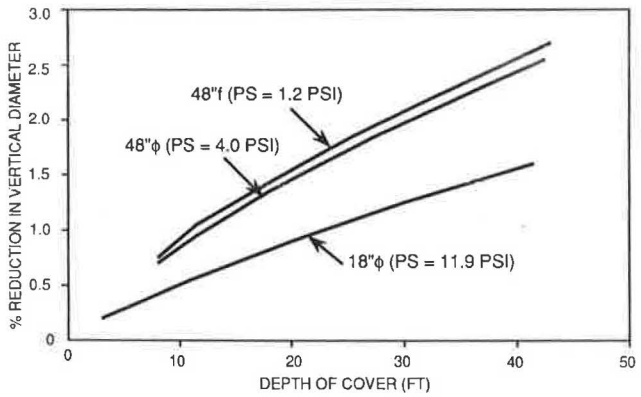

FIGURE 2 Vertical deflections for pipes of different stiffnesses.

great importance. A soil-pipe system with a soft backfill soil (K = 68) results in a higher stress level around the pipe and hence a larger soil modulus. In stiff backfill (K = 1,100), the stress level of the soil elements around the pipe is lower, leading to a lower soil modulus (but the imposed load on the pipe is also smaller). Figure 3 shows how pipe deflections can be reduced by increasing the degree of compaction on the embedment soil. Figure 3 also shows the exceptionally high deflection of a pipe backfilled with soft native soil only, that is, without any bedding material. The soil modulus resulting from the interaction between the different types of native soil and the different degrees of compaction of the embedment soil is shown in Figure 4.

Soil Arching

The degree of soil arching is described by the term A_f, which can take on values ranging from 1.0 to negative values. This term is given by

$$A_f = [1 - (1 - A_{fo})A_{fc}] \tag{8}$$

where

$$A_{fo} = [1 + (K_r - 622.7) \times 4.86 \times 10^{-4}]^{-1}$$

and

$$A_{fc} = 0.9054 - 1.07 \times 10^{-2}T_w + (8.18 \times 10^{-5} + 6.91 \times 10^{-6}T_w)K_r - [9.61 \times 10^{-5} + 1.30 \times 10^{-5}T_w - (6.75 \times 10^{-8} + 7.32 \times 10^{-9}T_w)K_r]E'$$

Figure 5 shows the arching values that can be obtained for various degrees of compaction in different native soils. It can be seen that in stiff native soil (K = 1,100), the arching value is close to 1.0, indicating that little of the imposed load from above the pipe is transmitted to the pipe. For the pipe surrounded by embedment material of slight compaction and buried in a soft native soil (K = 68), the arching factor is about 0.6. For a highly compacted embedment fill in a soft native soil, the arching factor falls below zero, indicating that the pipe must bear more load than the overburden pressure. It can be seen from the figure that the degree of arching tends to be constant after some depth. It can be shown that a larger trench width reduces soil arching.

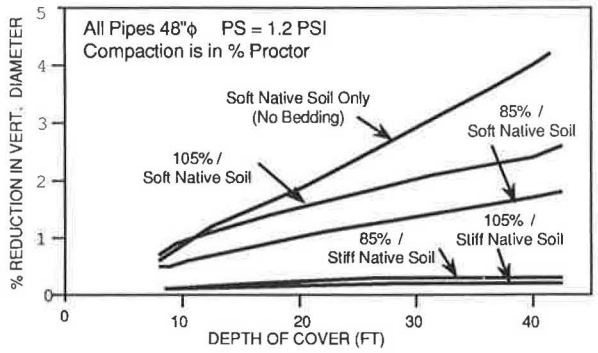

FIGURE 3 Vertical deflections of pipes in different soils.

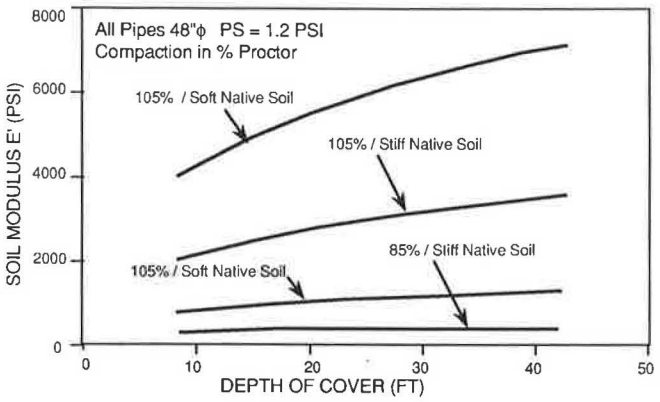

FIGURE 4 Soil moduli for different depths of cover.

Trench Width

When using a flexible pipe, generally, a trench width of about 1½ times the pipe diameter is preferred. It is not economical to overexcavate the trench, but sufficient clearance on both sides of the pipe is required to allow for proper compaction of the fill. As indicated earlier, an increase in the trench width will weaken the arch to be formed. To offset this, the application of a higher degree of compaction to the embedment material is required. In soft native soils, a better way to improve arching and hence reduce deflections is to increase the degree of compaction and not the trench width alone, unless soil exchange is the aim, as when organic soil or marine clay is encountered.

Groundwater

The effects of the presence of a hydrostatic load on the pipe exterior is a highly complicated consideration. In the design equation, W_f is the factor by which the percent pipe deflection for the dry case is multiplied to obtain the resultant deflection.

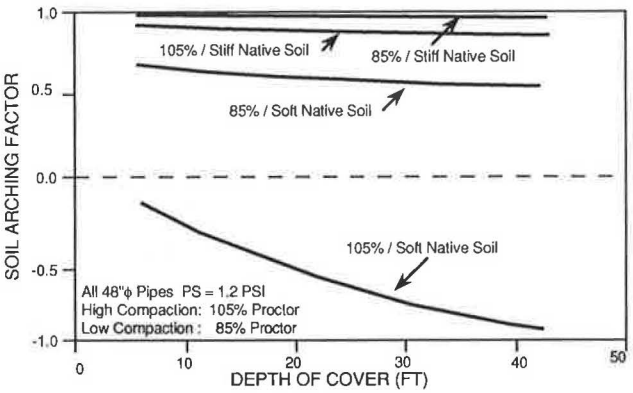

FIGURE 5 Arching factor of a soil-pipe system in different soils.

It is given by

$$W_f = 1 - 0.6718z_w + 2.83 \times 10^{-3}z_w K_r - 4.56 \times 10^6 \times K_r^2 z_w + 0.2520z_w^2 - 3.66 \times 10^{-3}K_r z_w^2 \times 7.84 \times 10^{-6}K_r^2 z_w^2 \quad (9)$$

where z_w is the ratio of the water table height above the springline to the depth of cover. As can be seen from Figure 6, the presence of groundwater will increase deflections only beyond a specific head, which varies with soil modulus. This is probably because beyond this point, the hydrostatic load increases faster than the support offered by the soil for the different depths of cover.

Ratio of Pipe Vertical to Horizontal Deflection

Pipe design engineers have been acutely interested in determining the ratio of the pipe vertical deflection, D_v (an absolute value), to the horizontal deflection, D_h, commonly referred to as the D_v/D_h ratio. This is because it has often been inaccurately presented that all pipes will approach failure if they do not conform to the ellipitical shape, where the D_v/D_h or D_h/D_v ratio is unity. The form of the regression equation that was obtained for the D_h/D_v ratio is

$$D_h/D_v = 1 - D_v/(A_o + D_v) \quad (10)$$

where A_o is a function of the pipe stiffness and the modulus numbers of the soil in the three zones. A regression equation has been obtained for A_o. Figure 7 shows the variation of the D_h/D_v ratio with respect to the pipe vertical deflection for pipes of various stiffnesses. It can be seen that a D_v/D_h ratio is of little value if the pipe deflection is not given at the same time. The horizontal line with the intercept at unity shows the relationship that can be expected for the D_h/D_v ratio and the pipe vertical deflection for a perfectly rigid pipe.

Bending Moment, Thrust, and Strain in the Pipe Wall

The bending moment at the crown (which can be assumed to represent the maximum bending moment) can be expressed

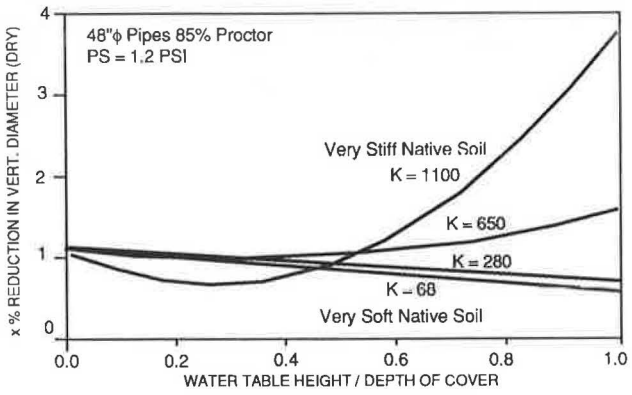

FIGURE 6 Effects of groundwater on pipe deflection.

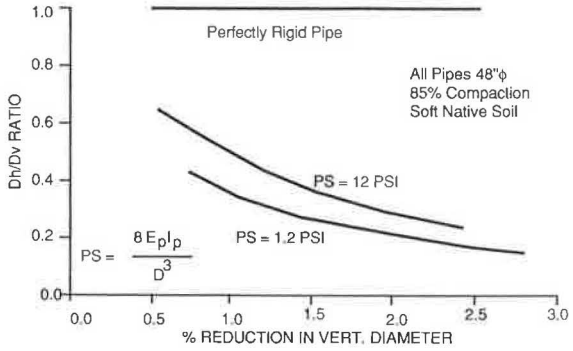

FIGURE 7 Ratio of pipe horizontal deflection to vertical deflection.

as

$$M = D_f 4E_p I_p(\Delta D/D)/D \quad (11)$$

where D_f is the deformation factor, which is given by

$$D_f = M_{c1} \times M_{c2}$$

where

$$M_{c1} = (0.2667T_w - 0.6) \times [3.2227 + 5.7 \times 10^{-3}K_r - 5.3 \times 10^{-6}K_r^2 - (4.4 \times 10^{-3} + 5.8 \times 10^{-6}K_r - 6.8 \times 10^{-9}K_r^2)K_e] - (0.2667T_w - 1.6) \times [1.8809 + 1.1 \times 10^{-3}K_r - 7.8 \times 10^{-7}K_r^2 - (1.4 \times 10^{-3} - 5.5 \times 10^{-7}K_r)K_e]$$

$$M_{c2} = (0.2667T_w - 0.6) \times [1.3690 - 2.1 \times 10^{-3}K_r + 1.7 \times 10^{-6}K_r^2 - 2.7 \times 10^{-3}K_e + 1.6 \times 10^{-5}K_rK_e - 1.3 \times 10^{-8}K_r^2K_e + 3.5 \times 10^{-3}K_e^2 - 2.0 \times 10^{-8} \times K_rK_e^2 + 1.6 \times 10^{-11}K_r^2K_e^2 + (1.94 \times 10^{-2}K_r - 2.6 \times 10^{-5}K_r^2 - 3.9 \times 10^{-3}K_e - 1.3 \times 10^{-4}K_rK_e + 1.7 \times 10^{-7}K_r^2K_e + 2.9 \times 10^{-5}K_e^2 + 9.9 \times 10^{-8} \times K_rK_e^2 + 1.8 \times 10^{10}K_r^2K_e^2)p_w + (-2.4 \times 10^{-2}K_r + 3.3 \times 10^{-5}K_r^2 + 4.9 \times 10^{-4}K_e + 1.7 \times 10^{-4}K_rK_e - 2.4 \times 10^{-7}K_r^2K_e - 2.5 \times 10^{-5}K_e^2 - 1.3 \times 10^{-7}K_rK_e^2 + 2.4 \times 10^{-10}K_r^2K_e^2)P_w^2]$$

The thrust at the pipe crown is given by

$$T = (C_1\sigma_x + C_2p_w\gamma_w z)D/2 \quad (12)$$

where

γ_w = the unit weight of water,
C_1 = 0.7285, and
C_2 = 0.9145.

The maximum pipe wall strain that can be assumed to occur at the crown is defined from the corresponding bending moment and thrust and is given by

$$\varepsilon - \frac{Mc}{2E_pI_p} + \frac{T}{A_pE_p} \quad (13)$$

where c is the distance to the outer fiber from the neutral axis. Figure 8 shows the variation of the strain at the crown at different levels of vertical deflection of a 48-in.-diameter

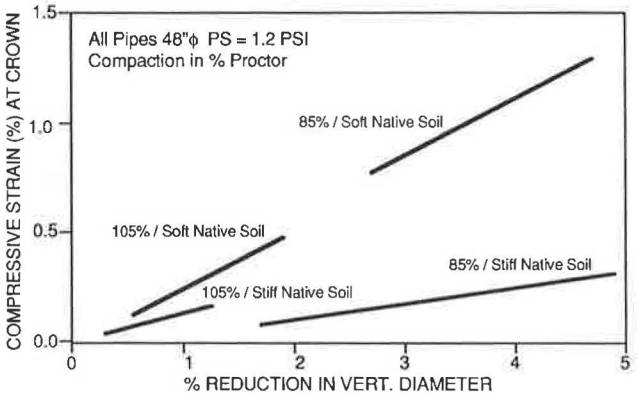

FIGURE 8 Pipe strains at crown for different in situ soils.

(*PS* = 1.2 psi) HDPE pipe for various installation cases after 1 year. This suggests that at, say, a 5 percent reduction in vertical diameter, the pipe material may or may not have reached yield, implying that a strain criterion rather than a deflection criterion may be more appropriate as a measure of the structural adequacy of a buried pipe. If the yield strain is to be used as the criterion, different types of pipes will be allowed to have different levels of pipe deflections, because the yield strain is different.

TIME-DEPENDENT DESIGN EQUATIONS

Viscoelastic Solutions

To model the elastic modulus as a function of time, the power law is used. It has been used on different types of plastics (*9*, pp. 201–221) as well as for rocks (*10*, pp. 293–301) and for soils (*11*,*12*). In the power law formulation, the relaxation modulus is given by

$$E(t) = E_1 t^{-m} \tag{14}$$

where E_1 and m are constants peculiar to the material.

The constitutive equation used to describe the stress-strain relationship of nonaging viscoelastic material is given by the following convolution integral:

$$E(t) = \int_{-\infty}^{t} E(t - \tau) \frac{\partial \varepsilon}{\partial \tau} d\tau \tag{15}$$

where $E(t - \tau)$ is the relaxation modulus as a function of time t and of the time when the input is applied, τ. The symbol ε refers to the step function strain input.

Biot (*13*) showed that the operational moduli of viscoelastic solutions can be manipulated algebraically as elastic moduli, hence establishing the correspondence rule by which "the classical theory of elasticity may be immediately extended to viscoelasticity by simply replacing their corresponding operators." Lee (*14*) showed that the time variable in the viscoelastic solution can be removed by applying the Laplace transform (LT), thus enabling it to be expressed in terms of an associated elastic problem. This is done by taking the LT of the governing field and boundary expressions with respect to time. The resulting expression is the LT of the viscoelastic solution. Taking the inverse LT of the resulting expression produces the desired result, which is the viscoelastic solution.

Consider a time-dependent response $u(t)$. Using the approximate method of the inversion of the LT as proposed by Schapery (*15*), the viscoelastic solution is given by

$$u(t) = [s\bar{u}(s)]_{s=\beta/t} \tag{16}$$

where s is the variable of integration in the LT. For the case in which the slope of the logarithm of the response versus log (t) is small ($-0.3 \leq m \leq 0.1$), $\beta = \frac{1}{2}$. This method had been shown to be very accurate (*16*) in approximating the rigorously determined LT. A discussion of this method of time-dependent analysis using elastic solutions for linear and nonlinear materials can be found elsewhere (*17*).

The viscoelastic form of the design equations was developed by using the correspondence principle with the approximate method of the inversion of the LT.

The Laplace-transformed time-dependent pipe vertical deflection is given by

$$\mathcal{L}\left\{\frac{\Delta D}{D}\right\} = \frac{1}{s} \cdot \frac{B_f(1 - A_f)\gamma z W_f}{8E_p I_p/(1 - \nu^2)D^3 + S_c E'} \tag{17}$$

where the Carson transforms of the pipe relaxation modulus as a power law, $E_p(t) = E_{p1}t^{-mp}$, and for the soil relaxation modulus, $E'(t) = E'_1 t^{-m}s$, are as follows

$$\bar{E}' = s_{ms}E'_1\Gamma(1 - m_s) \tag{18}$$

$$\bar{E}_p = s_{mp}E_{1p}\Gamma(1 - m_p) \tag{19}$$

Symbols are as defined earlier with the appropriate subscript to show the material that is described.

In the trench condition where there are three different soil zones, the value of m_s can be estimated using the following regression equation:

$$m_s = \{1 - \exp[-0.47 \times (T_w/D)^{0.31}]\} \times m_e + \exp[-0.47 \times (T_w/D)^{0.31}] \times m_i \tag{20}$$

where m_e and m_i are power law exponents for the embedment and in situ soil, respectively.

The Laplace-transformed time-dependent bending moment in the pipe wall is given by

$$\mathcal{L}\{M\} = 4D_f\bar{E}_p I_p(\Delta D/D)/sD \tag{21}$$

In the preceding development, it was assumed that the parameters related to the loading term, A_f and W_f, are independent of time. This may not be strictly true, but in view of the lack of evidence to the contrary, and because their influence is not critical, they were assumed to be constant. For practical reasons, the Poisson's ratios of the soils and the pipe material were also taken to be constants.

The following sections will discuss results obtained using the viscoelastic solutions and may help explain time-dependent soil-pipe interaction.

TABLE 1 EXPONENTS OF RELAXATION POWER LAW FOR SOILS AND PIPE MATERIALS

Descriptions and m values		Remarks
Allenfarm (ML)	0.106	Texas Soil at Optimum
Moscow (CH)	0.101	Moisture Content
Floydada (CL)	0.079	(18)
Mississippi Delta (CH)	0.082 to 0.104	5 Samples (19)
Louisiana Coast (MH)	0.029 to 0.104	8 Samples (20)
Haney Clay N.C.	0.300 to 0.600	(11)
Seattle Clay O.C.	0.500	(21)
Redwood City Clay	0.250	
Osaka Clay	0.000	
Tonegaw Loam	0.200	
Bangkok Mud	0.200	
Concrete	0.028	
High Density Polyethylene	0.098	
Polyvinyl Chloride	0.031	
Reinforced Plastic Mortar	0.048	

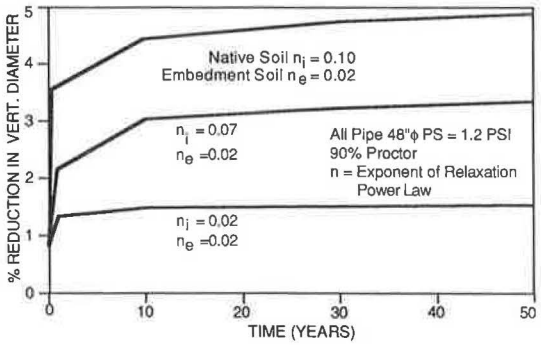

FIGURE 9 Variation of pipe vertical deflection over time.

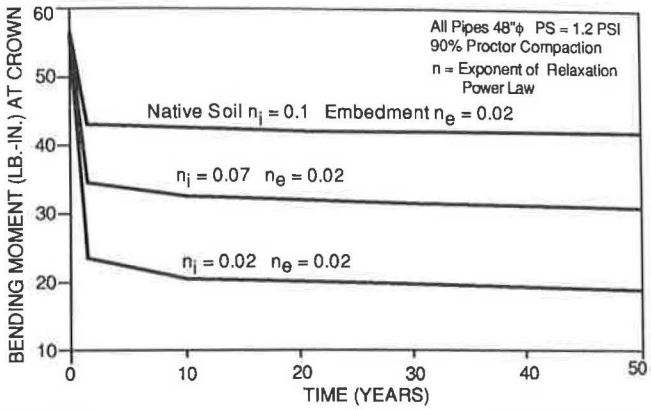

FIGURE 10 Variation of bending moment at crown over time.

Relaxation in a Soil-Pipe System

A flexible pipe deflects noticeably with time because the pipe material as well as the soil surrounding the pipe relaxes. Whether the soil load on a pipe increases or decreases with time depends on the difference between the relaxation rate (exponent of the power law) of the pipe material and the surrounding soil. In the case of a pipe made of stiff material, the soil tends to creep faster than the pipe, and hence the soil load increases. With pipes made of compliant materials, such as HDPE pipe, the pipe material relaxes faster than the soil and, in effect, redistributes the imposed loads back to the soil.

Table 1 gives the values of relaxation rates for various soils and pipe materials.

Pipe Vertical Deflection with Time

Figure 9 shows the predicted percentage reduction in vertical diameter of pipes with coarse-grained embedment materials (compacted to 90 percent Proctor) and buried in in situ (native) soils of the same stiffness (K = 200) but of different relaxation rates. The pipes deflect from two to five times the initial deflection during the 50-year period. The exponent of the power law for coarse-grained soils is assumed to be 0.02 (22) and for fine-grained soils is usually around 0.1. Silty soils can be assumed to have relaxation rates between the two. The figure also compares the results that can be obtained for m-values of 0.02, 0.07, and 0.10 for the different types of in situ soils.

Bending Moment Pipe Strains with Time

Figure 10 shows the variation of bending moment at the crown over time. In these cases, the bending moment at the crown reduces with time. This is because the exponent of the power law of the HDPE pipe material is about 0.098, which is higher than that of the surrounding soil. The converse will happen if a rigid pipe is buried in the same soil.

COMPARISON WITH FIELD MEASUREMENTS

To validate the design equations, field installation conditions as described by soil reports and installation procedures were studied, and the pipe vertical deflections were predicted for various time periods. The predictions were compared with the pipe deflections that were observed during the same period.

The field data were obtained for a variety of sites in the United States from a pipe manufacturer. The site that will be illustrated here is in Kansas. Six 48-in.-diameter HDPE pipe sections (PS = 5 psi), each 20 ft long, were installed as a single line with 18 ft of cover measured to the springline. The soil profile along the line was basically silty clay down to the springline. The modulus number of the backfill soil was K_b = 100; the in situ soil was estimated to have K_i = 200 and a modulus number n = 0.4. The embedment material was compacted to 85 percent Proctor. The soil modulus used in Spangler's equation was 3,000 psi, because crushed rocks were used (*23*) as bedding materials. Five pipe vertical deflections were measured at each section, and readings were taken at 2 days and 1, 2, 6, and 42 weeks after installation.

At the beginning of the installation, the six pipes were buried at different depths of cover ranging from 1 to 18 ft, and the pipe vertical deflections were measured. Figure 11 compares the results of the design equations and Spangler's equation with the average of five pipe vertical deflections per section. The design equations predicted the deflections well. It also appears that the level of compaction may be more than the 85 percent Proctor that was assumed.

The trench was backfilled a depth of cover of 18 ft after 2 days with the exception of the first two sections. The pipe deflections measured during the 10-month period were plotted in Figure 12. A relaxation rate of 0.02 was assumed for the embedment material, and 0.07 was assumed for the silty soil. A lag factor of 1.0 was used for Spangler's equation because lag factors from 1.25 to 1.5 are recommended only if the time periods are on the order of a few years (*23*). It can be seen that the design equations were able to match the deflection behavior. Again, the deflections were slightly more than predicted, probably because of the low compaction assumed for the embedment material. The field data also indicate a nonlinear increase in values over time, just as predicted by the design equations.

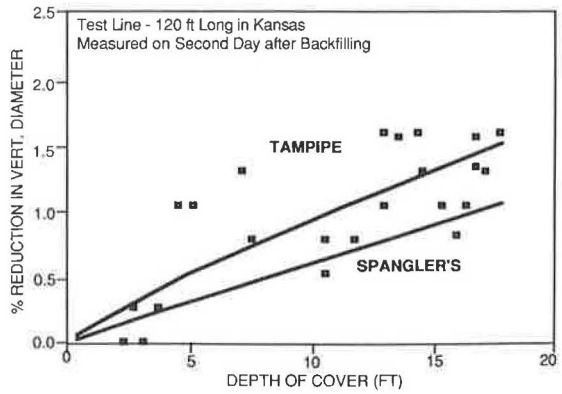

FIGURE 11 Predicted and measured pipe vertical deflections for different depths of cover.

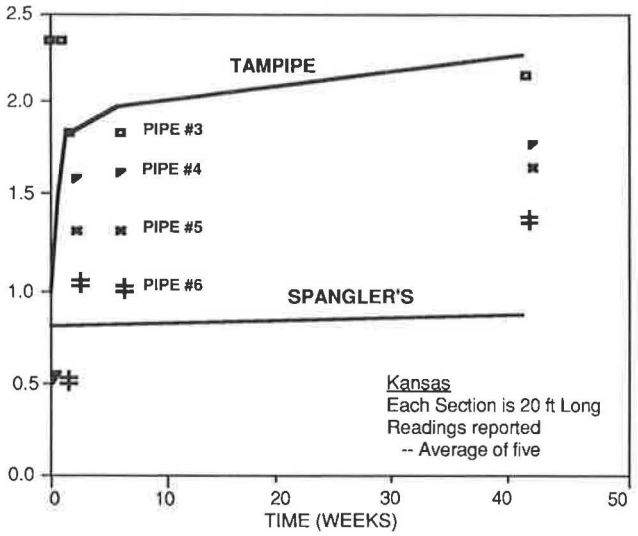

FIGURE 12 Predicted and measured pipe vertical deflection for different time periods.

CONCLUSIONS

Design equations that can be used to determine the deflections, loadings, and strains in flexible pipes and their behavior over time have been presented. The main factors affecting the soil-pipe system were identified. They include pipe characteristics, properties of the different types of soils, arching in the soil, trench width, and presence of groundwater. The time-dependent behavior of the soil-pipe system was also presented, and results were obtained by using the viscoelastic form of the design equations. It was shown that it is possible to quantify the effects of the various factors on pipe deflections over time and that the design equations were able to match field measurements. The ability to describe the details of soil-pipe behavior with a sound engineering approach can be expected to provide a major benefit to the design, construction, and performance of buried flexible pipes.

REFERENCES

1. M. G. Spangler. *Soil Engineering* (3rd ed.). International Textbook Co., Scranton, Pa., 1973.
2. R. L. Kondner. Hyperbolic Stress-Strain Response: Cohesive Soils. *Journal, Soil Mechanics and Foundations Division*, ASCE, Vol. 89, No. SM1, Feb., 1983.
3. N. Janbu. Soil Compressibility as Determined by Oedometer and the Triaxial Tests. *European Conference on Soil Mechanics and Foundation Engineering*, Wiesbaden, Germany, Vol. 1, 1963, pp. 19–25.
4. J. M. Duncan, P. Byrne, K. S. Wong, and P. Mabry. *Strength, Stress-Strain and Bulk Modulus Parameters for Finite Element Analysis of Stresses and Movements in Soil Masses*. Report UCB/GT/80-01, University of California, Berkeley, 1980.
5. M. G. Katona, J. M. Smith, R. S. Odello, and J. R. Allgood. *CANDE—A Modern Approach for the Structural Design and Analysis of Buried Culverts*. Rept. FHWA-RD-77-5, Oct. 1976.
6. *Spiral Engineered Systems*. Chevron Oil, Norcross, Ga., 1985.
7. E. Gaube and W. Mueller. 12 Years of Deformation Measurements on Sewer Pipes from Hostalen GM5010. *Proc., International Conference on Underground Plastic Pipes*, ASCE, New Orleans, La., 1981.

8. K. Hoeg. Stresses Against Underground Structural Cylinders. *Journal, Soil Mechanics and Foundations Division*, ASCE, No. SM1, July 1968, pp. 833–858.
9. *Structural Plastics Design Manual*. ASCE Manuals and Reports on Engineering Practice 63., May 1984.
10. L. Obert and W. I. Duvall. *Rock Mechanics and the Design of Structures in Rocks*. John Wiley and Sons, Inc., New York, 1967.
11. J. K. Mitchell, R. C. Campanella, and A. Singh. Soil Creep as a Rate Process. *Journal, Soil Mechanics and Foundations Division*, ASCE, Vol. 94, No. SM1, 1968, pp. 231–253.
12. R. A. Schapery and M. Riggins. Development of Cyclic Nonlinear Viscoelastic Constitutive Equations for Marine Sediments. *Proc., International Symposium on Numerical Models in Geomechanics*, Zurich, Switzerland, 1982.
13. M. A. Biot. Dynamics of Viscoelastic Anisotropic Media. *Proc., 4th Midwestern Conference*, 1955, pp. 94–108.
14. E. H. Lee. Stress Analysis in Viscoelastic Bodies. *Quarterly Journal of Applied Mathematics*, Vol. 13, 1955, pp. 183–190.
15. R. A. Schapery. Approximate Methods of Transform Inversion for Viscoelastic Stress Analysis. *Proc., 4th U.S. National Congress of Applied Mechanics*, ASME, 1962.
16. T. L. Cost. Approximate Laplace Transform Inversions in Viscoelastic Stress Analysis. *AIAA Journal*, Vol. 2, No. 12, 1964, pp. 2157–2166.
17. K. M. Chua and R. L. Lytton. Short Communication: A Method of Time-Dependent Analysis Using Elastic Solutions for a Non-Linear Material. *International Journal for Numerical And Analytical Methods in Geomechanics*, Vol. 11, No. 4, 1987.
18. A. M. Marimon. *The Effects of Suction and Temperature on the Material Characteristics of Fine-Grained Soils*. Texas A&M University, College Station, 1977.
19. M. Riggins. *The Viscoelastic Characterization of Marine Sediments in Large-Scale Simple Shear*. Ph.D. dissertation, Texas A&M University, College Station, 1981.
20. H. S. Stevenson. *Vane Shear Determination of the Viscoelastic Shear Modulus of Submarine Sediments*. M.S. thesis. Texas A&M University, College Station, 1973.
21. A. Singh and J. K. Mitchell. Creep Potential and Creep Rupture of Soils. *Proc., 7th International Conference of Soil Mechanics and Foundations Division*, ASCE, Vol. SM3, 1970, pp. 1011–1043.
22. K. M. Chua and R. L. Lytton. Time-Dependent Properties of Embedment Soils Back-Calculated from Deflections of Buried Pipes. *Specialty Geomechanics Symposium*, Institute of Engineers, Adelaide, Australia, Aug. 1986.
23. A. K. Howard. The USBR Equation for Predicting Flexible Pipe Deflection. *Proc., International Conference on Underground Plastic Pipes*, ASCE, New Orleans, La., 1981, pp. 37–55.

Publication of this paper sponsored by Commitee on Subsurface Soil-Structure Interaction.

Investigation of the Structural Adequacy of *C* 850 Box Culverts

G. R. FREDERICK, C. V. ARDIS, K. M. TARHINI, AND B. KOO

The structural behavior of American Society for Testing and Materials *C* 850 box culvert sections resulting from live load was investigated using theoretical analyses, field testing, and model testing. The field testing was performed on box culvert sections that were put into service after testing. These box culvert sections were installed on state routes in Ohio using construction crews and normal construction procedures. An overview of these analyses is presented in this paper. The initial purposes were to determine whether shear connector plates are required to transfer the load across a joint between adjacent box culvert sections, and if the recommended maximum spacing of 30 in. was appropriate. Testing at the first site indicated that shear connector plates are not required to transfer the load. The primary purpose of testing at the second site was to verify the results from testing at the first site. For these box culvert sections, there were no provisions for shear connectors, hence the reinforcing steel was not cut because the shear connector attachments were not installed. The results verified those from testing done at the first site. Additionally, it was concluded that *C* 850 box culvert sections are overdesigned structurally. Before testing was undertaken at the third site, a redesign was executed for *C* 850 box culvert sections. The redesigned *C* 850 box culvert section was essentially the same as the *C* 789 design with 4 ft of earth cover and HS 20 loading. Testing at this site demonstrated that the redesigned *C* 850 box culvert section performed satisfactorily. The major conclusions are that shear connectors are not required on American Society for Testing and Materials *C* 850 box culvert sections and that these sections are overdesigned structurally. It was also concluded that the deflection along an edge of the top slab was so low, even with the wheel load applied at that edge, that the American Association of State Highway and Transportation Officials' edge beam requirement need not be enforced.

The design requirements for box culvert sections installed with less than 2 ft of cover and subjected to highway loadings are enumerated in American Society for Testing and Materials (ASTM) Specification *C* 850 (*1*). These requirements generally follow the American Association of State Highway and Transportation Officials (AASHTO) *Standard Specifications for Highway Bridges* (*2*). The requirements of interest in this paper (as applied to box culvert sections) are

1. Use of shear connector plates,
2. AASHTO edge-beam requirement, and
3. Applicability of AASHTO distribution width for wheel loads.

Department of Civil Engineering, The University of Toledo, Toledo, Ohio 43606

Two separate studies were undertaken to investigate these requirements. These studies included theoretical analyses, model testing in a laboratory, and field testing of prototypes.

THEORETICAL ANALYSES

In the theoretical analyses, the structures were idealized into plane frames with a unit width. The corresponding live load was determined using the AASHTO distribution width for a wheel load. The dead load associated with 2 ft of earth cover and the weight of the box culvert, as well as the lateral earth pressure on the side walls, was also considered. The analyses were performed using classical methods of structural analyses and the finite element method.

A three-dimensional stress analysis was also performed using the finite element method. STRUDL was used for this analysis; prismatic elements with triangular cross sections and six nodes were selected. There were three linear degrees of freedom at each node of the element.

In these analyses, deflections, bending moments, shear, and normal forces were calculated. Reinforced concrete design was performed using the ultimate strength method.

FIELD TESTING

During the field testing of prototype structures, deflections of the top slab were observed and recorded along both edges of a joint that was subjected to load. Additionally, electric resistance strain gages had been mounted at selected locations and strain magnitudes were recorded. Primarily, strain values were recorded for the top slab.

All prototype structures were cast by the same manufacturer, Hyway Concrete Pipe Company in Findlay, Ohio, with tongue-and-groove joints. The cylinder strength of the concrete was a minimum of 5,000 lb/in.^{2} and the minimum yield strength of the welded wire fabric reinforcing was 65,000 lb/in.^{2}. Normal construction techniques were followed except that over-reinforcing was minimized. The theoretical steel areas were matched as closely as practicable.

For the first investigation (*3*), strain gauges were mounted on both the welded wire fabric and the concrete. Also, a few strain gauges were mounted on the shear connector plates. Deflection and strain data were recorded for three load conditions:

1. Wheel load applied directly to the top slabs of *C* 850 box culvert sections without shear connector plates installed,

2. Wheel load applied directly to the top slabs with shear connector plates installed, and
3. Wheel load applied to the asphalt pavement placed over the box culvert sections with shear connector plates installed.

For these conditions, a (simulated) wheel load of 20,800 lb (AASHTO HS 20 16,000-lb wheel load plus 30 percent impact) was applied to a simulated tire print (a 10-in. by 20-in. wooden block). Only one wheel load was applied on the structure at a time. The structure was Ohio DOT bridge number MAR-309-09.42 (located in Marion County) and used six box culvert sections with 12-ft span by 6-ft rise and a total laying length of 36 ft. The primary purposes of this investigation were to determine whether shear connectors were required and whether the 30-in. maximum spacing was appropriate. The geometry of an individual box culvert is presented in Figure 1; the overall configuration of the structure is shown in Figure 2. Because this structure was to be placed in highway service after testing, it was decided to limit the magnitude of the loading to 20,800 lb.

For the second investigation (*4*), strain gages were mounted on the concrete only. Two prototype structures were field tested in this investigation: PUT-109-02.67 and CRA-19-17.10. Deflection and strain data were recorded at each site. Based on the results of testing at the Marion County site, it was decided to load these box culvert sections until a hairline crack developed.

At Ohio Department of Transportation (DOT) bridge No. PUT-109-02.67 (located in Putnam County), the primary purpose was to verify the conclusions from MAR-309-09.42 on box culvert sections that did not have the reinforcing steel cut as is necessary when installing the shear connector attachments. This structure consisted of 17 box culvert sections with 12-ft span by 4-ft rise. These sections conformed to ASTM *C* 789 (*5*) for 3 ft of cover; the geometry of an individual box culvert is presented in Figure 3. However, they were subjected to live loading as though they were *C* 850 box culvert sections. After the sides had been backfilled to the elevation of the top slabs, the box culvert sections were loaded directly on the top slabs with a load of at least 20,800 lb before any earth cover

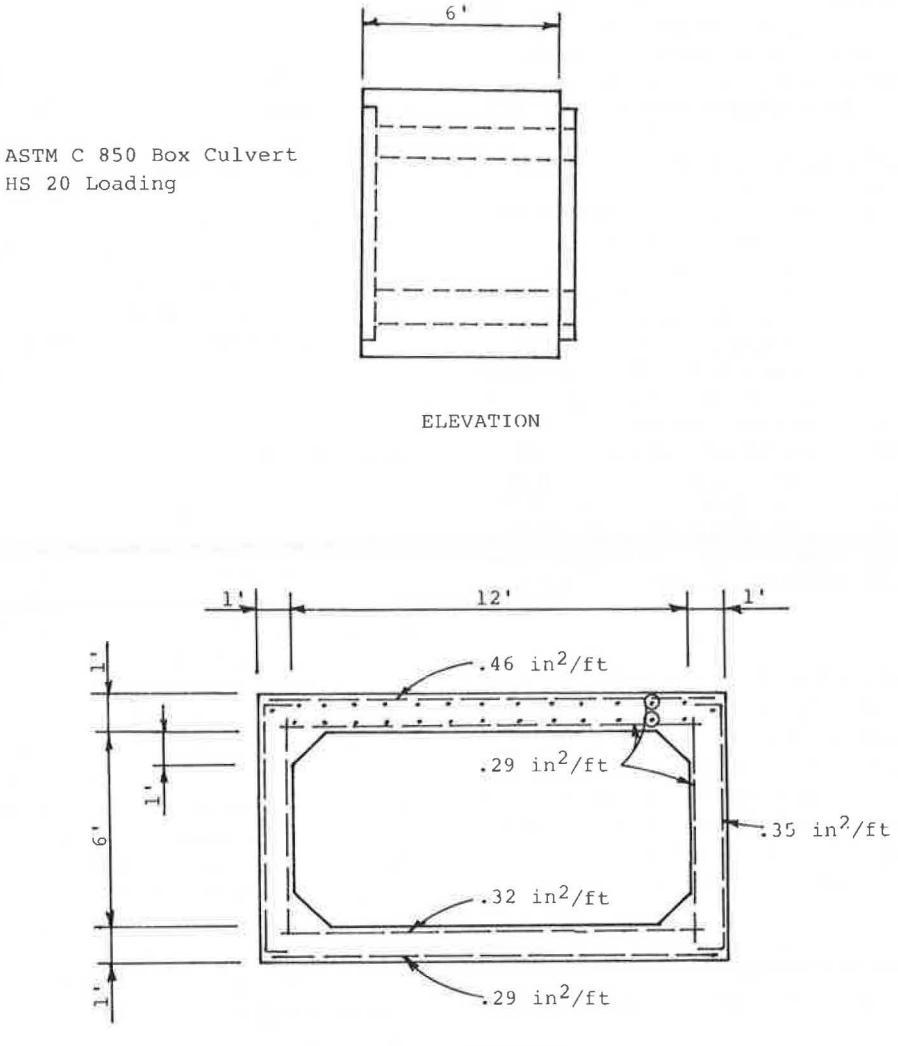

FIGURE 1 Details of 12-ft by 6-ft box culvert (Ohio DOT bridge MAR-309-09.42).

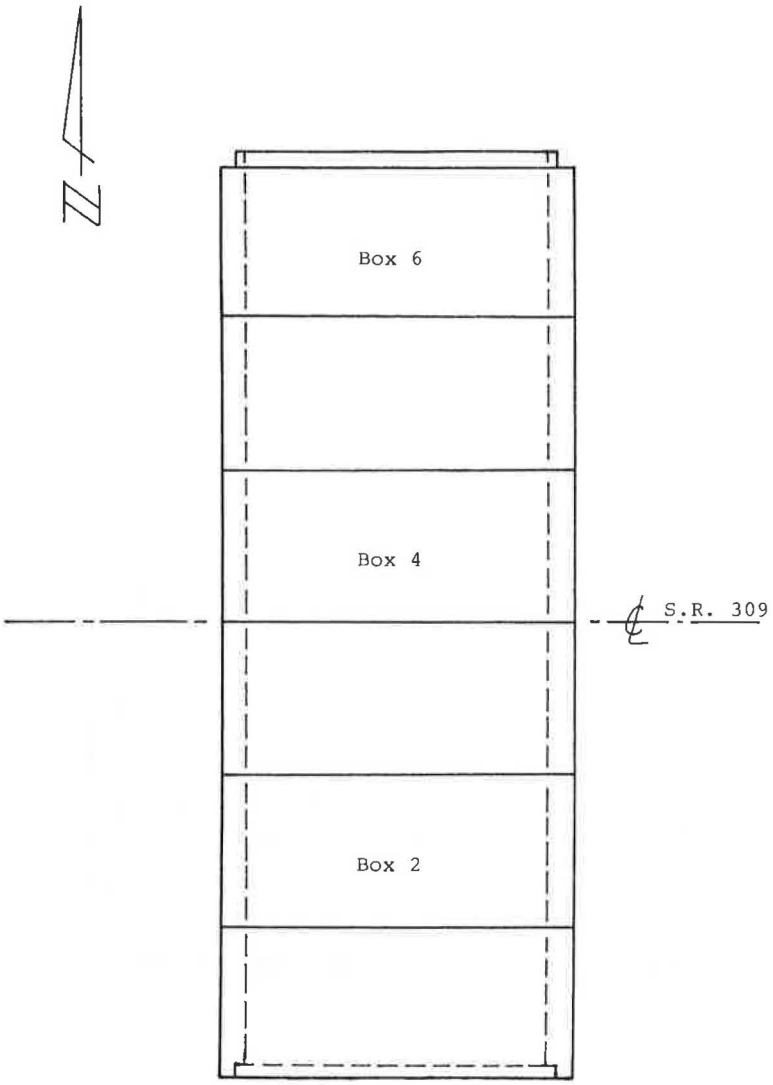

FIGURE 2 Arrangement of box culvert sections (Ohio DOT bridge MAR-309-09.42).

was placed. Four of the box culvert sections in this structure, as indicated in Figure 4, were subjected to single (simulated) wheel loads to produce a hairline flexural crack in the bottom sides of the top slabs.

At Ohio DOT bridge No. CRA-19-17.10 (located in Crawford County), the primary purpose was to verify a redesigned box culvert section that would be subjected to AASHTO HS 20 loading with asphalt pavement placed directly on the top slab. This structure consisted of 10 box culvert sections with 10-ft span by 6-ft rise. All walls of these sections were maintained at thicknesses of 10 in. so that conventional forms could be used in their manufacture. However, the reinforcing steel areas were less than those specified in ASTM *C* 850. The details of the redesigned box culvert are presented in Figure 5; the overall structure is shown in Figure 6.

MODEL TESTING

Model testing (*6*) was performed in a laboratory on ⅙ size scale models of each of the prototypes that were field tested. These models were cast in plywood forms using portland cement concrete and hardware cloth for the reinforcing steel. The concrete was proportioned to provide a 28-day compressive strength of 4,000 lb/in.^{2}. The aggregate used had a maximum particle size of ¼ in. The wires in the hardware cloth were spaced at ⅜ in. in both directions. To achieve the required areas of reinforcing steel, ⅛-in. diameter steel rods were wired to the hardware cloth as necessary. No attempt was made to match the distribution reinforcing or the shrinkage and temperature reinforcing. Each model was subjected to a scaled wheel load. The models were not subjected to lateral earth pressure or dead load (other than the weight of the model).

RESULTS AND CONCLUSIONS

The primary observations (at a wheel load of 20,800 lb) from the investigations of MAR-309-09.42 were as follows:

1. The maximum compressive strain in the concrete in top slabs is very low—of the order of 120 microin./in.

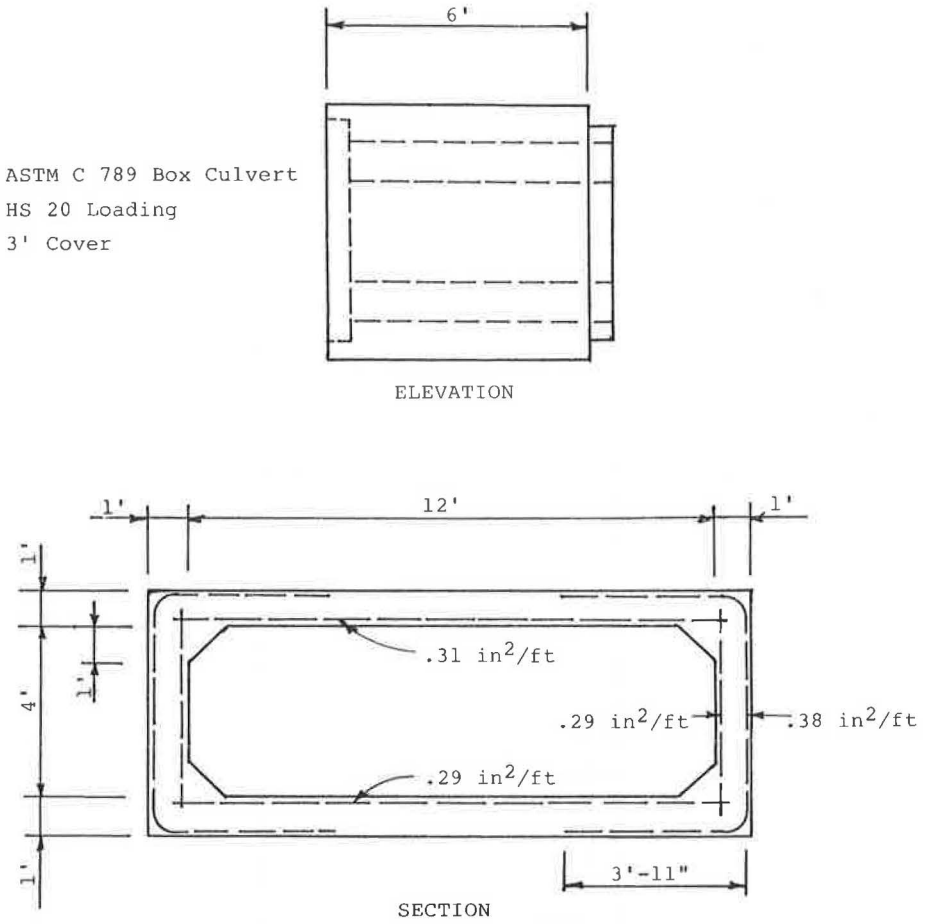

FIGURE 3 Details of 12-ft by 4-ft box culvert (Ohio DOT PUT-109-02.67).

2. The maximum tensile strain in the reinforcing steel is very low—of the order of 120 microin./in. (This is so low that the concrete did not develop tensile flexural cracks.)
3. The maximum deflection along a joint between adjacent box culvert sections was 0.027 in. without shear plates in place.
4. The average values of the deflections without shear plates for the loaded edge and relative deflection across the joint were 0.018 in. and 0.012 in., respectively.
5. The average values of the deflections were 0.014 in. and 0.006 in., respectively, with shear plates and without pavement.
6. The average values remained virtually the same after the pavement was in place.
7. The strain in the shear plates was very low—on the order of 120 microin./in.

Hence, because the deflections and strains were very low, it was concluded that shear connectors are not required to transfer load across a joint. Further, it was concluded that the AASHTO edge-beam requirement does not need to be enforced for box culverts. Note that it was necessary to cut the reinforcing steel to install the anchorages for shear connectors. Often this required cutting the reinforcing steel in locations of greatest bending moments. This did not appear to adversely affect the structural behavior of the box culvert sections. All of the above observations led to the conclusion that ASTM *C* 850 box culvert sections are overdesigned structurally.

The primary observations from the investigations of PUT-109-02.67 were

1. The maximum strain in the concrete was very low at design load plus impact.
2. The average deflection along a joint was very low at design load plus impact—of the order of 0.020 in. The average relative deflection was 0.012 in.
3. The average load required to produce a hairline flexural crack was twice the design wheel load plus impact.

The results of this testing confirmed the results from testing of MAR-309-09.42. It is emphasized that box culvert sections conforming to ASTM *C* 789 for 3 ft of earth cover were tested using *C* 850 live load conditions. Because none of the four box culvert sections subjected to load exhibited a hairline flexural crack at 20,800 lb, it is concluded that a *C* 789 design without shear plates is adequate for *C* 850 live-load conditions. The hairline cracks that developed at twice the design load plus impact virtually closed after the load was removed. This indicated that the reinforcing steel had not yielded. Note that

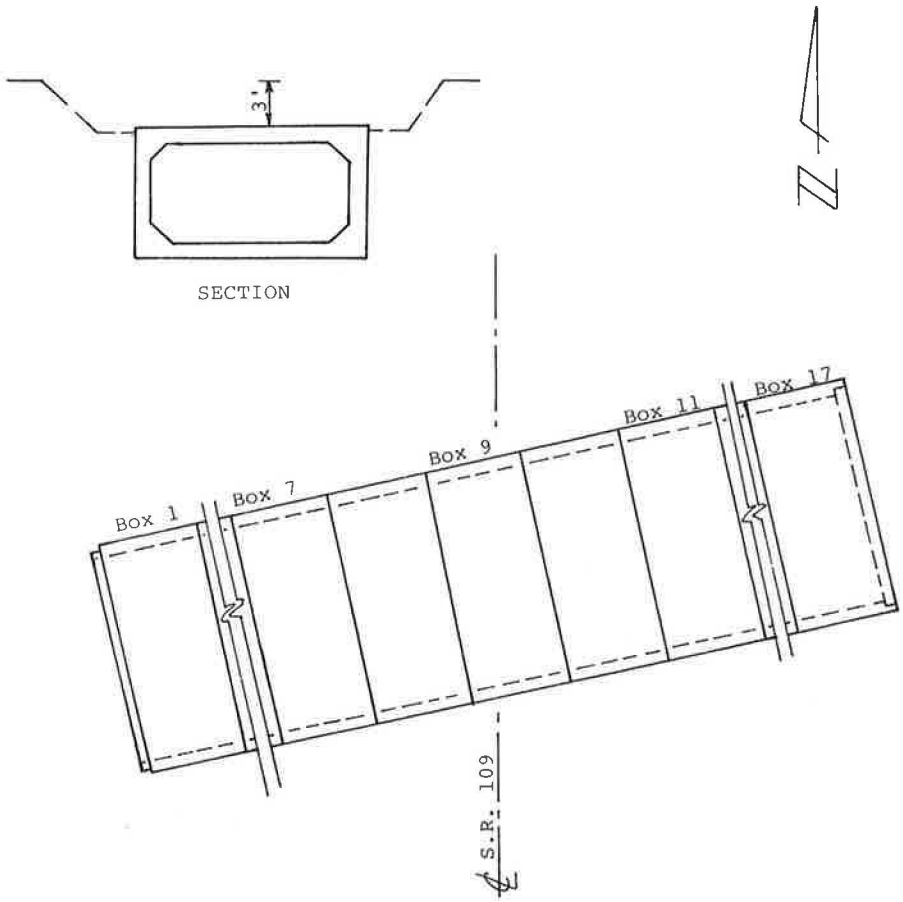

FIGURE 4 Arrangement of box culvert sections (Ohio DOT bridge PUT-109-02.67).

the average cracking load of 41,600 lb is almost equal to the ultimate design load of 45,140 lb (calculated using AASHTO load factors).

The deflection data from both MAR-309-09.42 and PUT-109-02.67 indicated that on the average a moderate amount of load is transferred across a joint between adjacent box culvert sections even when shear connectors are not used. A butyl rubber (ribbon) gasket was installed in each joint. It is believed that this transfer is due primarily to friction in the joint and the presence of the butyl rubber gasket. In many instances the unloaded side of the joint deflected as much as 50 percent of the loaded side. This load transfer appeared to be largely independent of whether the tongue end or the groove end was the loaded side of the joint. As might be suspected, the transfer resulting from friction was sensitive to how tightly the joint was made.

The primary observations (at a wheel load of 20,800 lb) from the investigations of CRA-19-17.10 were

1. The maximum strain in the concrete was very low both with and without the asphalt pavement in place.
2. The average deflection along a joint was very low without the pavement in place—of the order of 0.009 in. The average relative deflection was 0.003 in.
3. The average deflection along a joint was very low with the pavement in place—of the order of 0.013 in. The average relative deflection was 0.006 in.

Additionally, no hairline cracking was observed in the box culvert section subjected to a load of 30,350 lb without the pavement in place.

The results of this testing confirmed the results from testing of MAR-309-09.42 and PUT-109-02.67. It is emphasized that the box culvert sections for CRA-19-17.10 were redesigned box culverts. The redesigned box culverts used for *C* 850 live load conditions were very close to the *C* 789 design for 4 ft of earth cover. Hence, for CRA-19-17.10, the ASTM *C* 789 design for 4 ft of earth cover was used for a redesigned *C* 850 box culvert. It should also be noted that the box culvert sections for CRA-19-17.10 had a 10-ft span by 6-ft rise with wall thicknesses of 10 in.

A visual inspection of the box culvert sections for CRA-19-17.10 performed 21 months after they were installed revealed no signs of distress. Hence, the redesigned box culvert sections appear to be performing satisfactorily.

For the three box culvert sizes indicated, ⅙ size scale models were constructed and tested in a laboratory. These tests were performed on individual sections with the load applied along an edge. The measured strains on the concrete and deflections along the loaded edge agreed well with those quantities measured in the field. The strain values resulting from the application of the design wheel load plus impact on a scale model of the 12-ft by 6-ft box culvert are shown in Figure 7. The models exhibited a hairline flexural crack in the upper slab at approximately 2½ times the scaled design wheel load plus impact.

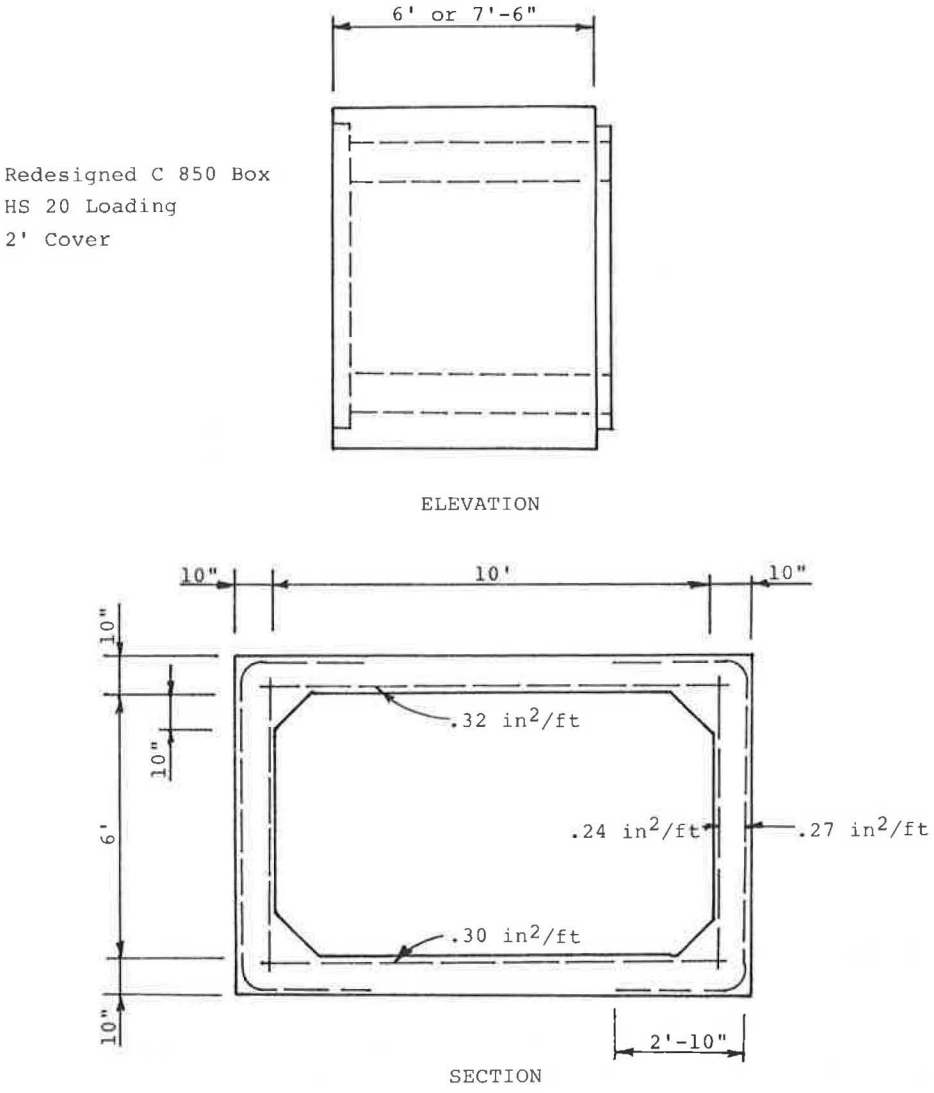

FIGURE 5 Details of redesigned 10-ft by 6-ft box culvert (Ohio DOT bridge CRA-19-17.10).

CLOSURE

Based on the findings described in this paper, the Ohio DOT no longer requires the use of shear connectors on box culvert sections conforming to ASTM *C* 850. The Ohio DOT does not enforce the AASHTO edge-beam requirement for slabs with main reinforcing parallel to traffic in box culverts, even though shear connectors are not used.

Based on the performance of box culvert sections at CRA-19-17.10, it appears that the structural design of ASTM *C* 850 box culvert sections can be economized. In this study only the steel reinforcement areas were changed. However, it is also possible to reduce the wall thicknesses. This may be undesirable because box culvert manufacturers would be required to modify existing forms or to purchase new forms.

It is further concluded that the ASTM *C* 850 specification, as well as the *C* 789 designs for less than 4 ft of cover, can be eliminated. The *C* 789 design for 4 ft of cover is recommended for these cases. For cover depths greater than 4 ft, the *C* 789 designs should be reevaluated.

In the redesigned box culvert section for *C* 850 live load conditions used in this study, the AASHTO distribution width for a wheel load was not used. Accounting for the transfer of load to adjacent sections by friction at a joint, a distribution width somewhat larger than the AASHTO recommendation, was used. Additional research should be undertaken to define a more appropriate expression for distribution width for a wheel load. In this redesign, a distribution width of 7.5 ft was used. This width corresponded to the largest laying length for these box culvert sections.

Note that the results and conclusions relative to MAR-309-09.42 are in agreement with those of James (*7*), who concurrently and independently investigated *C* 850 box culverts. Additionally, at least in Ohio, the authors' recommendation

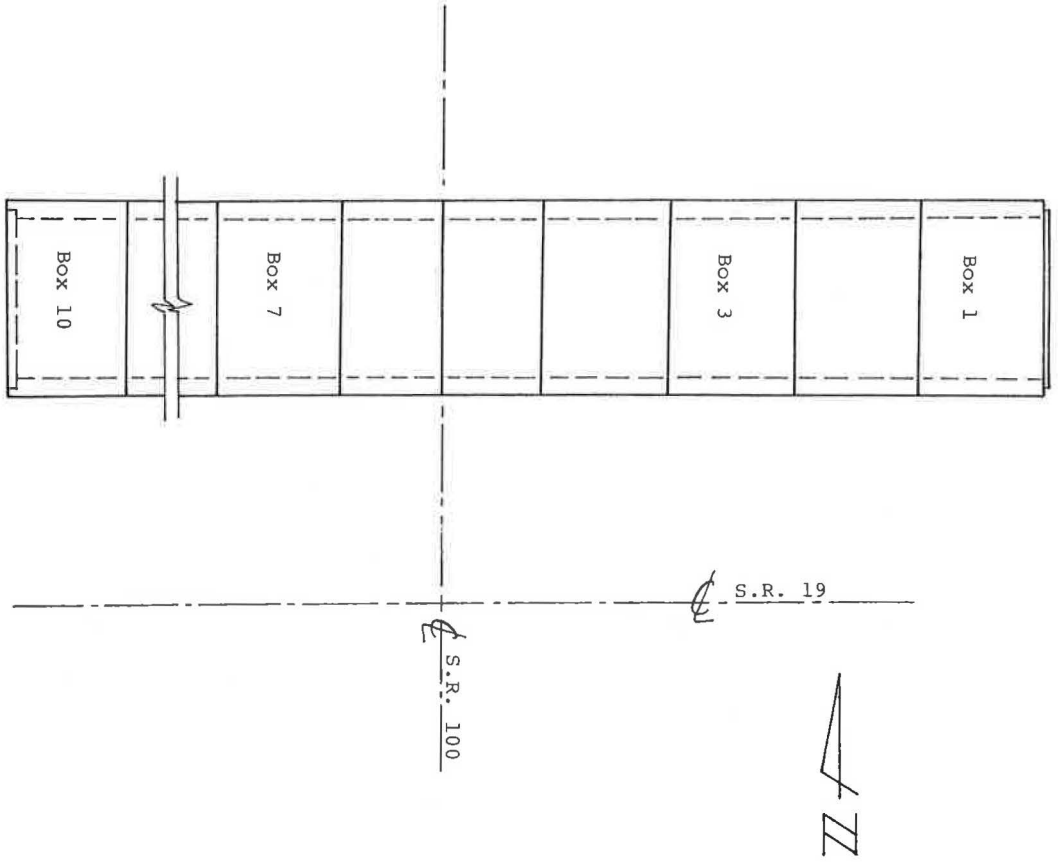

FIGURE 6 Arrangement of box culvert sections (Ohio DOT bridge CRA-19-17.10).

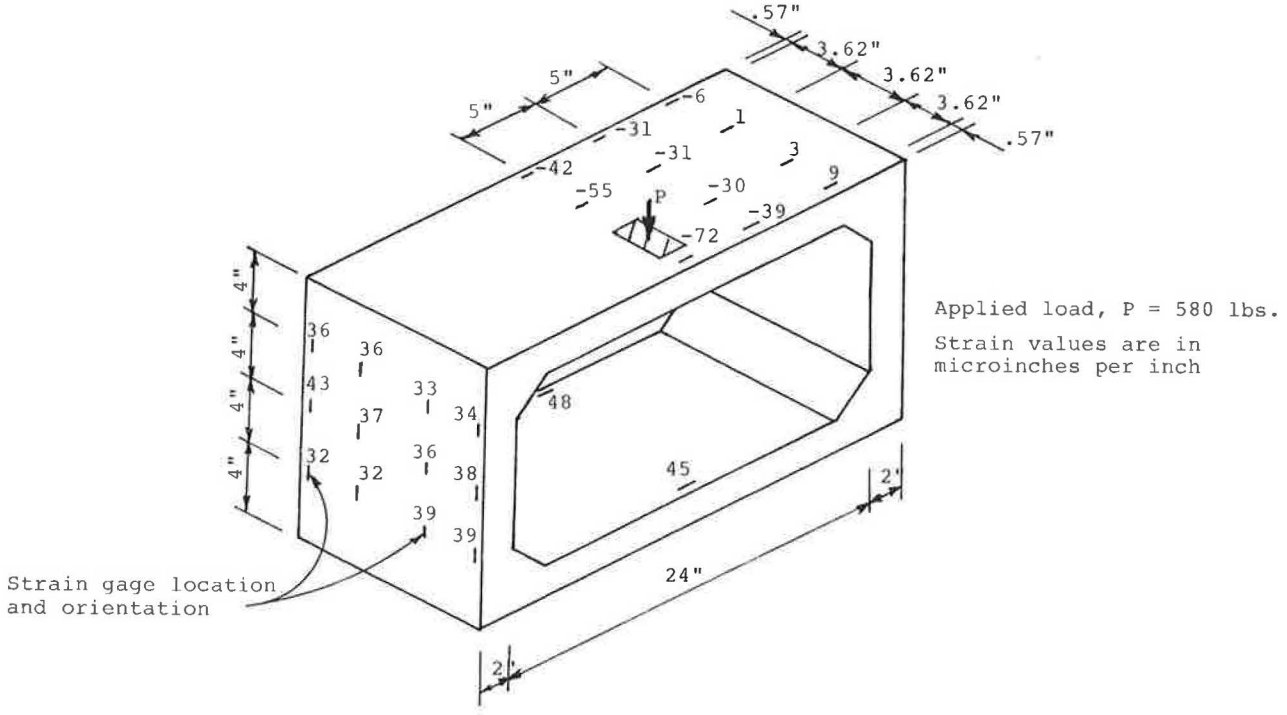

FIGURE 7 Strain data model of 12-ft by 6-ft box culvert.

(as well as that of James) regarding elimination of shear connectors has been implemented. Furthermore, our investigations at all three sites satisfy his second recommendation of field tests of box culverts installed without shear connectors.

ACKNOWLEDGMENTS

The work reported here was jointly funded by the Federal Highway Administration and the Ohio DOT under two separate grants.

The cooperation of personnel at Hyway Concrete Pipe Company in Findlay, Ohio, for providing space and arranging their work schedules for the installation of strain gauges is acknowledged.

The cooperation of the following contractors at the three job sites is also acknowledged:

Wren-Reese Construction Company at Ohio DOT bridge MAR-309-09.42,
Sherburn Construction Company at Ohio DOT bridge PUT-109-02.67, and
Ohio Engineering Company and Crawford Construction Company at Ohio DOT bridge CRA-19-17.10.

Finally, the assistance of several students who helped with the prototype and laboratory testing is acknowledged.

REFERENCES

1. *Standard Specification for Precast Reinforced Concrete Box Sections for Culverts, Storm Drains, and Sewers with Less than 2 Feet of Cover Subjected to Highway Loadings*. Standard C 850-82, American Society for Testing and Materials, 1983 Annual Book of Standards, Vol. 04.05, Philadelphia, Pa., 1983.
2. *Standard Specifications for Highway Bridges*, 12th ed. American Association of State Highway and Transportation Officials, Washington, D.C., 1977.
3. G. R. Frederick, B. Koo, and C. V. Ardis. *Evaluation of Shear Connectors on Precast Reinforced Concrete Box Sections*. Ohio Department of Transportation Project 3612, Department of Civil Engineering, The University of Toledo, Toledo, Ohio, 1984.
4. G. R. Frederick and C. V. Ardis. *Evaluation of Precast Reinforced Box Sections Installed Without Shear Connectors*. Ohio Department of Transportation Project 14370(0), Department of Civil Engineering, University of Toledo, Toledo, Ohio, 1987.
5. *Standard Specification for Precast Reinforced Concrete Box Sections for Culverts, Storm Drains, and Sewers*. Standard C 789-82, 1983 Annual Book of ASTM Standards, Vol. 04.05, American Society for Testing and Materials, Philadelphia, Pa., 1983.
6. G. R. Frederick and K. M. Tarhini. Model Analysis of Box Culverts Subjected to Highway Loading. In *Proc., VI International Congress on Experimental Mechanics*, Society for Experimental Mechanics, Portland, Oreg., June 1988.
7. Ray W. James. Behavior of ASTM C 850 Box Culverts Without Shear Connectors. In *Transportation Research Record 1001*, TRB, National Research Council, Washington, D.C., 1984, pp. 104–111.

Publication of this paper sponsored by Committee on Culverts and Hydraulic Structures.